

• REVIEW •



## Overview and Prospect of Data Assimilation in Numerical Weather Prediction

Lili LEI<sup>1</sup>, Fuzhong WENG<sup>2</sup>, Wansuo DUAN<sup>3</sup>, Yaodeng CHEN<sup>4</sup>, Lin ZHANG<sup>2</sup>, Ruichun WANG<sup>2</sup>, Jun YANG<sup>2</sup>, Xiaohao QIN<sup>3</sup>, Wei HAN<sup>2</sup>, Jun LI<sup>5</sup>, Jinzhong MIN<sup>4</sup>, Zhifang XU<sup>2</sup>, Qifeng LU<sup>2</sup>, and Jiandong GONG<sup>2\*</sup>

<sup>1</sup> School of Atmospheric Sciences, Nanjing University, Nanjing 210008

<sup>2</sup> CMA Earth System Modeling and Prediction Centre, China Meteorological Administration (CMA), Beijing 100081

<sup>3</sup> Institute of Atmospheric Physics, Chinese Academy of Sciences, Beijing 100029

<sup>4</sup> Key Laboratory of Meteorological Disaster of Ministry of Education, Nanjing University of Information Science & Technology, Nanjing 210044

<sup>5</sup> National Satellite Meteorological Centre, China Meteorological Administration, Beijing 100081

(Received 23 January 2025; in final form 10 April 2025)

### ABSTRACT

For numerical weather prediction (NWP), data assimilation (DA) combines short-term forecasts and various atmospheric observations to achieve optimal initial conditions, based on which subsequent forecasts are launched. With the rapid advancements in numerical models and observing systems, DA has been significantly evolved. Modern methods now can account for uncertainties of state variables across various spatiotemporal scales, incorporate multiscale observation error statistics, and enforce dynamical constraints and model balances. Meanwhile, observations from various platforms, such as ground-based, aircraft, and satellite, have been assimilated. These include data from polar-orbiting and geostationary satellites, radar-derived radial winds and reflectivity, Global Navigation Satellite System (GNSS) radio occultations, etc. To further utilize the advanced observing systems and DA techniques for high-impact weather predictions, target observation strategies have been developed to identify areas where additional observations can yield the greatest predict improvements. Based on the advancements of DA theories and methods, China's operational systems have made significant progress, establishing advanced operational DA systems. Over the past decade, the forecast skill of 5-day global weather prediction has improved by approximately 15%. The article reviews a century of development in DA, and discusses future directions, including the advanced DA methods, operational frameworks, integration of novel observations, and the synergy between DA and artificial intelligence.

**Key words:** data assimilation, multi-source observations, atmospheric predictability, numerical weather prediction

**Citation:** Lei, L. L., F. Z. Weng, W. S. Duan, et al., 2025: Overview and prospect of data assimilation in numerical weather prediction. *J. Meteor. Res.*, **39**(3), 559–592, <https://doi.org/10.1007/s13351-025-4905-8>.

## 1. Introduction

As an initial value problem, numerical weather prediction (NWP) can be achieved by advancing a numerical model, given the current state of the atmosphere, its associated lateral boundary, and top and bottom boundary conditions. More accurate initial conditions can lead to improved numerical weather forecasts, while the initial conditions are the best possible estimate of the atmospheric state using all available information (Talagrand, 1997). Data assimilation (DA) is a sophisticated process to combine the noisy observations with uncertain short-term forecasts, resulting in the optimal estimate of the at-

mospheric state (Daley, 1991; Kalnay, 2003; Zou, 2025).

In the early stages of DA for weather forecasting, empirical methods were developed, such as the interpolation schemes (Panofsky, 1949; Gilchrist and Cressman, 1954), successive correction method (Cressman, 1959), and Newton relaxation method (Hoke and Anthes, 1976). At the same time, Chinese scholars innovatively proposed to use recent historical weather data for future state forecasting, which transformed the NWP initial value problem into an extrapolation forecast process based on historical weather evolutions (Koo, 1958a, b). Chou (1974) further proposed using functional extreme value problem with multi-time historical observations as an

Supported by the National Natural Science Foundation of China (42192553).

\*Corresponding author: [gongjd@cma.gov.cn](mailto:gongjd@cma.gov.cn)

© The Chinese Meteorological Society 2025

equivalent way to solve the differential equations that approximately describe the atmospheric processes, which is the primary concept of the variational methods later developed and widely used in NWP. As numerical models advanced, Chinese scholars deepened the theoretical basis of DA, pointing out that NWP is an initial value problem and also an inverse problem (Chou, 2007), through which the initial conditions, boundary conditions, and model parameters can be optimally estimated. But challenges remain due to the ill-posed problems, which could be solved by introducing regularization from inverse problems to DA and adding stabilization functionals to the objective functional (Huang et al., 2003). The China Meteorological Administration (CMA) operational system initially relied on the imported DA technology. Since 2000, CMA has been dedicated to developing variational DA methods and systems, gradually establishing the operational regional three-dimensional variational DA system (GRAPES-MESO, now CMA-MESO) and global four-dimensional variational DA system (GRAPES, now CMA-GFS) (Xue and Chen, 2008; Zhang L. et al., 2019; Shen et al., 2020), which significantly improves the accuracy of global operational forecasts (Fig. 1).

In addition to the fundamental DA theories and methods, the effective and efficient integration of observation data into DA systems is crucial for NWP. The assimilation of satellite retrievals into numerical models began in the 1970s, marking a significant contribution to the field of numerical forecasting (Smith et al., 1970). Since the 1990s, the direct assimilation of satellite radiances has been made possible through advancements in fast radiat-

ive transfer models and variational assimilation methods (Saunders et al., 2018; Weng et al., 2020; Johnson et al., 2023). This development has further enhanced the role of satellite data in NWP (Eyre et al., 2020). In 2009, China's global/regional integrated numerical forecast model (GRAPES) was quasi-operational implemented, significantly advancing the utilization of satellite data, particularly from the Fengyun (FY) series. In 2015, FY-2D cloud motion vectors were operationally assimilated into GRAPES, followed by the operational assimilation of FY-3C microwave radiances and occultation data in 2016 (Li and Liu, 2016; Li G. et al., 2016; Li J. et al., 2016). Since then, a variety of satellite observations from FY-4A/B and FY-3D/E have been operationally assimilated, marking a significant milestone in the quantitative application of FY satellite data. Moreover, radar data has played an important role for monitoring and forecasting the convective-scale weather systems. Chinese researchers have demonstrated the effectiveness to assimilate radar data in improving the accuracy of forecasts for convective-scale weather systems (Chen et al., 2014; Shao et al., 2016; Chen et al., 2018; Sun et al., 2020b).

The concept of target observation (i.e., adaptive observation) strategy has refined DA by collecting and assimilating additional high-quality observations in limited "sensitive areas", in order to improve the initial conditions and then the subsequent forecasts of high-impact weather events. To identify the sensitive areas for target observations, Chinese scholars considered the nonlinear nature of atmospheric and oceanic motions, and proposed the conditional nonlinear optimal perturbation (CNOP) method. The additionally collected observations

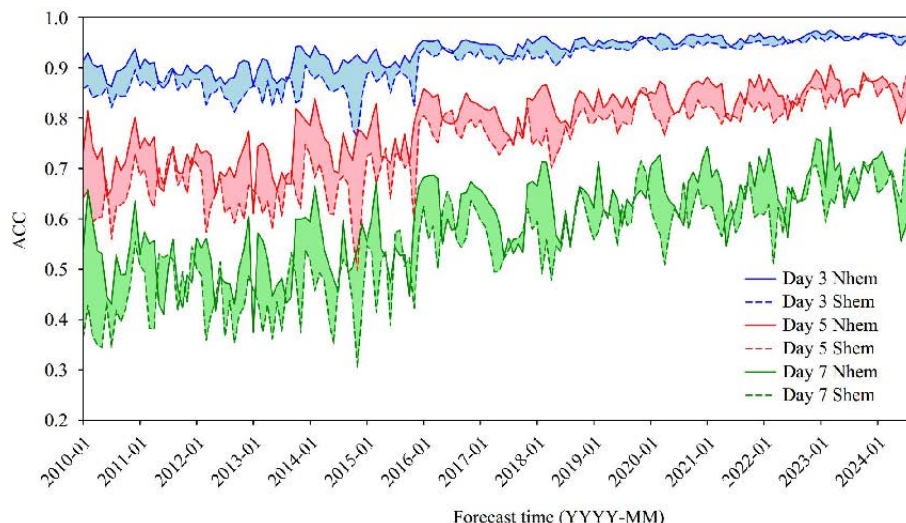


**Fig. 1.** Progress of global NWP by CMA. Monthly mean evolution of anomaly correlation coefficients (ACC) of 500-hPa geopotential height on the 3rd, 5th, and 7th forecast day, respectively, from January 2010 to August 2024 (solid lines for Northern Hemisphere and dashed lines for Southern Hemisphere).

based on the CNOP-identified sensitive areas have been proved to more effectively improve the forecast of high-impact weather events, compared to those collected upon sensitive areas identified by traditional linear approximation methods.

This paper reviews the development of DA theories and methods, the progress in assimilating multi-source observations, the development of targeted observation strategies, and advances in China's operational DA systems for NWP. The challenges and opportunities for DA in the context of rapid development of numerical models, observing systems, data science, and artificial intelligence are also discussed.

## 2. Theories and methods of DA

Along with the development of numerical models, observing systems, and computational science, the DA theories and methods have evolved from early empirical objective analysis to analysis theories based on statistics, and then to assimilation methods that incorporate atmospheric dynamics. This section focuses on the DA methods that are supported by statistical theories and have been operationally used in NWP. The nonlinear DA and coupled DA methods that are yet to be operationally applied are discussed in the prospect.

### 2.1 Variational methods

Analysis methods with statistical foundations began to develop around the 1980s. [Eliassen et al. \(1960\)](#) first derived the multivariate optimal interpolation equations based on observations and background fields. Subsequently, the optimal interpolation (OI) method was proposed, which seeks the optimal weight matrix in the physical space, such as at grid points ([McPherson et al., 1979](#)) or over finite volume elements ([Lorenc, 1981](#)). OI utilizes estimated background error covariances based on the differences between short-term forecasts and radiosonde observations ([Hollingsworth et al., 1986; Thiébaux and Pedder, 1987](#)). [Gandin \(1963\)](#) independently derived the multivariate OI equations and applied them to objective analysis in the Soviet Union. OI became the operational analysis method from the 1980s to the early 1990s.

Different from the OI that locally updates the weights given an “influence radius”, the three-dimensional variational method (3DVar; [Sasaki, 1970](#)) uses global optimization algorithms to minimize the cost function and directly obtains the minimum of control variables. 3DVar also has an observation-space form known as the physical-space statistical analysis system (PSAS; [Da Silva et al., 1995](#)), which seeks the minimum of the cost function in

the observation (physical) space. Although 3DVar, PSAS, and OI are equivalent in terms of their solutions ([Lorenc, 1986](#)), 3DVar and PSAS use more general and global background error covariances than OI, such as those based on forecast differences at the same forecast time ([Parrish and Derber, 1992; Rabier et al., 1998](#)).

As an extension of 3DVar, four-dimensional variational method (4DVar; [Lewis and Derber, 1985; Courtier and Talagrand, 1990](#)) considers temporal distributions of observations within an assimilation window ([Daley, 1991](#)) and can implicitly account for temporal evolutions of background error covariances ([Thépaut et al., 1993](#)). To efficiently obtain the optimal solution, 4DVar can be expressed in an incremental form ([Courtier et al., 1994; Lorenc, 1997](#)), by which the optimal perturbation relative to a reference state rather than the whole optimal state is solved, and the solving process can be accelerated through the “preconditioning” ([Parrish and Derber, 1992; Derber and Bouttier, 1999](#)). Strong-constrain 4DVar assumes the model being perfect ([Sasaki, 1970](#)), and the perfect-model assumption can be relaxed by model error corrections ([Derber, 1989; Zupanski, 1993](#)) or model error representation using weak constraints ([Bennett, 1992; Egbert et al., 1994; Bennett et al., 1996](#)). When the model is perfect and the background error covariances at the initial time are accurate, the analysis of 4DVar at the end of the assimilation window is equivalent to that of the generalized Kalman filter ([Lorenc, 1986](#)). Since the mid-1990s, 3DVar and 4DVar have become mainstream operational DA methods.

### 2.2 Ensemble Kalman filters

Both OI and 3DVar methods use static background error covariances, but “errors of the day” reveal the importance of flow-dependent background error covariances ([Kalnay et al., 1997](#)). Kalman filter (KF; [Kalman, 1960; Kalman and Bucy, 1961](#)) uses background error covariances that evolve with the numerical model over time, which establishes the mathematical framework for four-dimensional DA. Extended Kalman filter (EKF; [Ghil et al., 1981; Daley, 1995](#)), as an extension of KF to nonlinear models, can provide the best linear unbiased estimate (BLUE) for the state and its error covariances. EKF is considered the “gold standard” of DA, but it requires massive computations due to the update of background error covariances based on linear model matrices.

Ensemble Kalman filter (EnKF; [Evensen, 1994; Houtekamer et al., 1996](#)) uses the Monte Carlo method to estimate the background error covariances based on samples of ensemble forecasts, which can be seen as a simplified EKF. EnKF can approximate the KF’s analysis

solution and is suitable for high-dimensional dynamical systems, while providing ensemble initial conditions for subsequent ensemble forecasts (Houtekamer et al., 2005, 2014). The original EnKF is a stochastic one, by use of perturbed observations for each ensemble member to achieve consistent analysis and associated error covariances (Burgers et al., 1998; Houtekamer and Mitchell, 1998). To avoid sampling errors caused by perturbing observations, deterministic EnKFs have been proposed, such as the ensemble adjustment Kalman filter (EAKF; Anderson, 2001), ensemble square-root filter (EnSRF; Whitaker and Hamill, 2002), and local ensemble transform Kalman filter (LETKF; Bishop et al., 2001; Hunt et al., 2007). Deterministic EnKFs solve for optimal Kalman gains using the analysis error covariances and achieve equivalent solutions without covariance localization (Tippett et al., 2003). As an extension of EnKF, ensemble Kalman smoother (EnKS; Evensen and van Leeuwen, 2000) further assimilates future observations to update the analysis of EnKF based on temporal sample correlations.

EnKF faces the challenges of filter divergence, especially when it is applied to high-dimensional dynamical systems, due to limited ensemble sizes, model errors, and linear correlations. One way to combat the filter divergence is covariance localization (Hamill, 2001; Anderson, 2012), which is typically a function of the distance between observations and model variables (Gaspari and Cohn, 1999). Covariance localization can be implemented through the background error covariance matrix (Houtekamer and Mitchell, 2001; Lei et al., 2018) or the observation error covariance matrix (Hunt et al., 2007). The localization function varies with observation types (Zhang et al., 2009a; Lei and Anderson, 2014b), state variable kinds (Kang et al., 2011; Lei et al., 2015), and assimilation times (Anderson, 2007; Chen and Oliver, 2010). Thus, adaptive localization methods have been developed (Bishop and Hodges, 2009; Lei and Anderson, 2014a; Zhen and Zhang, 2014; Flowerdew, 2015; Lei et al., 2020). Another approach to address the filter divergence is covariance inflation (Anderson and Anderson, 1999; Houtekamer and Mitchell, 2005). It can be implemented by empirically or adaptively multiplying the ensemble perturbations (Anderson, 2009; Miyoshi, 2011; El Gharani, 2018), increasing posterior ensemble perturbations relative to prior ensemble perturbations or prior ensemble spread (Zhang et al., 2004; Whitaker and Hamill, 2012; Ying and Zhang, 2015), or augmenting additive noises (Wang et al., 2013; Yang et al., 2015), particularly accounting for model uncertainties (Buizza et al., 1999; Berner et al., 2009; Ha et al., 2015; Zeng et al.,

2020). Since the early 2000s, EnKF has been operationally used at Environmental Canada and NCEP (Houtekamer and Mitchell, 2005; Whitaker et al., 2008).

### 2.3 Hybrid ensemble-variational methods

The static background error covariance matrix used by the variational methods is full rank, but unable to capture the “errors of the day”. On the other hand, EnKF constructs flow-dependent background error covariance matrix using short-term ensemble forecasts, but the flow-dependent one is often rank-deficient and affected by sampling errors and model errors. Thus, hybrid ensemble-variational methods that combine the advantages of variational methods and EnKFs have been developed. The hybrid ensemble-variational method can directly combine the static and flow-dependent background error covariance matrices (Hamill and Snyder, 2000), to mitigate the impact of rank deficiency and sampling errors in the flow-dependent background error covariances (Wang et al., 2008, 2013; Zhang et al., 2009b; Kleist and Ide, 2015a, b). The static background error covariances can also be incorporated into the EnKF to represent model errors (Meng and Zhang, 2008). Ensemble-4DVar (En4DVar; Lorenc, 2003; Bonavita et al., 2012) embeds the flow-dependent background error covariances into the cost function of the variational method through the alpha control vector, which is equivalent to directly combining the static and flow-dependent background error covariances (Wang et al., 2007). En4DVar outperforms either standalone 4DVar or EnKF (Zhang et al., 2009b; Buehner et al., 2010a, b).

Compared to En4DVar, the 4D ensemble-variational method (4DEnVar; Liu et al., 2008) captures the temporal evolution of error covariances based on ensemble forecasts, eliminating the need for tangent-linear and adjoint models. Similar to 4DEnVar, the dimension-reduced projection 4DVar (DRP-4DVar; Wang et al., 2010; He et al., 2017) and the nonlinear least-squares ensemble 4DVar (NLS-En4DVar; Tian and Feng, 2015; Tian et al., 2018) have been proposed. However, 4DEnVar cannot account for the evolution of static background error covariances within the assimilation window (Wang and Lei, 2014) and struggles to handle time-varying localization (Bishop and Hodges, 2009). Consequently, 4DEnVar is inferior to En4DVar (Lorenc et al., 2015; Poterjoy and Zhang, 2015, 2016).

Unlike the hybridization of static and flow-dependent background error covariances, the hybrid gain approach (Penny, 2014) mixes the analyses from the variational method and EnKF. The hybrid gain approach also outperforms the standalone EnKF and 4DVar with static

background error covariances (Bonavita et al., 2015). Since the early 2010s, the hybrid ensemble 4DVar has been operational at centers such as ECMWF and the Met Office (Bonavita et al., 2012; Clayton et al., 2013). 4DEnVar has later been implemented at operational centers of Canada, the U.S., and so on (Buehner et al., 2015; Caron et al., 2015; Kleist and Ide, 2015b).

Hybrid ensemble-variational methods require a variational system and an EnKF system, but inconsistencies between the two systems could result in suboptimal analyses. The ensemble variational integrated localized method (EVIL; Auligné et al., 2016) constructs the ensemble analyses using the analysis error covariances from the variational solution, to avoid the need for an ensemble framework. The integrated hybrid ensemble-variational method (IHEnKF; Lei et al., 2021) approximates the static background error covariances by a large size of climatological perturbations, and achieves the solutions of hybrid ensemble-variational and hybrid gain methods within a pure ensemble framework. Moreover, IHEnKF can update the ensemble perturbations by the hybrid background error covariances, which leads to superior ensemble analyses than the traditional hybrid ensemble-variational methods.

#### 2.4 Multi-scale and balanced DA

The atmospheric state and its evolution span multiple spatial and temporal scales, and multi-source observations also capture information across different scales. Thus, multiscale DA methods have been proposed to effectively use the multi-source observations to constrain the multiscale atmospheric state. Multiscale DA methods can be iteratively and sequentially implemented. Observations representing large scales (e.g., conventional observations) are first assimilated using a broad localization lengthscale; then small-scale observations (e.g., radar data) are assimilated with a tight localization lengthscale, aiming to effectively extract information from observations at different scales (Zhang et al., 2009a; Xie et al., 2011; Sodhi and Fabry, 2022). Alternatively, all observations can be assimilated using different localization lengthscales, and the final analysis is constructed by combining the analysis increments with various localization lengthscales (Miyoshi and Kondo, 2013). Different from the iterative assimilation methods, multiscale DA can be performed in a single step within the ensemble-variational framework or pure ensemble assimilation framework. Different localization lengthscales are applied to the background error covariances at different scales, and then the multiscale state variables are simultaneously updated by the multi-source observations

across all resolvable scales (Buehner, 2012; Buehner and Shlyaea, 2015; Wang X. G. et al., 2021; Wang and Wang, 2023).

When the numerical models use the analyses produced by DA methods as initial conditions to advance, they face “insertion noises” or “initialization shocks”. Thus, balanced DA is required to minimize the insertion noises caused by unbalanced initial conditions, which could result in spurious gravity waves and adversely affect subsequent forecasts (Temperton and Roch, 1991). It is straightforward for 4DVar to include balance constraints in the cost function. However, intermittent EnKF faces the issue of imbalances, and then continuous EnKF that transforms the intermittent EnKF to a continuous form has been proposed (Bergemann and Reich, 2010; Lei et al., 2012). Moreover, to mitigate the initialization shocks, EnKF can utilize shorter assimilation windows (He et al., 2020; Slivinski et al., 2022), or leverage additional current observations to obtain more accurate past initial conditions (Kalnay and Yang, 2010). There have been general initialization methods, such as the digital filter that eliminates rapid oscillations (Lynch and Huang, 1992), the incremental analysis update that preserves large-scale analysis increments (Bloom et al., 1996), and the four-dimensional incremental analysis update that retains the evolution of both large- and small-scale increments within the assimilation window (Lorenc et al., 2015; Lei and Whitaker, 2016).

### 3. Multi-source atmospheric observations

#### 3.1 Satellite data

Over the past five decades, the role of satellite DA in NWP has grown significantly. Following the launch of the “Nimbus 3” satellite in April 1969, which carried the first temperature detector, the retrieval products from the Satellite Infrared Spectrometer (SIRS) were first “incorporated” into the objective analysis of the U.S. National Meteorological Center and had a significant impact on the analyses in the Pacific region and the forecasts across the U.S. (Smith et al., 1970). Subsequently, a series of international experiments on satellite product assimilation were conducted (Atkins and Jones, 1975; Desmarais et al., 1978; Druyan et al., 1978; Kelly et al., 1978; Gilchrist, 1982; Uppala et al., 1984). However, due to the low vertical resolution of satellite data and relatively large temperature retrieval errors of 2–3 K, the assimilation experiments during this period generally had a neutral impact on forecasts, with a more pronounced effect in the Southern Hemisphere (Ohring, 1979). Eye and Lorenc (1989) pioneered the direct assimilation of the ra-

diative brightness temperature observed by satellites in NWP, successfully integrating the radiative information from the Television Infrared Observation Satellite Program (TIROS) vertical sounding through one-dimensional variational assimilation (Eyre et al., 1993). In October 1995, the NCEP (Derber and Wu, 1998) and in January 1996, the ECMWF (Andersson et al., 1994; McNally and Vesperini, 1996; Saunders et al., 1997) led the way in directly assimilating satellite radiances using 3DVar. ECMWF further advanced this by adopting direct satellite DA in 4DVar in November 1997. Subsequently, other operational centers successively directly assimilated radiances in 3DVar and 4DVar systems (Chouinard et al., 2002; Joo and Lee, 2002; Okamoto et al., 2002; Li J. et al., 2016).

### 3.1.1 Fast radiative transfer model

The fast radiative transfer model quickly maps the atmospheric state variables to the observed quantities, serving as an observation forward operator. It mainly consists of an atmospheric gas absorption module, a particle scattering module, a surface emissivity module, a radiative transfer solution module, and the corresponding tangent linear and adjoint modules. Currently, three fast radiative transfer models are widely used in satellite DA for NWP: the Radiative Transfer for the TIROS Operational Vertical Sounder (RTTOV) model developed by the European Organisation for the Exploitation of Meteorological Satellites (EUMETSAT) (Saunders et al., 2018), the Community Radiative Transfer Model (CRTM) model developed by the NOAA of the U.S. (Johnson et al., 2023), and the Advanced Radiative Transfer Modeling System (ARMS) model developed by the CMA (Weng et al., 2020; Yang et al., 2020). ARMS, a fast radiative transfer model independently developed by China, has replaced RTTOV in CMA-GFS since 2023. Its innovations are mainly reflected in the following aspects. (1) A calculation scheme for atmospheric transmittance coupled with the real spectral response function, effectively enhancing the simulation accuracy of microwave channels (Kan et al., 2024). (2) A scattering database for non-spherical cloud particles and aerosol particles based on the  $T$ -matrix and the Discrete Dipole Approximation (DDA) methods, supporting all-sky satellite DA (Yang et al., 2020). (3) A polarized Bidirectional Reflectance Distribution Function (pBRDF) based on a two-scale ocean roughness model, improving the physical mechanism of the bidirectional reflection at the sea-air interface and enhancing the simulation of the satellite radiative transfer with integrated active and passive sensors (He and Weng, 2023). (4) An improved physical model of microwave land surface emissivity

(LandEM) and the development of the Chen–Weng rough surface reflectivity model, increasing the estimation accuracy of complex surface emissivity (Liu et al., 2024). (5) Refinement of the discrete ordinate radiative transfer theory, overcoming assumptions and dependences on the azimuthal symmetry property in atmospheric scattering and surface reflection process, and developing a general vector radiative transfer solution scheme (VDISORT) for simulating Stokes vector radiation of satellites across the full spectrum range (Zhu et al., 2024).

### 3.1.2 Infrared radiance DA

Due to the spectral limitations and challenges in assimilating radiative quantities in cloud areas (Li et al., 2022a), infrared radiance DA mainly focuses on the direct assimilation of clear-sky radiances or radiances with partial cloud cover. For clear-sky radiances, precise cloud detection is essential. The clear-sky channel cloud detection scheme sorts the channels to determine cloud top height and assimilates channels above the cloud top, improving utilization of the satellite data (McNally and Watts, 2003). For assimilating infrared sounding with partial cloud cover, Li et al. (2005) proposed the “optimal cloud clearing” technique, converting partially cloud-covered infrared sounding into equivalent clear-sky radiative quantities, effectively improving the utilization rate of infrared sounding data in rain and cloud areas and improving tropical cyclones forecasts (Wang P. et al., 2014, 2017). To address challenges in directly assimilating the infrared radiances in rain and cloud areas, Jones et al. (2013) and Chen et al. (2015) successfully assimilated satellite cloud water and cloud ice path products retrieved from visible and near-infrared soundings by using the EnKF and variational methods, respectively. Meng D. M. et al. (2019) introduced hydrometeors into the extended control variables and achieved the hybrid assimilation of infrared retrievals in cloudy areas.

In addition, techniques such as channel correlation processing and principal component analysis have been developed to optimized channel assimilation, addressing the computational costs and spectral-related observational errors of infrared hyperspectral data (Rabier et al., 2002; Collard, 2007; Matricardi and McNally, 2014; Zhou et al., 2024). Typically, about 200 channels per instrument are assimilated, which also avoids spectral regions affected by trace gases like ozone. CMA-GFS currently has the ability to assimilate the infrared hyperspectral data of China’s polar-orbiting and geostationary satellites, such as *FY-3D/E HIRAS* (Liu and Xue, 2014), *FY-4A/B GIIRS* (Yin et al., 2020, 2021; Han et al., 2023), and is also capable of assimilating the infrared hyperspectral

data such as *METOP-B/C IASI* (Li G. et al., 2016) and *NOAA 20 CRIS* in real time. In addition, infrared imager data, including *FY-2 VISSR*, *FY-4A/B AGRI* (Wang et al., 2018), *H8/H9 AHI* and *GOES-18 ABI* data, etc., have also achieved operational application in CMA-GFS.

### 3.1.3 Microwave radiance DA

Among numerous satellite instruments, microwave sounding data can penetrate the cloud and rain, and provide information on the vertical distribution of atmospheric temperature and water vapor over the whole sky and the entire surface, significantly improving the forecasting accuracy (Bormann et al., 2019; Li et al., 2024; Luo et al., 2025). In 2009, ECMWF implemented the world's first operational assimilation system for all-sky satellite data (Bauer et al., 2010). Subsequently, satellite DA techniques in rain and cloud areas were successively applied to the operational models of the Japan Meteorological Agency and NCEP (Okamoto et al., 2014; Zhu et al., 2014). Initially, ECMWF adopted an indirect assimilation strategy of 1D–4DVar for rain and cloud areas. For satellite observations affected by rain and clouds, the temperature and humidity in the background field were used as the first guess values. Through 1DVar, the total water vapor content (TWPC) corresponding to satellite data was retrieved, and then TWPC was taken as a virtual observation and assimilated by 4DVar (Geer et al., 2008). Since 1DVar can retrieve the atmospheric state matching the rain and cloud conditions of satellite observations, it can avoid the mismatch between the background and observations under the cloudy and rainy conditions. Meanwhile, it can also conduct all-sky quality control through 1DVar without the need to adopt a complex cloud detection scheme. However, the TWPC retrieved by this method has already implied the humidity information of the background field, and false observation increments will be generated when it is subsequently brought into 4DVar to update the background (Geer et al., 2010). Therefore, this method was later replaced by the direct all-sky assimilation at ECMWF (Bauer et al., 2010; Geer et al., 2010). CMA-GFS has also successfully carried out the all-sky assimilation of FY satellite microwave imager, significantly improving global water vapor analyses and forecasts (Xie et al., 2023). In the past decade, the most important progress in satellite DA in NWP has been the DA techniques under the influence of clouds and precipitation (Geer et al., 2018).

Microwave radiance assimilation affected by surface conditions has also gained attention. Accurate surface emissivity estimation is crucial, with methods including physical model method, statistical model method, and

dynamic inversion method (Tian et al., 2015). The physical model method aims to establish a numerical model based on the physical relationship between surface emissivity and various surface parameters (such as surface type, vegetation parameters, and soil parameters.). However, its calculation accuracy depends on the accurate estimation of a large amount of input information of surface parameters, which is difficult to obtain, hindering the wide application of this method (Weng et al., 2001). The statistical model method refers to using the historical data set of surface emissivity as the empirical or semi-empirical estimated value of the actual instantaneous emissivity, such as the TELSEM data set (Aires et al., 2011) and the CNRM data set (Karbou et al., 2010). This type of method is easy to use, but the historical statistical data set is difficult to represent the current instantaneous emissivity state and cannot estimate the temporal changes of surface features or spatial changes of surface features at the sub-pixel scale. The dynamic inversion method refers to obtaining the surface emissivity given observed brightness temperature by calculating the upward and downward radiation of the atmosphere, as well as the atmospheric transmittance and surface temperature (Karbou et al., 2006). This method not only has strong usability but also can consider the dynamic changes of emissivity under complex conditions, so it has been widely used in the assimilation of land surface microwave data (Krzeminski et al., 2009; Baordo and Geer, 2016; Xiao et al., 2023b). Based on the dynamic inversion method, the CMA-GFS model has successfully achieved the operational assimilation of the near-surface channels of the AMSU data on land, significantly improving global lower atmosphere analyses and forecasts, particularly in the Northern Hemisphere (Xiao et al., 2023b).

### 3.1.4 From dual-satellite constellation to three-satellite constellation

Joo et al. (2013) found that 64% of the reduction in numerical forecast errors of NWP was contributed by satellite observations, with polar-orbiting meteorological satellites contributing approximately 90% of this reduction. Before 2010, the international polar-orbiting meteorological satellites operated in a dual-satellite constellation (“AM” satellite and “PM” satellite). Recognizing the limitations of the dual-satellite system could not provide complete global coverage within the 6-h assimilation window of the global NWP model, the World Meteorological Organization (WMO) proposed a three-satellite constellation model (“Dawn”, “AM”, and “PM”) in 2009. In 2014, the CMA clearly stated the plan to launch the “Dawn” satellite in the feasibility study report for the

third batch of FY-3 satellites. In 2021, *FY-3E* was successfully launched, and the Chinese researchers realized that the observation system of the three-satellite constellation could effectively make up the observation gap of polar-orbiting satellites within the 6-h assimilation window (Zhang et al., 2022). The observation data of *FY-3E* have been applied not only in China's NWP operational system (Li et al., 2024), but also in the operational models of many organizations such as the ECMWF, the Met Office, the Japan Meteorological Agency (JMA), and the Korea Meteorological Administration (KMA), ensuring global observation needs for NWP (Zhang et al., 2024).

### 3.2 Radar data

Radar data has high temporal and spatial resolutions, allowing it to capture fine information for convective-scale weather systems. Proper utilization of radar data can significantly improve the dynamical and microphysical characteristics of convective weather systems in the initial conditions. Thus, the effective assimilation of radar observations is one of the key factors in improving convective-scale NWP (Wan et al., 2005; Sun et al., 2014; Sun et al., 2020b).

#### 3.2.1 Radar observation operators

Traditional Doppler weather radar detects variables mainly including the radial wind and reflectivity. Radial wind represents important dynamical features of the internal structure of convective-scale weather systems, while reflectivity contains microphysical information about these systems. Radar radial wind has been widely used in various DA systems, including the VDRAS 4DVar system (Sun and Crook, 1997), ARPS 3DVar system (Gao et al., 1999), WRFDA system (Xiao et al., 2005), and GRAPES 3DVar system (Liu et al., 2010). But conventional radial wind observation forward operators only introduce information of radial wind, and could be insufficient to analyze tangential wind. Based on the assumption of a uniform wind field within the regional azimuth, Luo et al. (2014) incorporated radar radial wind speed and its spatial variations into the radial wind forward operator, enabling the analysis of tangential wind information during radial wind assimilation. This radial wind forward operator was introduced into both the GSI (Chen et al., 2017) and GRAPES (Ma et al., 2016) assimilation systems.

Compared to radial wind forward operators, reflectivity observation forward operators are more complex. Early studies established reflectivity forward operators based on the empirical relationship between reflectivity and rainfall (Sun and Crook, 1998; Xiao and Sun, 2007). Tong and Xue (2005) and Gao and Stensrud (2012) fur-

ther incorporated ice-phase particles such as snow and hail, developing reflectivity forward operators based on the Lin microphysical parameterization scheme, and implemented direct assimilation of reflectivity within the EnKF and variational frameworks. Similarly, Hawkness-Smith and Simonin (2021) constructed reflectivity forward operators to achieve direct assimilation of reflectivity within the Met Office assimilation system. Liu et al. (2022) introduced raindrop number concentration based on the Thompson microphysics scheme, developing a reflectivity forward operator for 2-moment hydrometeors. However, reflectivity observation forward operators remain somewhat empirical, and the associated errors are relatively large.

Jung et al. (2008b) estimated the backscatter cross-section parameters of various precipitation particles using the *T*-matrix algorithm, developing a more accurate forward reflectivity forward operator and achieving successfully assimilated reflectivity in an EnKF. Following Jung et al. (2008a), Wang and Liu (2019) developed the tangent linear and adjoint operators to perform direct reflectivity assimilation within a variational framework. Zeng et al. (2013; 2014) and Jerger (2013) incorporated different physical aspects into the reflectivity forward operator, developing a three-dimensional reflectivity forward operator. Wang and Liu (2019) further developed a forward reflectivity observation operator for ice-phase particles based on Jung et al. (2008a), parameterizing reflectivity as a rapid polynomial relationship for the mixed ratio. These more complex and accurate reflectivity forward operators significantly reduce the errors from forward operators, leading to better assimilation of radar reflectivity.

In addition, many studies have focused on developing radar observation forward operators. Jung et al. (2008a) implemented a polarization radar data simulator, which uses spherical particles to represent hydrometeors and calculates spectral properties with either online Rayleigh approximations or offline lookup tables (Mishchenko et al., 1994). This polarization radar data simulator has been applied to low-frequency S-band, C-band, and X-band radar. Wolfensberger and Berne (2018) developed a cross-platform polarimetric radar observation forward operator, which includes hail particle radar simulations and represents all hydrometeor particles as uniform spherical bodies. Oue et al. (2020) developed a cloud-resolving model radar simulator that can simulate both polarimetric radar and lidar observations, though it is currently limited to ground platforms and does not explicitly handle melting particles. Zhejiang University (ZJU-AERO, Xie et al., 2024) designed an accurate and effi-

cient radar observation forward operator that incorporates scattering calculations for hydrometeors and constructs an optical property database, allowing it to handle non-spherical and inhomogeneous hydrometeor particles in the atmosphere.

### 3.2.2 Conventional radar DA

Radial wind observations contain important dynamical features of convective-scale weather systems and provide crucial tools for monitoring and studying convective-scale weather systems (Xu, 2003; Liang, 2007; Yang et al., 2008). Assimilation of radar radial wind is relatively mature and can significantly improve analyses and forecasts of convective-weather systems (Gao et al., 2004; Li et al., 2012; Zhu et al., 2013; Chen et al., 2014; Shao et al., 2016; Chen et al., 2019; Mu et al., 2019; Chen et al., 2025).

Comparing to assimilation of radial winds, the assimilation of reflectivity is more complex. Current methods of radar reflectivity assimilation are generally divided into two categories: direct and indirect assimilation. Direct assimilation projects model state variables into the observation space, directly comparing the background with the observed reflectivity. The innovation and associated uncertainties are used for assimilation and lead to the analysis. Direct assimilation of radar reflectivity has been applied effectively (Sun and Crook, 1997; Tong and Xue, 2005; Sheng et al., 2006).

However, direct assimilation of radar reflectivity using variational methods also faces challenges. When the background hydrometeor content is low, the gradient of the observation term in the cost function can be large, which often prevents effective convergence of the minimization. The nonlinear reflectivity forward operator is difficult to construct, often resulting in unrealistic hydrometeor analyses (Wang et al., 2013a, b; Liu C. S. et al., 2019). Incremental variational assimilation improves the nonlinearity of the reflectivity forward operator through multiple outer loops, but with increased computational cost. Compared to variational methods, EnKFs can use nonlinear forward operators of radar reflectivity (Lan et al., 2010a, b; Yussouf and Stensrud, 2010), thereby effectively use reflectivity observations with complex microphysical processes. However, nonlinear forward operators do not satisfy the assumption of Gaussian error distributions of EnKFs, and thus, suboptimal solutions are obtained, especially for dense and strongly nonlinear reflectivity observations. Moreover, the EnKF is also affected by sampling errors and model errors (Liu et al., 2020).

Background error covariances play a crucial role in convective-scale DA, and appropriate background error

covariances can lead to more coherent analyses (Chen et al., 2013, 2022; Zheng et al., 2023). Wang and Wang (2021) developed static background error covariances including hydrometeor control variables, which are incorporated into a hybrid ensemble-variational framework, leading to improved supercell predictions than ensemble-based background error covariances. Furthermore, assimilating radar reflectivity with hydrometeor-included background error covariances can significantly improve thermodynamic conditions and heavy rainfall forecasts, due to the vertical and multivariable correlations (Zheng et al., 2023).

To avoid linearization errors caused by the nonlinear reflectivity forward operator during direct assimilation, many studies and operational systems often use indirect assimilation for radar reflectivity. In indirect assimilation, the radar reflectivity is first inverted into model variables during the assimilation process, where the type and proportion of hydrometeors are determined using the prior temperature, and then these inverted model variables are assimilated (Wang et al., 2013a). Some studies have proposed a new background-dependent hydrometeor inversion method, which updates the type and proportion of hydrometeors in real time based on the background characteristics. This improves reflectivity assimilation and enhances weather forecasts (Chen et al., 2020, 2021; Huang J. et al., 2022). The indirect assimilation method avoids constructing tangent linear and adjoint operators for reflectivity observation operators, improving the mathematical conditions for solving the cost function, while having relatively lower computational costs compared to direct assimilation. As a result, it is widely used in various studies and operational systems (Fan et al., 2013; Lai et al., 2020; Zhang L. et al., 2019).

### 3.2.3 Dual-polarization radar data assimilation

In recent years, several countries, including China, have started upgrading their dual-polarization radar networks (Wu et al., 2018). Dual-polarization radar can improve the identification the phase state characteristics of hydrometeors, and the effective use of dual-polarization radar data can improve microphysical initial conditions, such as hydrometeor content (Zhao et al., 2019). Assimilation of dual-polarization radar observations has made progress. Chinese researchers have developed dual-polarization observation forward operators based on single- and double-moment microphysical schemes and directly assimilated simulated dual-polarization radar observations using EnKFs (Jung et al., 2008a, b; Xue et al., 2010). Further, Putnam et al. (2019) used an EnKF to assimilate real dual-polarization radar observations, leading to improved analyses and forecasts of polarimetric

quantities, although their assimilation was limited to horizontal reflectivity factor and differential reflectivity below 2 km.

The EnKF is constrained by the limited size of the ensemble, which complicates the accurate estimation of background error covariances due to rank deficiencies. Additionally, it encounters challenges related to imbalances in analyses and model errors. Consequently, research on dual-polarization radar assimilation based on variational methods has also been carried out. Li et al. (2017) conducted case studies of single-station dual-polarization radar DA using variational methods, and their results showed that additional assimilation of differential reflectivity and specific differential phase could further improve reflectivity analyses and forecasts. Variational methods require the construction of tangent linear and adjoint operators for dual-polarization observations. To establish more reasonable tangent linear and adjoint operators, Kawabata et al. (2018) constructed the tangent linear and adjoint operators for dual-polarization observations based on liquid-phase particles, and Wang et al. (2019) developed the tangent linear and adjoint operators for horizontal/vertical reflectivity, including ice-phase particles.

### 3.3 Other types of observations

The radio occultation technique is regarded as one of the most promising means in current atmospheric detection. It can provide information on the neutral atmosphere and ionosphere with global distribution over the whole sky. In particular, the “Constellation Observing System for Meteorology, Ionosphere, and Climate (COSMIC)” implemented in 2006 created conditions for the operational application of occultation DA. For the assimilation of occultation data, the most suitable assimilation quantities are the bending angle and refractivity and there are two kinds of forward operator, namely one-dimensional or two-dimensional. Currently, nearly all the advanced global operational centers have assimilated occultation data, indicating the importance of occultation data for NWP (Healy et al., 2005; Poli et al., 2009; Liu and Xue, 2014). The CMA-GFS model started to operationally assimilate occultation data in 2009. The assimilated quantity is the refractivity with height ranging from 1 to 50 km. The CMA-GFS achieved a relatively earlier assimilation of *FY-3D* GNOS occultation refractivity (Wang et al., 2020). Occultation data have always played an important role in the numerical prediction system of CMA, with the contribution to the 24-h forecast error always ranked among the top three in CMA-GFS.

Atmospheric motion vectors (AMV) are one of the

satellite data that were among the earliest usage in DA. Even with a large amount of satellite data assimilated by the DA system, the role of AMV in improving NWP remains non-negligible (Forsythe et al., 2007). In the past decade, satellite wind retrieval algorithms have achieved remarkable progress in aspects such as the selection of tracer representative pixels and height assignment (Xu, 2020). In particular, due to the improvements of the selection of motion representative pixels and the estimation of translucent cloud height for *FY* satellite cloud motion winds (Zhang et al., 2017a, b), the cloud motion wind data of *FY-2E* had reached the level of similar international products as early as 2011 (Salonen and Bornmann, 2015). Compared to other observation means, the errors of AMV are still relatively large. In particular, the error in specifying the height of clouds makes the height of the atmospheric motion represented by AMV highly uncertain. The thousands of channels in the vertical of the *FY-4A* GIIRS have brought new opportunities for the height assignment of the three-dimensional wind field. Studies have shown that the three-dimensional horizontal wind field can be effectively retrieved in clear-sky and partially cloudy areas (Ma et al., 2021; Li et al., 2022b), and reasonable assimilation of three-dimensional dynamic information has a positive effect on the track and intensity forecasts of typhoons (Meng et al., 2024).

A scatterometer is a spaceborne radar that measures the backscatter of the sea surface from multiple directions, from which the wind direction and wind speed of the sea surface can be derived (Stoffelen and Anderson, 1997). Satellites measure a set of backscatter values in different directions for the same sea surface area, but these can correspond to multiple different wind directions, thus bringing new problems to DA. Currently, when assimilating the scatterometer data, one wind direction closest to the background is generally selected from several possible wind directions. There are also cases where the wind speeds of multiple different wind directions are assimilated simultaneously, allowing the assimilation system to provide adaptive weights. In 2022, the assimilation of the scatterometer wind data of China’s *HY-2B* satellite was achieved in the CMA-GFS 4DVar, significantly improving the analyses in the lower troposphere over the ocean surface (Wang et al., 2023).

In 2018, the European Space Agency (ESA) successfully launched the world’s first spaceborne wind lidar satellite, i.e., *ADM-Aeolus*. It can provide high spatial and temporal resolutions and near-real-time global radial wind speed information with vertical resolutions ranging from 0.25 to 2 km from the ground to 30 km. In 2022, the operational application of Aeolus data was achieved

for the first time in CMA-GFS. The assimilation of Aeolus data can significantly reduce the wind analysis errors in the tropics and the Southern Hemisphere. In the tropics, the reduction in the average error (compared with ERA5) can reach 10%. The forecast improvements for the first three days in the Northern Hemisphere, Southern Hemisphere, and tropics are relatively significant, and the prediction contribution in the East Asian region is neutral.

Additionally, China's ground-based automatic weather station network has developed since 2008, reaching approximately 70,000 stations by 2023. High spatiotemporal resolution ground-based observations have become one of the key observation types of CMA-MESO. However, due to China's complex terrain, including the "Roof of the World" with an average elevation above 4000 m, plateaus such as the Yunnan–Guizhou Plateau, the Loess Plateau, and the Sichuan Basin with average elevations between 1000 and 2000 m, as well as hills and plains below 1000 m, there are significant height differences between the relatively smooth model terrain and the actual terrain of observation stations. Studies by Xu et al. (2006, 2007, 2009) have shown that failing to effectively resolve the height differences between the model and stations can negatively impact the assimilation of surface data. Therefore, Xu et al. (2021, 2023) developed DA schemes for 2-m relative humidity and temperature observations in complex terrain within the CMA-MESO 3DVar. These schemes improved both the quantity and quality of assimilated surface data and enhanced forecasts of surface state variables. Moreover, a DA scheme for the surface pressure based on the hydrostatic equation was implemented to replace the surface pressure extrapolation assimilation scheme by Lian and Xue (2010). This new approach not only increased the utilization of surface observations but also resolved the issue of deteriorating precipitation forecasts with increased number of ground observations.

#### 4. The target observation strategies

Large uncertainties often occur in high-impact weather forecasts, such as heavy rainfalls, typhoons. Not enough data with either quantity or quality is an important obstacle that limits the forecast skill for high-impact weather events. Hence, Snyder (1996) proposed the concept of target observation strategy, which adds a few observations with high quality in sensitive areas to improve the forecasts in concern. Extensive researches have demonstrated that additional observations in sensitive areas are greatly helpful for accurate forecasts of high-

impact weather events such as typhoons (Anderson, 2010). For example, the Observing System Research and Predictability Experiment (THORPEX) displayed the importance of target observations in improving the track forecasts of typhoons (Shapiro and Thorpe, 2004). In recent years, China has made significant advancements in the research and application of targeted observations for forecasting high-impact weather events. (Duan et al., 2023).

##### 4.1 Concept of target observations

THORPEX, under the auspices of WMO, is a world weather research programme accelerating improvements in the accuracy of one-day to two-week high-impact weather forecasts for the benefit of society, economy, and environment. As an important part of THORPEX, target observations were highly promoted and refer to the augmentation of the regular observing networks with additional observations in some sensitive but data-sparse areas, aiming to reduce the initial condition errors and improve the subsequent forecasts.

The field campaigns of target observations have advanced rapidly under THORPEX. The Atlantic-THORPEX Regional Campaign (A-TReC) started during the autumn of 2003 for the Northern Hemisphere. A large quantity of in-situ and remotely sensed observations was collected, targeted at 1- to 3-day forecasts of potential high-impact weather events over Europe (Rabier et al., 2008). The African Monsoon Multidisciplinary Analysis campaign, utilizing the rawinsonde and driftsonde balloons, was aimed at improving short-range forecasts of western African rainfall and easterly waves that may lead to tropical cyclogenesis (Agustí-Panareda et al., 2010). Several campaigns over Europe, aimed partially at improving short-range forecasts of specific high-impact weather events such as winter flow distortion past Greenland, summer rainfall in Central Europe, or autumn heavy precipitation events in the Mediterranean region have taken place between 2007 and 2009 (Wulfmeyer et al., 2008; Prates et al., 2009; Jansa et al., 2011). The THORPEX Pacific Asian Regional Campaign (T-PARC) possessed a broader scope than aforementioned experiments and focused on the large northern Pacific basin. The summer phase in 2008 was aimed at investigating a wide variety of issues related to the science and predictability of the life cycle of typhoons from formation through recurvature and extratropical transition, including the impact on the flow far downstream in the mid-latitude storm track (Elsberry and Harr, 2008). In the winter phase, the primary purpose was to investigate the potential for targeted aircraft and rawinsonde obser-

vations to improve forecasts of weather systems over North America beyond the 1- to 3-day ranges. In order to improve forecasts over Scandinavia and the use of data from polar-orbiting satellites over the Antarctic, field campaigns of target observations also covered the polar areas (IPY; Irvine et al., 2011).

#### 4.2 Target observation strategies

The target observation strategy requires additional observations in some key sensitive areas to reduce the initial condition errors and further improve the forecast skills of high-impact weather events. The methods to identify the sensitive areas can be classified into two types: one based on the analysis sensitivity and the other based on the observation sensitivity.

Analysis sensitivity captures the dependence of forecast uncertainty on initial perturbations at different sites. The higher the sensitivity, the larger forecast errors are induced by the initial errors at these sites. Hence, these sites are identified as the sensitive areas for target observations. The typical analysis sensitivity methods include the adjoint sensitivity (Bergot, 1999; Wu et al., 2007), singular vectors (SVs; Palmer et al., 1998), ensemble transform technique (Bishop and Toth, 1999), etc. The former two methods have been widely utilized in the field campaigns of target observations as T-PARC and IPY.

Observation sensitivity introduces observations and DA techniques, which identifies the sensitive areas by evaluating the reduction of the forecast errors led by the simulated observations at different sites. The sites where the observations can bring the maximum reduction of forecast errors are identified as the sensitive areas. The typical observation sensitivity methods include the Hessian SVs (Barkmeijer et al., 1998) and ensemble transform Kalman filter (ETKF; Bishop et al., 2001). The latter has been utilized in many field campaigns as ATReC, T-PARC, and IPY. Results from the T-PARC summer phase showed improved track forecasts of two long-lived typhoons, with 20%–40% error reduction in numerical models of NCEP and KMA, while little track forecast improvements in the models of ECMWF and JMA with forecast lead times longer than 72 h (Weissmann et al., 2011).

All the methods mentioned above utilize linear approximation to some degrees; however, the atmospheric state and its evolutions are characterized by nonlinear nature. Mu et al. (2009) proposed to identify the sensitive areas of target observations according to the structures and locations of initial perturbations through the CNOP method (Mu et al., 2003). Plenty of observation system simulated experiments demonstrated that assimil-

ating observations in the sensitive areas identified by the CNOP method can improve the track forecasts of typhoons, which is more prominent than that by traditional SVs (Qin and Mu, 2012; Chen et al., 2013; Feng et al., 2022; Chan et al., 2023; Qin et al., 2023). In recent years, the CNOP method has also been used in theoretical research and field campaigns of offshore ocean environment forecasts, which greatly improved the ocean forecast skills (Liu et al., 2021). As an effective method to identify the sensitive areas of target observations for both atmosphere and ocean (Mu et al., 2017; Duan et al., 2018; Jiang et al., 2022, 2024; Yang et al., 2022, 2023), the CNOP method is expected to be further applied in real-time operational forecasts and improve the NWP forecasts (Fig. 2).

#### 4.3 Practices and experiences in China

The national Landfalling Tropical Cyclone Research Project (LTCRP) in China was conceived and funded in 2009. The main objectives of the project are to investigate the characteristics of structure and intensity changes during TC landfall and associated physical mechanisms, and then to develop new technology to advance the forecast skills for landfalling TCs (Duan et al., 2019). The China's LTCRP has been ongoing for about 10 years from 2008 to 2018 and includes three main components: field campaigns, scientific research, and technical developments. Field campaigns for 24 TCs under the national LTCRP have obtained a large amount of observations, which helps understanding the boundary structure of TCs (Zhang et al., 2011, 2015; Ming et al., 2014; Bi et al., 2015; Tang et al., 2015; Zhao et al., 2015; Wang et al., 2016, 2018; Zhao et al., 2017; Ming and Zhang, 2018; Wen et al., 2018; Wu et al., 2018) and promotes the developments of new DA technique, nowcast system, and assessment system (Cha and Wang, 2013; Wen et al., 2017; Li et al., 2018; Liu et al., 2018; Lu et al., 2018; Chen et al., 2019; Bao et al., 2023).

The operational GRAPES model achieved identifying sensitive areas using the SVs in 2013 (Liu et al., 2013; Li and Liu, 2019) and started to conduct field campaigns of target observations for TC forecasts. The forecasts in GRAPES-SVs usually concern a wide area ( $10^{\circ}$ – $35^{\circ}$ N,  $105^{\circ}$ – $125^{\circ}$ E) of southern China and near sea (Liu C. S., et al., 2019; Zhang et al., 2019). A few years later, several operational and scientific research departments have started cooperation in 2020 to utilize the CNOP method to identify the sensitive areas of target observations for TCs (Duan and Qin, 2022; Duan et al., 2023). Field campaigns were conducted for TCs Higos (2020), Maysak (2020), Chanhom (2020), Conson (2021), Chanthu (2021), and Mulan (2022), and the forecasts have been

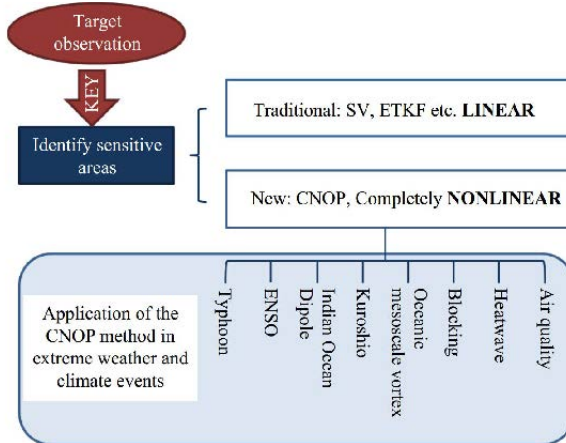


**Fig. 2.** The CNOP method and its application in forecasts of extreme weather and climate events.

improved (Feng et al., 2022; Chan et al., 2023; Qin et al., 2023).

Field campaigns of target observations for TCs have been going on after the China's LTCRP. The Hong Kong Observatory has conducted field campaigns for the TCs over South China Sea using dropsondes since 2006 (Chan et al., 2018). In 2020, Meteorological Observation Centre of CMA organized a field campaign for TC Sinlaku (2020) using an unmanned aerial vehicle. The collected data help understand the formation and effect of helical roll in the TC boundary layer (Chen et al., 2021; Tang et al., 2021) and improve the forecast skills of TC track and intensity. Taking the TC Atsani (2020) for example, assimilating several dropsonde data in the sensitive areas identified by the CNOP method has obtained comparable track forecasts as assimilating all available dropsonde data.

The successful launched *FY-4A* in December 2006 supplements a new and powerful observing technique for field campaigns of target observations (Han et al., 2023). In 2018–2021, *FY-4A* conducted nine field campaigns of target observations, of which eight were aimed at TCs (Lei et al., 2019; Meng Z. Y. et al., 2019; Han et al., 2025). Taking the TC Maria (2018) for example, *FY-4A* scanned it at every 15 m. Such high frequent data help profile the atmospheric structure around the TC (Yin et al., 2021). Feng et al. (2022) showed that the data obtained by *FY-4A* improved the TC track forecasts with lead time longer than 2.5 day, especially with a 50% reduction of track forecast errors in 3- to 3.5-day forecasts. In particular, assimilation of the *FY-4A* data corrected the wrong landfall forecast of TC Chanthu in Taiwan Island.

*FY-4B* was successfully launched in June 2021 and rapidly conducted target observations three times from 2021 to 2023, including two for TCs. In 2022, assimilat-

ing the *FY-4B* data improved forecast skills for TC Mulan (2022) in track, intensity, and precipitation (Chan et al., 2023). Without the *FY-4B* target observations, TC Mulan (2022) was forecasted to make landfall in Leizhou Peninsula. However, TC Mulan was forecasted to move westward and then turn northward with the *FY-4B* target observations assimilated, which is much closer to the fact.

In summary, China has made breakthrough in target observations for TCs, promoted interactions between forecasts and observations, fulfilled a combination of nonlinear method in identifying sensitive areas and field campaigns of target observations. All these achievements have provided theories and techniques for field campaigns of target observations for TCs and other high-impact weather event forecasts.

## 5. China's operational DA systems for NWP

### 5.1 Development of operational DA systems for NWP

DA systems built on theoretical and methodological foundations are a critical component of operational NWP systems. Operational DA systems typically include real-time observation acquisition modules, observation pre-processing modules, and assimilation modules, along with the core methods of observation quality control and DA. Since the 1980s, as China's operational NWP systems have advanced, the DA systems have evolved from simple to complex, from primarily imported systems to independently developed ones (Fig. 3).

China's earliest operational NWP models were the three-layer primitive equation model (Model A), starting in July 1980, and the five-layer Northern Hemisphere primitive equation model (Model B), operational since February 1982. At that time, assimilation, also called objective analysis, employed the relatively simple SCM method, primarily assimilating conventional observations (Wang et al., 1984).

From the late 1980s, the National Meteorological Centre of China (NMC) gradually established and developed the limited area forecast system model (LAFS), operational in 1991, and the high-resolution LAFS model (HLAFS), operational in May 1996, and meanwhile regional DA was also achieved. The assimilation scheme was an improved version of OI from the U.S. National Meteorological Center, performing 3D multivariate analysis for height and wind fields and univariate analysis for relative humidity, along with nonlinear normal mode initialization (Xue et al., 1992), to assimilate conventional and non-conventional observations, including the satellite-derived moisture, temperature profiles, and cloud-

tracked winds (Guo et al., 1995). During the “Ninth Five-year Plan” period, the NMC adopted the Mesoscale Model 5 (MM5) from the NCAR and updated the SCM method to a dynamical relaxation method for assimilating conventional observations (Jiao, 2010).

Later on, CMA imported the ECMWF spectral model to establish a global medium-range NWP operational system, which included the T42L9 system (operational in June 1991), the T63L16 system (operational on the domestically developed Galaxy-II supercomputer in October 1993), the T106L19 system (operational on CRAY C92 in July 1997), and the T213L31 system (operational in September 2002) (Jiao, 2010). In these T-series global medium-range forecasting systems, a global DA system based on OI was established, with nonlinear normal mode initialization to ensure more coherent alignment between the analyses and forecasts. Assimilated observations included the weather reports received via domestic communication lines and GTS (Li and Qiu, 1992; Li, 1994). The T639L60 system, operational right before the 2009 flood season, introduced NCEP’s GSI variational assimilation system, marking a transition from OI to 3DVar, with the ability of assimilating microwave sounding data from polar-orbiting satellites (Guan et al., 2008).

By the late 20th and early 21st centuries, CMA shifted its strategy from importing systems to independently developing its own systems. This decision led to the development of the first-generation multiscale and unified DA and NWP system—GRAPES (Xue and Chen, 2008; Shen et al., 2020). In July 2006, the GRAPES regional model system (GRAPES-MESO V2.0) with a 30-km horizontal resolution became operational, featuring a regional isobaric 3DVar assimilating conventional observations, with twice-daily cold starts. Before the 2008 flood season, GRAPES-MESO was upgraded to V2.5 with a

15-km resolution and isobaric 3DVar system. In 2010, the GRAPES-RAFS (Rapid Analysis and Forecast System) began quasi-operational use, offering 3-h cycles of analyses and forecasts (Xu et al., 2013). In July 2014, GRAPES-MESO V4.0 was launched with a 10-km resolution, a new cloud analysis module, and the capability to assimilate GPS/PW, FY-2E cloud drift winds, and GNSS/RO data (Huang et al., 2017; Shen et al., 2020). In June 2020, CMA-MESO V5.0 became operational, upgrading the DA system to a 3DVar with 3-km resolution and 3-h cycles of analyses and forecasts (Huang J. et al., 2022).

The first formal version of the GRAPES global model, GRAPES-GFS V1.0, began quasi-operational use in 2009, with initial conditions provided by a global isobaric 3DVar system. In 2016, GRAPES-GFS V2.0 with a 25-km horizontal resolution became operational, upgrading to a model-level 3DVar to reduce errors introduced by spatial interpolation and variable transformation along with improved background error covariances (Wang J. C. et al., 2014). DA for the satellite and occultation data were also enhanced (Wang et al., 2015, 2016; Han and Bormman, 2016). GRAPES-GFS V2.2, operational in July 2018, upgraded the assimilation system from 3DVar to 4DVar (Zhang et al., 2019). This marked China’s entry into the international forefront of operational 4DVar systems, making CMA one of the few operational centers with self-developed and operational 4DVar systems (Shen et al., 2020). In 2021, GRAPES-GFS and GRAPES-MESO were renamed CMA-GFS and CMA-MESO. In May 2023, CMA-GFS V4.0 became operational, increasing the global 4DVar system’s resolution from 25 to 12.5 km and replacing the RTTOV radiative transfer model with the domestic ARMS model, a significant step toward independent control of core technologies in operational DA systems. According to the WMO



Fig. 3. Journey of the independently developed NWP operational DA systems at CMA.

model verification standards, forecast improvements can be measured by the historical evolution of the 500-hPa geopotential height anomaly correlation coefficient (ACC) in the Northern and Southern Hemispheres (Fig. 1). For the Northern Hemisphere, the 5-day ACC at 500 hPa improved from 0.695 in September 2010 to 0.768 in September 2015, and further reached 0.846 in September 2023.

In June 2024, CMA-MESO V6.0 with nationwide 1-km resolution passed the operational evaluation and began real-time parallel operational trials, upgrading the 3DVar system with 1-km horizontal resolution and 1-h cycle of analyses and forecasts. Meanwhile, CMA-GFS V4.2 upgraded its global 4DVar system to a global En4DVar system, with a year-long retrospective test showing systematically better analyses and forecasts than the global 4DVar operational system. Now the global En4DVar has been operationally implemented since 31 December 2024.

## 5.2 Global 4DVar operational system

4DVar is an extension of 3DVar in the time dimension, and thus 3DVar framework is the foundation for the 4DVar framework. The CMA-GFS global 3DVar and 4DVar systems use stream function, unbalanced velocity potential, unbalanced nondimensional pressure, and specific humidity as the analysis variables. The balanced components of velocity potential and nondimensional pressure are calculated using a combination of dynamical and statistical methods. Since the analysis variables are independent, the corresponding background error covariance matrix is diagonal. A second-order autoregressive correlation function is used for the horizontal correlation of univariate variable, computed via spectral filtering, while the lengthscales of horizontal and vertical correlations are statistically derived from ensemble samples.

Additionally, the CMA-GFS global 3DVar and 4DVar systems employ an incremental scheme. In this incremental scheme, the high-resolution forecast model is integrated to calculate the observation increments, while low-resolution tangent linear and adjoint models are used for the minimization process, significantly reducing the computational cost and improving the efficiency of functional minimization.

The global tangent linear model and adjoint model are the core components of the global 4DVar system. The CMA-GFS global tangent linear and adjoint models are the first non-hydrostatic ones applied in an operational 4DVar system internationally. Moreover, the computational time for the dynamical frameworks of the tangent linear and adjoint models is only about three times that of

the dynamical framework of the global forecast model, demonstrating outstanding computational performance. The tangent linear and adjoint models also incorporate comprehensively linearized physical processes, including vertical diffusion, subgrid-scale topography parameterization, large-scale condensation, and convective parameterization (Gong et al., 2019; Liu Y. Z. et al., 2019).

The CMA-GFS global 4DVar operational system developed preconditioned Lanczos-CG and L-BFGS algorithms. By default, the Lanczos-CG algorithm is used for its faster convergence and smoother process. However, the L-BFGS algorithm has better fault tolerance, and the system automatically switches to L-BFGS when the Lanczos-CG algorithm fails to converge.

The basic configuration of the CMA-GFS global 4DVar operational system (Version 4.0) includes a horizontal resolution of 0.125°/0.75° (outer loop/inner loop), 87 vertical layers, model integration time step of 300/900 s (outer loop/inner loop), a 6-h assimilation window, observation profiling interval of 30 m, and a maximum of 50 iterations for minimization. To balance the tradeoff between the quality of analyses and forecasts and timeliness, the CMA-GFS global 4DVar operational system runs one analysis–forecast cycling system and one analysis–forecast system. The CMA-GFS global 4DVar operational system is performed four times daily, producing model initial conditions for standard time points that are then used for subsequent 10-day forecasts.

The CMA-GFS global assimilation system has developed critical technologies for satellite DA, including quality control, cloud detection, and bias correction. It has also established a domestically developed fast radiative transfer model ARMS replacing the previously used RTTOV. CMA-GFS global 4DVar has successively incorporated satellite data from FY polar-orbiting microwave temperature and humidity sounders (Xiao et al., 2023a, b), microwave imagers (Xiao et al., 2020), occultation data (Wang et al., 2020), FY geostationary infrared hyperspectral (Yin et al., 2020, 2021; Han et al., 2023), infrared imagers (Wang and Han, 2018), HY-2B microwave imager SMR (Li and Han, 2024), scatterometer ocean winds (Wang et al., 2023), etc. Currently, the CMA-GFS global 4DVar operational system assimilates observations including radiosonde, surface, aircraft reports, cloud drift winds, occultation data, scatterometer winds, GPS precipitable water, GNSS reflectometry winds, NOAA, METOP, FY-3 microwave temperature and humidity sounders, infrared hyperspectral data, GCOM microwave imagers, and FY-2 imagers. Satellite observations account for approximately 80% of all observations, playing a critical role in global DA.

### 5.3 The regional 3DVar operational system

The regional numerical forecasting system implemented in CMA is CMA-MESO (formerly GRAPES-MESO), which is mainly used to improve the prediction of hazardous weather and lower tropospheric phenomena. In order to rapidly update the model trajectories, CMA-MESO uses a 3DVar assimilation system and a cloud analysis system to assimilate spatiotemporally dense observations. In June 2020, the CMA-MESO v5.0 system with 3-km horizontal resolution and 3-h update was operationally implemented (Shen et al., 2020; Huang L. P. et al., 2022). Since October 2024, the CMA-MESO v6.0 system with 1-km horizontal resolution and 1-h update has been operationally implemented.

The CMA-MESO kilometer-scale 3DVar is based on the GRAPES unified variational data assimilation framework, and has been further developed for convective-scale weather systems. In terms of the analysis framework, new minimization control variables are constructed based on the dynamical characteristics of the convective-scale system, and a simplified weak constraint of the continuum equation is introduced to get better balanced small- and medium-scale analyses (Wang et al., 2024). Meanwhile, multiscale analysis schemes are also developed to capture the large-scale patterns, which include a horizontal correlation model using multiple Gaussian scale superposition, a weak constrain with large-scale information, and a blending scheme that merges small- and medium-scale information to the global large-scale information (Zhuang et al., 2020; Wang R. C. et al., 2021). The kilometer-scale 3DVar mainly updates wind, temperature, pressure, and humidity variables, while the cloud fields are diagnostically updated by the cloud analysis system and introduced into the model trajectory by nudging (Zhu et al., 2017). Based on the operational 3DVar system, a prototype En3DVar system has also been developed to obtain flow-dependent analyses. In addition, cloud control variables have also been added into the En3DVar framework to provide a basis for direct assimilation of radar reflectivity.

In terms of the application of observations, CMA-MESO kilometer-scale 3DVar takes full advantages of shared observation operators of the unified variational framework and achieves the direct assimilation of conventional and satellite observations. On this basis, the CMA-MESO system further develops assimilation algorithms for spatiotemporally dense observations. For radar data, radial wind and wind profile radar data are directly assimilated in the kilometer-scale 3DVar, and reflectivity data is assimilated in the cloud analysis system.

The observations of China's new generation of geostationary satellites, *FY-4A* and *FY-4B*, can be directly assimilated in the kilometer-scale 3DVar, while the FY-2G brightness temperature and total cloud cover data are assimilated in the cloud analysis system. For automatic surface observations, kilometer-scale 3DVar can assimilate multiple observations such as 10-m wind, 2-m temperature, 2-m humidity, and surface pressure. In addition to conventional surface variables, GNSS/MET humidity data is also assimilated in the kilometer-scale 3DVar. Currently, a total of 17 types of observations are assimilated in the CMA-MESO system, with radar data contributed to the highest percentage.

The assimilation of radar reflectivity data can improve the TS of heavy precipitation forecasts by 5%–18%, and the assimilation of radial winds further improves the quality of low-level winds. The assimilation of wind profile radar observations can also improve the track and intensity forecasts of typhoons (Wang et al., 2019). Since the cloud analysis system relies on empirical relations and has limitations for the convective-scale numerical simulations, the development of direct assimilation techniques for radar reflectivity (including dual polarization quantities) is being carried out based on the CMA-MESO 1-km variational assimilation system. In addition, research on the assimilation of new types of ground-based remote sensing observations, including the X-band weather radar data, microwave radiometer temperature and humidity profile products, and cloud radar products, is also under way.

### 5.4 DA of TC observations

Since 2004, a set of TC initialization schemes (Qu et al., 2009), which consists of initial vortex formation, vortex relocation, and vortex adjustment, has been successively developed and adopted in operation on T213 global spectral model of CMA for TC forecasts. In 2014, the bogus vortex embedding in the initial vortex formation scheme was replaced by DA of vortex wind and pressure data, which were developed and applied to T639 Global Spectral Model (Qu et al., 2016). In 2018, with the continuous improvement of CMA's self-developed global modeling system (CMA-GFS), a new initialization scheme that assimilates the evolution trend of the TC position and central pressure profile based on the 4DVar assimilation system, was produced (Qu et al., 2022). The operational application shows that the new initialization scheme can significantly improve the TC track and intensity forecasts of CMA-GFS. There are two prospects for future advancements of improving the analyses and forecasts of TCs, one to develop TC initial perturbation

techniques, aiming to improve the flow-dependent background error statistics for TCs, and the other to develop En4DVar with effective and efficient assimilation of observation information for TCs.

## 6. Prospects for DA

### 6.1 Integrating DA for high resolutions and long lead times

One development aspect for NWP is persistently improving the model resolution, which leads to better resolved small-scale, nonlinear, and non-Gaussian processes. Meanwhile, advances in observing systems produce more indirect types of observations and increased observations with higher spatiotemporal resolutions (Fig. 4). Consequently, the current mainstream DA methods that often assume Gaussian error distributions and linear relationships may no longer be optimal (Yano et al., 2018). The iterative EnKF (IEnKF; Sakov et al., 2012) replaces linear regression with a transform matrix from the previous iteration, better capturing the nonlinear error growth. Other nonlinear filtering methods have been proposed, including the Gaussian mixture filters (Bengtsson et al., 2003), maximum likelihood ensemble filters (Zupanski, 2005), rank histogram filters (Anderson, 2010), rank-matching filters (Lei and Bickel, 2011), and quantile-conserving ensemble filters (Anderson, 2022, 2023).

A fully Bayesian, nonlinear method is the particle filter that provides particles following the Bayesian posterior distribution. Particle filter can be implemented through methods like bootstrap sampling (Gordon et al., 1993; Douc and Cappé, 2005), importance sampling (van Leeuwen, 2003; Robert and Cassela, 2004), and importance sampling with proposal (Doucet et al., 2000; Spiller et al., 2008). However, particle filter faces the “curse of dimensionality” when it was applied in high-dimensional dynamical systems (Snyder et al., 2008). To mitigate the “curse of dimensionality”, techniques such as the implicit particle filter combining filtering and smoothing (Chorin and Tu, 2009), hybrid ensemble-particle filters (Santitissadeekorn and Jones, 2015), equal-weight particle filters (Ades and van Leeuwen, 2015; Zhu et al., 2016), and localized particle filters (Penny and Miyoshi, 2016; Poterjoy, 2016) have been developed.

Another trend in NWP is extending the forecast lead times, from the current forecast limit of two weeks to seasonal-to-decadal (s2d) lead times (Fig. 4). To extend the predictability, coupling atmospheric models with slowly evolving components of the Earth system, such as the ocean, land surface, and cryosphere, becomes necessary.

Thus, the advance of coupled DA becomes essential. Weakly-coupled DA assimilates component-specific observations within each model component, using the coupled model to spread the observation information cross components (Zhang et al., 2007; Sugiura et al., 2008; Saha et al., 2010; Laloyaux et al., 2016). Comparatively, strongly-coupled DA uses cross-components observations to simultaneously update state variables from all components (Sluka et al., 2016; Sun et al., 2020a), providing more balanced analyses and reducing initialization shock, and strongly-coupled DA can lead to improved forecasts (Smith et al., 2015; Chen and Zhang, 2019).

### 6.2 Hybrid machine learning and DA

Machine learning (ML) has brought new opportunities for DA, numerical models, predictions, and projections, especially in efficiently and effectively assimilating the vast satellite observations. Both DA and ML can be viewed as inverse problems under the Bayes theory (Geer, 2021). Compared to traditional DA methods, ML has advantages for capturing nonlinear features, approximating nonlinear systems, and processing massive observation datasets, and thus, hybrid ML and DA approaches have been rapidly developed (Fig. 4). Direct integration of ML and DA can use data-driven ML models to replace numerical models, providing efficient forecasts for DA cycles. FengWu-4DVar combines the multimodal neural network-based FengWu model with 4DVar, to leverage the short-term forecasts and automatic differentiation capability of DL for efficiently solving the 4DVar analysis (Xiao et al., 2024a). Similarly, the Cli-maX based on the Vision Transformer (ViT) architecture can integrate with LETKF, enabling cyclical ensemble DA while diagnosing ML-based models (Kotsuki et al., 2024).

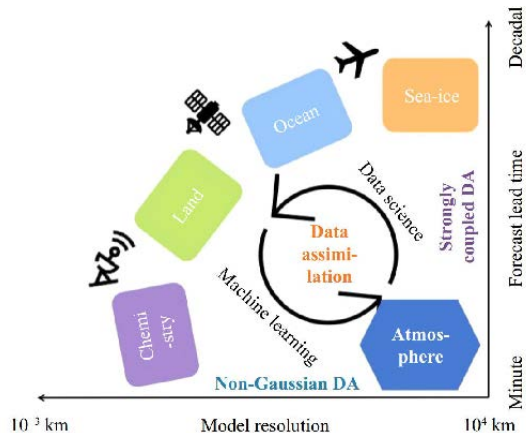


Fig. 4. Prospect for the development of DA in NWP.

ML can also enhance various DA components. Observation forward operators convert model state variables to estimated observations, but the Jacobians of forward operators could be computationally expensive. ML can efficiently approximate the forward operators, their Jacobians, and even the second-order Hessian matrices, especially for highly nonlinear forward operators (Storto et al., 2021). ML-based forward operator for satellite radiances can replace the fast radiative transfer model and simultaneously perform bias correction (Liang et al., 2023). The adjoint models required by 4DVAR are difficult to construct and also computationally expensive. ML offers an alternative by simulating the physical parameterizations to directly obtain the tangent linear and adjoint models, significantly improving the computational efficiency (Hatfield et al., 2021). Covariance localization is essential for EnKF successfully applied in high-dimensional dynamical systems, but the widely used localization functions are symmetric functions of distances. ML can extract nonlinear error characteristics from data, and generate non-symmetric and nonlinear localization functions (Wang and Wang, 2021).

As a major source of forecast errors, model errors need be appropriately addressed in DA. ML can learn model errors resulting from unresolved processes in numerical simulations (Rasp et al., 2018; Bolton and Zanna, 2019; Gagne II et al., 2020; Brajard et al., 2021). Neural networks and other ML architectures can learn model errors with nonlinear and multiscale characteristics from the analyses, forecasts, and observations, which can then be represented in DA through additive terms (Bonavita and Laloyaux, 2020; Farchi et al., 2021b). Moreover, through cycling DA, ML can learn and correct model errors online using priors and posteriors (Farchi et al., 2021a; Peng et al., 2024), or simultaneously estimate errors in state variables and model parameters (Bocquet et al., 2021; Malartic et al., 2022).

To address the computational complexity of high-dimensional dynamical systems, latent-space DA has been proposed, which assimilates data in the latent space created by ML-based autoencoders, combining ML's efficiency with DA's optimization (Binev et al., 2017; Arcucci et al., 2019; Casas et al., 2020). Compared to the variational methods and EnKFs that often assume Gaussian error distributions, variational autoencoders can estimate non-Gaussian error distributions, and the combined variational autoencoders and variational methods outperform the traditional variational methods (Xiao et al., 2024b). ML can also integrate with nonlinear filters, like the deep Kalman filters (Krishnan et al., 2015, 2017) and Kalman variational autoencoders (Fraccaro et al.,

2017). DiffDA, based on the GraphCast neural network, leverages similarities between numerical models and denoising diffusion models to directly produce the analysis (Huang et al., 2024). Furthermore, ML can facilitate reconstruction and assimilation based on incomplete or coarse-resolution observing networks (Wang et al., 2022; Howard et al., 2024).

### 6.3 DA for all-sky satellite radiances and dual-polarization radar data

In China's operational systems, the assimilated satellite data primarily focuses on clear-sky radiances, with the assimilation of satellite data in rain and cloud areas has not yet been operationally implemented. The assimilation and application of new remote sensing data, including active remote sensing instruments such as precipitation radars and wind lidars, as well as ground-based payload observation data, still need to be improved. For Earth system coupled DA, the fast radiative transfer model needs to consider an ultra-high spectral atmospheric transmittance calculation model covering the full spectrum range and containing multiple atmospheric components. Additionally, constructing a satellite and new payload coupled forward operator based on artificial intelligence is essential. The assimilation of visible data will be a very important direction for the future application of satellite DA. Specifically, the all-sky assimilation of infrared and visible data will provide more accurate analyses for numerical models, particularly at the convective scale (Schröttle et al., 2020). Developing advanced radiative transfer models that account for the scattering characteristics of cloud particles will enable better assimilate of infrared radiances affected by clouds. Meanwhile, an improved description of land surface processes is worth to develop, aiming to increase the assimilation of radiance in surface-sensitive channels. Microwave sounding data contribute the most to the forecast accuracy of NWP. But currently, microwave sounders are only carried on low-earth orbit meteorological satellites, with long revisit cycles and low temporal resolutions, making it difficult to provide continuous observation for weather systems. The geostationary orbit microwave sounding being designed and constructed for China's FY satellites is an important supplement to the existing microwave sounding system (Lu and Gu, 2016). It can not only provide high temporal resolution 3D information for the atmospheric thermodynamic structure but also generate wind field products at different heights over the whole sky using the water vapor tracking method, providing more dynamical information for NWP (Zhang et al., 2021). In addition, the current satellite DA tech-

niques basically neglect the synergy effect among the multi-instrument observations. Fully considering the synergy and complementary effects among the multi-instrument observations, such as the joint application of imaging and sounding data (Di et al., 2024), can lead to improved assimilation outcomes. This represents a significant future development direction for satellite DA.

Developing a reasonable variational-based dual-polarimetric radar observation forward operator is crucial. Based on the dual-polarization radar observation operator developed by Kawabata et al. (2018), Zhang et al. (2024) developed a variational direct assimilation scheme for dual-polarization radar based on hydrometeor control variables. Cycling assimilation and forecast experiments for real cases demonstrated that the assimilation of dual-polarization radar data can improve the thermodynamic and microphysical characteristics of both the analyses and forecasts. Research on the development of dual-polarization radar observation forward operators and adjoint operators provides foundational support for the variational assimilation of polarimetric radar quantities. However, due to the complexity of the tangent linear and adjoint operators of polarimetric radar and the uncertainties in parameterization schemes, further research for more refined polarimetric radar observation forward operators is needed, particularly with respect to the treatment of ice-phase and mixed-phase hydrometeors.

#### 6.4 Advanced operational DA systems

Currently, China's independently developed global and regional operational weather forecasting systems, CMA-GFS and CMA-MESO, can effectively assimilate multi-source observations, and play an important role in daily weather forecasts, warning, and meteorological disaster prevention and mitigation. However, the existing model dynamical frameworks are insufficient to meet the demand for seamless NWP of the Earth system. Major operational centers have been developing quasi-uniform grid numerical models, and China has also completed the next-generation high-precision scalable atmospheric model (Li et al., 2020). Development of the high-precision scalable atmospheric DA system for the next-generation model is progressing intensively. The goal for the next-generation atmospheric DA system is to establish an integrated global/regional hybrid ensemble-variational assimilation framework, with the basis of global 4DVar. Research on advanced assimilation techniques for multi-source observations, including the Beidou navigation soundings, satellite data in cloud and precipitation areas, radar reflectivity, X-band radar, dual-polarization radar, phased-array radar, and ground-based vertical remote

sensing, will be conducted to promote the operational use of innovative observations. Meanwhile, studies on applying artificial intelligence algorithms in various areas of multi-source DA are underway.

To address the multiscale seamless NWP for the Earth system from weather to climate, research on DA techniques across different components of the Earth system will be conducted. Based on the high-precision scalable atmospheric DA system, the goal is to develop an ocean–land–atmosphere–ice coupled DA system to achieve effective and efficient assimilation of multi-source observations across different components of the Earth system, providing coherent, balanced, and high-quality initial conditions for the Earth system model. As illustrated in Fig. 4, the aim is to establish an operational DA system for the Earth system prediction and projection, based on the advances in DA theories and methods.

#### REFERENCES

- Ades, M., and P. J. van Leeuwen, 2015: The equivalent-weights particle filter in a high-dimensional system. *Quart. J. Roy. Meteor. Soc.*, **141**, 484–503, <https://doi.org/10.1002/qj.2370>.
- Agustí-Panareda, A., A. Beljaars, C. Cardinali, et al., 2010: Impacts of assimilating AMMA soundings on ECMWF analyses and forecasts. *Wea. Forecasting*, **25**, 1142–1160, <https://doi.org/10.1175/2010WAF2222370.1>.
- Aires, F., C. Prigent, F. Bernardo, et al., 2011: A tool to estimate Land-Surface emissivities at microwave frequencies (TELSEM) for use in numerical weather prediction. *Quart. J. Roy. Meteor. Soc.*, **137**, 690–699, <https://doi.org/10.1002/qj.803>.
- Anderson, J. L., 2001: An ensemble adjustment Kalman filter for data assimilation. *Mon. Wea. Rev.*, **129**, 2884–2903, [https://doi.org/10.1175/1520-0493\(2001\)129<2884:AEAKFF>2.0.CO;2](https://doi.org/10.1175/1520-0493(2001)129<2884:AEAKFF>2.0.CO;2).
- Anderson, J. L., 2007: Exploring the need for localization in ensemble data assimilation using a hierarchical ensemble filter. *Phys. D Nonlinear Phenom.*, **230**, 99–111, <https://doi.org/10.1016/j.physd.2006.02.011>.
- Anderson, J. L., 2009: Spatially and temporally varying adaptive covariance inflation for ensemble filters. *Tellus A*, **61**, 72–83, <https://doi.org/10.1111/j.1600-0870.2008.00361.x>.
- Anderson, J. L., 2010: A non-Gaussian ensemble filter update for data assimilation. *Mon. Wea. Rev.*, **138**, 4186–4198, <https://doi.org/10.1175/2010MWR3253.1>.
- Anderson, J. L., 2012: Localization and sampling error correction in ensemble Kalman filter data assimilation. *Mon. Wea. Rev.*, **140**, 2359–2371, <https://doi.org/10.1175/MWR-D-11-00013.1>.
- Anderson, J. L., 2022: A quantile-conserving ensemble filter framework. Part I: Updating an observed variable. *Mon. Wea. Rev.*, **150**, 1061–1074, <https://doi.org/10.1175/MWR-D-21-0229.1>.
- Anderson, J. L., 2023: A quantile-conserving ensemble filter framework. Part II: Regression of observation increments in a probit and probability integral transformed space. *Mon. Wea.*

- Rev.*, **151**, 2759–2777, <https://doi.org/10.1175/MWR-D-23-0065.1>.
- Anderson, J. L., and S. L. Anderson, 1999: A Monte Carlo implementation of the nonlinear filtering problem to produce ensemble assimilations and forecasts. *Mon. Wea. Rev.*, **127**, 2741–2758, [https://doi.org/10.1175/1520-0493\(1999\)127<2741:AMCIOT>2.0.CO;2](https://doi.org/10.1175/1520-0493(1999)127<2741:AMCIOT>2.0.CO;2).
- Andersson, E., J. Pailleux, J. N. Thépaut, et al., 1994: Use of cloud-cleared radiances in three/four-dimensional variational data assimilation. *Quart. J. Roy. Meteor. Soc.*, **120**, 627–653, <https://doi.org/10.1002/qj.49712051707>.
- Arcucci, R., L. Mottet, C. Pain, et al., 2019: Optimal reduced space for Variational Data Assimilation. *J. Comput. Phys.*, **379**, 51–69, <https://doi.org/10.1016/j.jcp.2018.10.042>.
- Atkins, M. J., and M. Jones, 1975: An experiment to determine the value of satellite infrared spectrometer (SIRS) data in numerical forecasting. *Meteor. Mag.*, **104**, 125–142.
- Auligné, T., B. Ménétrier, A. C. Lorenc, et al., 2016: Ensemble-variational integrated localized data assimilation. *Mon. Wea. Rev.*, **144**, 3677–3696, <https://doi.org/10.1175/MWR-D-15-0252.1>.
- Bao, X. H., R. D. Xia, Y. L. Luo, et al., 2023: Efficiently improving ensemble forecasts of warm-sector heavy rainfall over coastal southern China: Targeted assimilation to reduce the critical initial field errors. *J. Meteor. Res.*, **37**, 486–507, <https://doi.org/10.1007/s13351-023-2140-8>.
- Baordo, F., and A. J. Geer, 2016: Assimilation of SSMIS humidity-sounding channels in all-sky conditions over land using a dynamic emissivity retrieval. *Quart. J. Roy. Meteor. Soc.*, **142**, 2854–2866, <https://doi.org/10.1002/qj.2873>.
- Barkmeijer, J., F. Bouttier, and M. van Gijzen, 1998: Singular vectors and estimates of the analysis-error covariance metric. *Quart. J. Roy. Meteor. Soc.*, **124**, 1695–1713, <https://doi.org/10.1002/qj.49712454916>.
- Bauer, P., A. J. Geer, P. Lopez, et al., 2010: Direct 4D-Var assimilation of all-sky radiances. Part I: Implementation. *Quart. J. Roy. Meteor. Soc.*, **136**, 1868–1885, <https://doi.org/10.1002/qj.659>.
- Bengtsson, T., C. Snyder, and D. Nychka, 2003: Toward a nonlinear ensemble filter for high-dimensional systems. *J. Geophys. Res. Atmos.*, **108**, 8775, <https://doi.org/10.1029/2002JD002900>.
- Bennett, A. F., 1992: *Inverse Methods in Physical Oceanography*. Cambridge University Press, Cambridge, 368 pp, <https://doi.org/10.1017/CBO9780511600807>.
- Bennett, A. F., B. S. Chua, and L. M. Leslie, 1996: Generalized inversion of a global numerical weather prediction model. *Met. Atmos. Phys.*, **60**, 165–178, <https://doi.org/10.1007/BF01029793>.
- Bergemann, K., and S. Reich, 2010: A mollified ensemble Kalman filter. *Quart. J. Roy. Meteor. Soc.*, **136**, 1636–1643, <https://doi.org/10.1002/qj.672>.
- Bergot, T., 1999: Adaptive observations during FASTEX: A systematic survey of upstream flights. *Quart. J. Roy. Meteor. Soc.*, **125**, 3271–3298, <https://doi.org/10.1002/qj.49712556108>.
- Berner, J., G. J. Shutts, M. Leutbecher, et al., 2009: A spectral stochastic kinetic energy backscatter scheme and its impact on flow-dependent predictability in the ECMWF ensemble prediction system. *J. Atmos. Sci.*, **66**, 603–626, <https://doi.org/10.1175/2008JAS2677.1>.
- Bi, X. Y., Z. Q. Gao, Y. G. Liu, et al., 2015: Observed drag coefficients in high winds in the near offshore of the South China Sea. *J. Geophys. Res. Atmos.*, **120**, 6444–6459, <https://doi.org/10.1002/2015JD023172>.
- Binev, P., A. Cohen, W. Dahmen, et al., 2017: Data assimilation in reduced modeling. *SIAM/ASA J. Uncertainty Quantif.*, **5**, 1–29, <https://doi.org/10.1137/15M1025384>.
- Bishop, C. H., and Z. Toth, 1999: Ensemble transformation and adaptive observations. *J. Atmos. Sci.*, **56**, 1748–1765, [https://doi.org/10.1175/1520-0469\(1999\)056<1748:ETAAO>2.0.CO;2](https://doi.org/10.1175/1520-0469(1999)056<1748:ETAAO>2.0.CO;2).
- Bishop, C. H., and D. Hodyss, 2009: Ensemble covariances adaptively localized with ECO-RAP. Part I: Tests on simple error models. *Tellus A*, **61**, 84–96.
- Bishop, C. H., B. J. Etherton, and S. J. Majumdar, 2001: Adaptive sampling with the ensemble transform Kalman filter. Part I: Theoretical aspects. *Mon. Wea. Rev.*, **129**, 420–436, [https://doi.org/10.1175/1520-0493\(2001\)129<0420:ASWTET>2.0.CO;2](https://doi.org/10.1175/1520-0493(2001)129<0420:ASWTET>2.0.CO;2).
- Bloom, S. C., L. L. Takacs, A. M. da Silva, et al., 1996: Data assimilation using incremental analysis updates. *Mon. Wea. Rev.*, **124**, 1256–1271, [https://doi.org/10.1175/1520-0493\(1996\)124<1256:DAUIAU>2.0.CO;2](https://doi.org/10.1175/1520-0493(1996)124<1256:DAUIAU>2.0.CO;2).
- Bocquet, M., A. Farchi, and Q. Malartic, 2021: Online learning of both state and dynamics using ensemble Kalman filters. *Found. Data Sci.*, **3**, 305–330, <https://doi.org/10.3934/fods.2020015>.
- Bolton, T., and L. Zanna, 2019: Applications of deep learning to ocean data inference and subgrid parameterization. *J. Adv. Model. Earth Syst.*, **11**, 376–399, <https://doi.org/10.1029/2018MS001472>.
- Bonavita, M., and P. Laloyaux, 2020: Machine learning for model error inference and correction. *J. Adv. Model. Earth Syst.*, **12**, e2020MS002232, <https://doi.org/10.1029/2020MS002232>.
- Bonavita, M., L. Isaksen, and E. Hólm, 2012: On the use of EDA background error variances in the ECMWF 4D-Var. *Quart. J. Roy. Meteor. Soc.*, **138**, 1540–1559, <https://doi.org/10.1002/qj.1899>.
- Bonavita, M., M. Hamrud, and L. Isaksen, 2015: EnKF and hybrid gain ensemble data assimilation. Part II: EnKF and hybrid gain results. *Mon. Wea. Rev.*, **143**, 4865–4882, <https://doi.org/10.1175/MWR-D-15-0071.1>.
- Bormann, N., H. Lawrence, and J. Farnan, 2019: Global Observing System Experiments in the ECMWF Assimilation System. ECMWF Technical Memoranda 839, ECMWF, Shinfield Park, 23 pp.
- Brajard, J., A. Carrassi, M. Bocquet, et al., 2021: Combining data assimilation and machine learning to infer unresolved scale parametrization. *Philos. Trans. Roy. Soc. A Math. Phys. Eng. Sci.*, **379**, 20200086, <https://doi.org/10.1098/rsta.2020.0086>.
- Buehner, M., 2012: Evaluation of a spatial/spectral covariance localization approach for atmospheric data assimilation. *Mon. Wea. Rev.*, **140**, 617–636, <https://doi.org/10.1175/MWR-D-10-0502.1>.
- Buehner, M., and A. Shlyaeva, 2015: Scale-dependent background-error covariance localisation. *Tellus A Dyn. Meteor. Oceanogr.*, **67**, 28027, <https://doi.org/10.3402/tellusa.v67.28027>

- 027.
- Buehner, M., P. L. Houtekamer, C. Charette, et al., 2010a: Inter-comparison of variational data assimilation and the ensemble Kalman filter for global deterministic NWP. Part I: Description and single-observation experiments. *Mon. Wea. Rev.*, **138**, 1550–1566, <https://doi.org/10.1175/2009MWR3157.1>.
- Buehner, M., P. L. Houtekamer, C. Charette, et al., 2010b: Inter-comparison of variational data assimilation and the ensemble Kalman filter for global deterministic NWP. Part II: One-month experiments with real observations. *Mon. Wea. Rev.*, **138**, 1567–1586, <https://doi.org/10.1175/2009MWR3158.1>.
- Buehner, M., R. McTaggart-Cowan, A. Beaulne, et al., 2015: Implementation of deterministic weather forecasting systems based on ensemble-variational data assimilation at Environment Canada. Part I: The global system. *Mon. Wea. Rev.*, **143**, 2532–2559, <https://doi.org/10.1175/MWR-D-14-00354.1>.
- Buizza, R., M. Milleer, and T. N. Palmer, 1999: Stochastic representation of model uncertainties in the ECMWF ensemble prediction system. *Quart. J. Roy. Meteor. Soc.*, **125**, 2887–2908, <https://doi.org/10.1002/qj.49712556006>.
- Burgers, G., P. J. van Leeuwen, and G. Evensen, 1998: Analysis scheme in the ensemble Kalman filter. *Mon. Wea. Rev.*, **126**, 1719–1724, [https://doi.org/10.1175/1520-0493\(1998\)126<171:ASITEK>2.0.CO;2](https://doi.org/10.1175/1520-0493(1998)126<171:ASITEK>2.0.CO;2).
- Caron, J. F., T. Milewski, M. Buehner, et al., 2015: Implementation of deterministic weather forecasting systems based on ensemble-variational data assimilation at Environment Canada. Part II: The regional system. *Mon. Wea. Rev.*, **143**, 2560–2580, <https://doi.org/10.1175/MWR-D-14-00353.1>.
- Casas, C. Q., R. Arcucci, P. Wu, et al., 2020: A reduced order deep data assimilation model. *Phys. D Nonlinear Phenom.*, **412**, 132615, <https://doi.org/10.1016/j.physd.2020.132615>.
- Cha, D.-H., and Y. Q. Wang, 2013: A dynamical initialization scheme for real-time forecasts of tropical cyclones using the WRF Model. *Mon. Wea. Rev.*, **141**, 964–986, <https://doi.org/10.1175/MWR-D-12-00077.1>.
- Chan, P. W., N. G. Wu, C. Z. Zhang, et al., 2018: The first complete dropsonde observation of a tropical cyclone over the South China Sea by the Hong Kong Observatory. *Weather*, **73**, 227–234, <https://doi.org/10.1002/wea.3095>.
- Chan, P.-W., W. Han, B. Mak, et al., 2023: Ground-space-sky observing system experiment during tropical cyclone Mulan in August 2022. *Adv. Atmos. Sci.*, **40**, 194–200, <https://doi.org/10.1007/s00376-022-2267-z>.
- Chen, B. Y., M. Mu, and X. H. Qin, 2013: The impact of assimilating dropwindsonde data deployed at different sites on typhoon track forecasts. *Mon. Wea. Rev.*, **141**, 2669–2682, <https://doi.org/10.1175/MWR-D-12-00142.1>.
- Chen, F., X. D. Liang, and H. Ma, 2017: Application of IVAP-based observation operator in radar radial velocity assimilation: The case of Typhoon Fitow. *Mon. Wea. Rev.*, **145**, 4187–4203, <https://doi.org/10.1175/MWR-D-17-0002.1>.
- Chen, H. Q., Y. D. Chen, J. D. Gao, et al., 2020: A radar reflectivity data assimilation method based on background-dependent hydrometeor retrieval: An observing system simulation experiment. *Atmos. Res.*, **243**, 105022, <https://doi.org/10.1016/j.atmosres.2020.105022>.
- Chen, H.-Y., H. Yu, G.-J. Ye, et al., 2019: Return period and the trend of extreme disastrous rainstorm events in Zhejiang Province. *J. Trop. Meteor.*, **25**, 192–200, <https://doi.org/10.16555/j.1006-8775.2019.02.006>.
- Chen, M., M. X. Chen, and S. Y. Fan, 2014: The real-time radar radial velocity 3DVar assimilation experiments for application to an operational forecast model in North China. *Acta Meteor. Sinica*, **72**, 658–677, <https://doi.org/10.11676/qxb2014.070>. (in Chinese)
- Chen, N., J. Tang, J. A. Zhang, et al., 2021: On the distribution of helicity in the tropical cyclone boundary layer from dropsonde composites. *Atmos. Res.*, **249**, 105298, <https://doi.org/10.1016/j.atmosres.2020.105298>.
- Chen, X. C., and F. Q. Zhang, 2019: Development of a convection-permitting air-sea-coupled ensemble data assimilation system for tropical cyclone prediction. *J. Adv. Model. Earth Syst.*, **11**, 3474–3496, <https://doi.org/10.1029/2019MS001795>.
- Chen, X. Y., Y. D. Chen, and D. M. Meng, 2022: Assimilation of radar data based on cloud-dependent background error covariance and its impact on rainfall forecasting. *Acta Meteor. Sinica*, **80**, 243–256, <https://doi.org/10.11676/qxb2022.011>. (in Chinese)
- Chen, Y., and D. S. Oliver, 2010: Cross-covariances and localization for EnKF in multiphase flow data assimilation. *Comput. Geosci.*, **14**, 579–601, <https://doi.org/10.1007/s10596-009-9174-6>.
- Chen, Y. D., H. L. Wang, J. Z. Min, et al., 2015: Variational assimilation of cloud liquid/ice water path and its impact on NWP. *J. Appl. Meteor. Climatol.*, **54**, 1809–1825, <https://doi.org/10.1175/JAMC-D-14-0243.1>.
- Chen, Y. D., H. Q. Chen, J. Z. Sun, et al., 2018: Nonlinear characteristics of model variables corresponding to radar observations and its effects on 4D-VAR assimilation. *J. Trop. Meteor.*, **34**, 721–732, <https://doi.org/10.16032/j.issn.1004-4965.2018.06.001>. (in Chinese)
- Chen, Y. D., X. Z. Liu, S. Y. Fan, et al., 2025: Assimilation of radar radial velocity in the clear-air region and its impact on forecasting. *J. Meteor. Res.*, **39**, 272–287, <https://doi.org/10.1007/s13351-025-4186-2>.
- Chorin, A. J., and X. M. Tu, 2009: Implicit sampling for particle filters. *Proc. Natl. Acad. Sci. USA*, **106**, 17,249–17,254, <https://doi.org/10.1073/pnas.0909196106>.
- Chou, J. F., 1974: The usage of past observations in numerical weather prediction. *Sci. China*, **4**, 635–644. (in Chinese)
- Chou, J. F., 2007: An innovative road to numerical weather prediction—from initial value problem to inverse problem. *Acta Meteor. Sinica*, **65**, 673–682, <https://doi.org/10.11676/qxb2007.061>. (in Chinese)
- Chouinard, C., J. Hallé, C. Charette, et al., 2002: Recent improvements in the use of TOVS satellite radiances in the Unified 3D-Var system of the Canadian Meteorological Centre. ITSC XII Proceedings, Lorne, Australia, 27 pp.
- Clayton, A. M., A. C. Lorenc, and D. M. Barker, 2013: Operational implementation of a hybrid ensemble/4D-Var global data assimilation system at the Met Office. *Quart. J. Roy. Meteor. Soc.*, **139**, 1445–1461, <https://doi.org/10.1002/qj.2054>.
- Collard, A. D., 2007: Selection of IASI channels for use in numerical weather prediction. *Quart. J. Roy. Meteor. Soc.*, **133**, 1977–1991, <https://doi.org/10.1002/qj.178>.
- Courtier, P., and O. Talagrand, 1990: Variational assimilation of meteorological observations with the direct and adjoint shal-

- low-water equations. *Tellus A Dyn. Meteor. Oceanogr.*, **42**, 531–549, <https://doi.org/10.1034/j.1600-0870.1990.t01-4-0004.x>.
- Courtier, P., J.-N. Thépaut, and A. Hollingsworth, 1994: A strategy for operational implementation of 4D-Var, using an incremental approach. *Quart. J. Roy. Meteor. Soc.*, **120**, 1367–1387, <https://doi.org/10.1002/qj.49712051912>.
- Cressman, G. P., 1959: An operational objective analysis system. *Mon. Wea. Rev.*, **87**, 367–374, [https://doi.org/10.1175/1520-0493\(1959\)087<0367:AOOAS>2.0.CO;2](https://doi.org/10.1175/1520-0493(1959)087<0367:AOOAS>2.0.CO;2).
- Da Silva, A., J. Pfandtner, J. Guo, et al., 1995: Assessing the effects of data selection with the DAO physical-space statistical analysis system. Proceedings of the 2nd WMO Symposium on Assimilation of Observations in Meteorology and Oceanography, World Meteorological Organization, Geneva, 273–278.
- Daley, R., 1991: *Atmospheric Data Analysis*. Cambridge University Press, Cambridge, 472 pp.
- Daley, R., 1995: Estimating the wind field from chemical constituent observations: Experiments with a one-dimensional extended Kalman filter. *Mon. Wea. Rev.*, **123**, 181–198, [https://doi.org/10.1175/1520-0493\(1995\)123<0181:ETWFFC>2.0.CO;2](https://doi.org/10.1175/1520-0493(1995)123<0181:ETWFFC>2.0.CO;2).
- Derber, J., and F. Bouttier, 1999: A reformulation of the background error covariance in the ECMWF global data assimilation system. *Tellus A Dyn. Meteor. Oceanogr.*, **51**, 195–221, <https://doi.org/10.3402/tellusa.v51i2.12316>.
- Derber, J. C., 1989: A variational continuous assimilation technique. *Mon. Wea. Rev.*, **117**, 2437–2446, [https://doi.org/10.1175/1520-0493\(1989\)117<2437:AVCAT>2.0.CO;2](https://doi.org/10.1175/1520-0493(1989)117<2437:AVCAT>2.0.CO;2).
- Derber, J. C., and W.-S. Wu, 1998: The use of TOVS cloud-cleared radiances in the NCEP SSI analysis system. *Mon. Wea. Rev.*, **126**, 2287–2299, [https://doi.org/10.1175/1520-0493\(1998\)126<2287:TUOTCC>2.0.CO;2](https://doi.org/10.1175/1520-0493(1998)126<2287:TUOTCC>2.0.CO;2).
- Desmarais, A. J., S. Tracton, R. McPherson, et al., 1978: The NMC Report on the Data Systems Test. NASA Contract S-70252-AG, National Meteorological Center, Camp Springs, Maryland, 313 pp.
- Di, D., J. Li, Z. L. Li, et al., 2024: Enhancing clear radiance generation for geostationary hyperspectral infrared sounder using high temporal resolution information. *Geophys. Res. Lett.*, **51**, e2023GL107194, <https://doi.org/10.1029/2023GL107194>.
- Douc, R., and O. Cappé, 2005: Comparison of resampling schemes for particle filtering. Proceedings of the 4th International Symposium on Image and Signal Processing and Analysis, IEEE, Zagreb, Croatia, 64–69, <https://doi.org/10.1109/ISPA.2005.195385>.
- Doucet, A., S. Godsill, and C. Andrieu, 2000: On sequential Monte Carlo sampling methods for Bayesian filtering. *Stat. Comput.*, **10**, 197–208, <https://doi.org/10.1023/A:1008935410038>.
- Druyan, L. M., T. Ben-Amram, Z. Alperson, et al., 1978: The impact of VTPR data on numerical forecasts of the Israel Meteorological Service. *Mon. Wea. Rev.*, **106**, 859–869, [https://doi.org/10.1175/1520-0493\(1978\)106<0859:TIOVDO>2.0.CO;2](https://doi.org/10.1175/1520-0493(1978)106<0859:TIOVDO>2.0.CO;2).
- Duan, W. S., and X. H. Qin, 2022: Application of nonlinear optimal perturbation methods in the targeting observations and field campaigns of tropical cyclones. *Adv. Earth Sci.*, **37**, 165–176, [\(in Chinese\)](https://doi.org/10.11867/j.issn.1001-8166.2022.010)
- Duan, W. S., X. Q. Li, and B. Tian, 2018: Towards optimal observational array for dealing with challenges of El Niño–Southern Oscillation predictions due to diversities of El Niño. *Climate Dyn.*, **51**, 3351–3368, <https://doi.org/10.1007/s00382-018-4082-x>.
- Duan, W. S., L. C. Yang, M. Mu, et al., 2023: Recent advances in China on the predictability of weather and climate. *Adv. Atmos. Sci.*, **40**, 1521–1547, <https://doi.org/10.1007/s00376-023-2334-0>.
- Duan, Y. H., Q. L. Wan, J. Huang, et al., 2019: Landfalling tropical cyclone research project (LTCRP) in China. *Bull. Amer. Meteor. Soc.*, **100**, ES447–ES472, <https://doi.org/10.1175/BAMS-D-18-0241.1>.
- Egbert, G. D., A. F. Bennett, and M. G. G. Foreman, 1994: TOPEX/POSEIDON tides estimated using a global inverse model. *J. Geophys. Res. Oceans*, **99**, 24821–24852, <https://doi.org/10.1029/94JC01894>.
- El Gharanti, M., 2018: Enhanced adaptive inflation algorithm for ensemble filters. *Mon. Wea. Rev.*, **146**, 623–640, <https://doi.org/10.1175/MWR-D-17-0187.1>.
- Eliassen, A., J. S. Sawyer, and J. Smagorinsky, 1960: Upper Air Network Requirements for Numerical Weather Prediction. Technical Note No. 29, World Meteorological Organization, Geneva, Switzerland, 135 pp.
- Elsberry, R. L., and P. A. Harr, 2008: Tropical cyclone structure (TCS08) field experiment science basis, observational platforms, and strategy. *Asia-Pacific J. Atmos. Sci.*, **44**, 209–231.
- Evensen, G., 1994: Sequential data assimilation with a nonlinear quasi-geostrophic model using Monte Carlo methods to forecast error statistics. *J. Geophys. Res. Oceans*, **99**, 10,143–10,162, <https://doi.org/10.1029/94JC00572>.
- Evensen, G., and P. J. van Leeuwen, 2000: An ensemble Kalman smoother for nonlinear dynamics. *Mon. Wea. Rev.*, **128**, 1852–1867, [https://doi.org/10.1175/1520-0493\(2000\)128<1852:AEKSFN>2.0.CO;2](https://doi.org/10.1175/1520-0493(2000)128<1852:AEKSFN>2.0.CO;2).
- Eyre, J. R., and A. C. Lorenc, 1989: Direct use of satellite sounding radiances in numerical weather prediction. *Meteor. Mag.*, **118**, 13–16.
- Eyre, J. R., G. A. Kelly, A. P. McNally, et al., 1993: Assimilation of TOVS radiance information through one-dimensional variational analysis. *Quart. J. Roy. Meteor. Soc.*, **119**, 1427–1463, <https://doi.org/10.1002/qj.49711951411>.
- Eyre, J. R., S. J. English, and M. Forsythe, 2020: Assimilation of satellite data in numerical weather prediction. Part I: The early years. *Quart. J. Roy. Meteor. Soc.*, **146**, 49–68, <https://doi.org/10.1002/qj.3654>.
- Fan, S. Y., H. L. Wang, M. Chen, et al., 2013: Study of the data assimilation of radar reflectivity with the WRF 3D-Var. *Acta Meteor. Sinica*, **71**, 527–537, [\(in Chinese\)](https://doi.org/10.11676/qxb2013.032)
- Farchi, A., M. Bocquet, P. Laloyaux, et al., 2021a: A comparison of combined data assimilation and machine learning methods for offline and online model error correction. *J. Comput. Sci.*, **55**, 101468, <https://doi.org/10.1016/j.jocs.2021.101468>.
- Farchi, A., P. Laloyaux, M. Bonavita, et al., 2021b: Using machine learning to correct model error in data assimilation and forecast applications. *Quart. J. Roy. Meteor. Soc.*, **147**, 3067–3084, <https://doi.org/10.1002/qj.4116>.
- Feng, J., X. H. Qin, C. Q. Wu, et al., 2022: Improving typhoon

- predictions by assimilating the retrieval of atmospheric temperature profiles from the *FengYun-4A*'s Geostationary Interferometric Infrared Sounder (GIIRS). *Atmos. Res.*, **280**, 106391, <https://doi.org/10.1016/j.atmosres.2022.106391>.
- Flowerdew, J., 2015: Towards a theory of optimal localisation. *Tellus A Dyn. Meteor. Oceanogr.*, **67**, 25257, <https://doi.org/10.3402/tellusa.v67.25257>.
- Forsythe, M., H. Berger, C. Velden, et al., 2007: Atmospheric motion vectors: Past, present and future. ECMWF seminar on recent development in the use of satellite observations in NWP, Exeter, UK, 3–7 September, ECMWF, 79 pp.
- Fraccaro, M., S. Kamronn, U. Paquet, et al., 2017: A disentangled recognition and nonlinear dynamics model for unsupervised learning. Proceedings of the 31st International Conference on Neural Information Processing Systems, Curran Associates Inc., Long Beach, 3601–3610.
- Gagne II, D. J., H. M. Christensen, A. C. Subramanian, et al., 2020: Machine learning for stochastic parameterization: Generative adversarial networks in the Lorenz' 96 model. *J. Adv. Model. Earth Syst.*, **12**, e2019MS001896, <https://doi.org/10.1029/2019MS001896>.
- Gandin, L. S., 1963: *Objective Analysis of Meteorological Fields*. Hydromet Press, Leningrad, 242 pp.
- Gao, J. D., and D. J. Stensrud, 2012: Assimilation of reflectivity data in a convective-scale, cycled 3DVAR framework with hydrometeor classification. *J. Atmos. Sci.*, **69**, 1054–1065, <https://doi.org/10.1175/JAS-D-11-0162.1>.
- Gao, J. D., M. Xue, A. Shapiro, et al., 1999: A variational method for the analysis of three-dimensional wind fields from two Doppler radars. *Mon. Wea. Rev.*, **127**, 2128–2142, [https://doi.org/10.1175/1520-0493\(1999\)127<2128:AVMFTA>2.0.CO;2](https://doi.org/10.1175/1520-0493(1999)127<2128:AVMFTA>2.0.CO;2).
- Gao, J. D., M. Xue, K. Brewster, et al., 2004: A three-dimensional variational data analysis method with recursive filter for Doppler radars. *J. Atmos. Oceanic Technol.*, **21**, 457–469, [https://doi.org/10.1175/1520-0426\(2004\)021<0457:ATVDAM>2.0.CO;2](https://doi.org/10.1175/1520-0426(2004)021<0457:ATVDAM>2.0.CO;2).
- Gaspari, G., and S. E. Cohn, 1999: Construction of correlation functions in two and three dimensions. *Quart. J. Roy. Meteor. Soc.*, **125**, 723–757, <https://doi.org/10.1002/qj.4971255417>.
- Geer, A. J., 2021: Learning earth system models from observations: Machine learning or data assimilation? *Philos. Trans. Roy. Soc. A Math. Phys. Eng. Sci.*, **379**, 20200089, <https://doi.org/10.1098/rsta.2020.0089>.
- Geer, A. J., P. Bauer, and P. Lopez, 2008: Lessons learnt from the operational 1D + 4D-Var assimilation of rain- and cloud-affected SSM/I observations at ECMWF. *Quart. J. Roy. Meteor. Soc.*, **134**, 1513–1525, <https://doi.org/10.1002/qj.304>.
- Geer, A. J., P. Bauer, and P. Lopez, 2010: Direct 4D-Var assimilation of all-sky radiances. Part II: Assessment. *Quart. J. Roy. Meteor. Soc.*, **136**, 1886–1905, <https://doi.org/10.1002/qj.681>.
- Geer, A. J., K. Lonitz, P. Weston, et al., 2018: All-sky satellite data assimilation at operational weather forecasting centres. *Quart. J. Roy. Meteor. Soc.*, **144**, 1191–1217, <https://doi.org/10.1002/qj.3202>.
- Ghil, M., S. Cohn, J. Tavantzis, et al., 1981: Applications of estimation theory to numerical weather prediction. *Dynamic Meteorology: Data Assimilation Methods*, L. Bengtsson, M. Ghil, and E. Källén, Eds., Springer, New York, 139–224, [https://doi.org/10.1007/978-1-4612-5970-1\\_5](https://doi.org/10.1007/978-1-4612-5970-1_5).
- Gilchrist, A., 1982: JSC Study Conference on Observing Systems Experiments, 19–22 April 1982. Numerical Experimentation Programme report No. 4, Geneva, Switzerland, WMO, 55 pp.
- Gilchrist, B., and G. P. Cressman, 1954: An experiment in objective analysis. *Tellus A Dyn. Meteor. Oceanogr.*, **6**, 309–318, <https://doi.org/10.3402/tellusa.v6i4.8762>.
- Gong, J. D., Y. Z. Liu, and L. Zhang, 2019: A study of simplification and linearization of the NSAS deep convection cumulus parameterization scheme for 4D-Var. *Acta Meteor. Sinica*, **77**, 595–616, <https://doi.org/10.11676/qxb2019.048>. (in Chinese)
- Gordon, N. J., D. J. Salmond, and A. F. M. Smith, 1993: Novel approach to nonlinear/non-Gaussian Bayesian state estimation. *IEE Proc. F (Radar Signal Process.)*, **140**, 107–113, <https://doi.org/10.1049/ip-f-2.1993.0015>.
- Guan, C. G., Q. Y. Chen, H. Tong, et al., 2008: Experiments and evaluations of global medium range forecast system of T639L60. *Meteor. Mon.*, **34**, 11–16, <https://doi.org/10.7519/j.issn.1000-0526.2008.06.002>. (in Chinese)
- Guo, X. R., Y. L. Zhang, Z. H. Yan, et al., 1995: The limited area analysis and forecast system and its operational application. *Acta Meteor. Sinica*, **53**, 306–318, <https://doi.org/10.11676/qxb1995.036>. (in Chinese)
- Ha, S., J. Berner, and C. Snyder, 2015: A comparison of model error representations in mesoscale ensemble data assimilation. *Mon. Wea. Rev.*, **143**, 3893–3911, <https://doi.org/10.1175/MWR-D-14-00395.1>.
- Hamill, T. M., 2001: Interpretation of rank histograms for verifying ensemble forecasts. *Mon. Wea. Rev.*, **129**, 550–560, [https://doi.org/10.1175/1520-0493\(2001\)129<0550:IORHFV>2.0.CO;2](https://doi.org/10.1175/1520-0493(2001)129<0550:IORHFV>2.0.CO;2).
- Hamill, T. M., and C. Snyder, 2000: A hybrid ensemble Kalman filter-3D variational analysis scheme. *Mon. Wea. Rev.*, **128**, 2905–2919, [https://doi.org/10.1175/1520-0493\(2000\)128<2905:AHEKVF>2.0.CO;2](https://doi.org/10.1175/1520-0493(2000)128<2905:AHEKVF>2.0.CO;2).
- Han, W., and N. Bormman, 2016: Constrained Adaptive Bias Correction for Satellite Radiance Assimilation in the ECMWF 4D-Var System. ECMWF Technical Memoranda, No. 783, ECMWF, Shinfield Park, 1–60, <https://doi.org/10.21957/rex0omex>.
- Han, W., R. Y. Yin, J. Li, et al., 2023: Assimilation of geostationary hyperspectral infrared sounders (GeoHIS): Progresses and perspectives. *Numerical Weather Prediction: East Asian Perspectives*, S. K. Park, Ed., Springer, Cham, 205–216, [https://doi.org/10.1007/978-3-031-40567-9\\_8](https://doi.org/10.1007/978-3-031-40567-9_8).
- Han, W., R. Y. Yin, J. Li, et al., 2025: Targeted sounding observations from geostationary satellite and impacts on high impact weather forecasts. *Sci. China Earth Sci.*, **68**, 963–976, <https://doi.org/10.1007/s11430-024-1489-5>.
- Hatfield, S., M. Chantry, P. Dueben, et al., 2021: Building tangent-linear and adjoint models for data assimilation with neural networks. *J. Adv. Model. Earth Syst.*, **13**, e2021MS002521, <https://doi.org/10.1029/2021MS002521>.
- Hawkins-Smith, L. D., and D. Simonin, 2021: Radar reflectivity assimilation using hourly cycling 4D-Var in the Met Office Unified Model. *Quart. J. Roy. Meteor. Soc.*, **147**, 1516–1538, <https://doi.org/10.1002/qj.3977>.
- He, H., L. L. Lei, J. S. Whitaker, et al., 2020: Impacts of assimilation frequency on ensemble Kalman filter data assimilation

- and imbalances. *J. Adv. Model. Earth Syst.*, **12**, e2020MS002 187, <https://doi.org/10.1029/2020MS002187>.
- He, L. L., and F. Z. Weng, 2023: Improved microwave ocean emissivity and reflectivity models derived from two-scale roughness theory. *Adv. Atmos. Sci.*, **40**, 1923–1938, <https://doi.org/10.1007/s00376-023-2247-y>.
- He, Y. J., B. Wang, M. M. Liu, et al., 2017: Reduction of initial shock in decadal predictions using a new initialization strategy. *Geophys. Res. Lett.*, **44**, 8538–8547, <https://doi.org/10.1002/2017GL074028>.
- Healy, S. B., A. M. Jupp, and C. Marquardt, 2005: Forecast impact experiment with GPS radio occultation measurements. *Geophys. Res. Lett.*, **32**, L03804, <https://doi.org/10.1029/2004GL020806>.
- Hoke, J. E., and R. A. Anthes, 1976: The initialization of numerical models by a dynamic-initialization technique. *Mon. Wea. Rev.*, **104**, 1551–1556, [https://doi.org/10.1175/1520-0493\(1976\)104<1551:TIONMB>2.0.CO;2](https://doi.org/10.1175/1520-0493(1976)104<1551:TIONMB>2.0.CO;2).
- Hollingsworth, A., D. B. Shaw, P. Lönnberg, et al., 1986: Monitoring of observation and analysis quality by a data assimilation system. *Mon. Wea. Rev.*, **114**, 861–879, [https://doi.org/10.1175/1520-0493\(1986\)114<0861:MOOAAQ>2.0.CO;2](https://doi.org/10.1175/1520-0493(1986)114<0861:MOOAAQ>2.0.CO;2).
- Houtekamer, P. L., and H. L. Mitchell, 1998: Data assimilation using an ensemble Kalman filter technique. *Mon. Wea. Rev.*, **126**, 796–811, [https://doi.org/10.1175/1520-0493\(1998\)126<0796:DAUAEK>2.0.CO;2](https://doi.org/10.1175/1520-0493(1998)126<0796:DAUAEK>2.0.CO;2).
- Houtekamer, P. L., and H. L. Mitchell, 2001: A sequential ensemble Kalman filter for atmospheric data assimilation. *Mon. Wea. Rev.*, **129**, 123–137, [https://doi.org/10.1175/1520-0493\(2001\)129<0123:ASEKFF>2.0.CO;2](https://doi.org/10.1175/1520-0493(2001)129<0123:ASEKFF>2.0.CO;2).
- Houtekamer, P. L., and H. L. Mitchell, 2005: Ensemble Kalman filtering. *Quart. J. Roy. Meteor. Soc.*, **131**, 3269–3289, <https://doi.org/10.1256/qj.05.135>.
- Houtekamer, P. L., L. Lefavre, J. Derome, et al., 1996: A system simulation approach to ensemble prediction. *Mon. Wea. Rev.*, **124**, 1225–1242, [https://doi.org/10.1175/1520-0493\(1996\)124<1225:ASSATE>2.0.CO;2](https://doi.org/10.1175/1520-0493(1996)124<1225:ASSATE>2.0.CO;2).
- Houtekamer, P. L., H. L. Mitchell, G. Pellerin, et al., 2005: Atmospheric data assimilation with an ensemble Kalman filter: Results with real observations. *Mon. Wea. Rev.*, **133**, 604–620, <https://doi.org/10.1175/MWR-2864.1>.
- Houtekamer, P. L., X. X. Deng, H. L. Mitchell, et al., 2014: Higher resolution in an operational ensemble Kalman filter. *Mon. Wea. Rev.*, **142**, 1143–1162, <https://doi.org/10.1175/MWR-D-13-00138.1>.
- Howard, L. J., A. Subramanian, and I. Hoteit, 2024: A machine learning augmented data assimilation method for high-resolution observations. *J. Adv. Model. Earth Syst.*, **16**, e2023MS003774, <https://doi.org/10.1029/2023MS003774>.
- Huang, J., Y. D. Chen, H. Q. Chen, et al., 2022: Real-time background-dependent indirect assimilation of radar reflectivity factor and experiments for multi heavy rainfall cases. *Chinese J. Atmos. Sci.*, **46**, 691–706, <https://doi.org/10.3878/j.issn.1006-9895.2201.21145>. (in Chinese)
- Huang, L. P., D. H. Chen, L. T. Deng, et al., 2017: Main technical improvements of GRAPES\_Meso V4.0 and verification. *J. Appl. Meteor. Sci.*, **28**, 25–37, <https://doi.org/10.11898/1001-7313.20170103>. (in Chinese)
- Huang, L. P., L. T. Deng, R. C. Wang, et al., 2022: Key technologies of CMA-MESO and application to operational forecast. *J. Appl. Meteor. Sci.*, **33**, 641–654, <https://doi.org/10.11898/1001-7313.20220601>. (in Chinese)
- Huang, L. W., L. Gianinazzi, Y. J. Yu, et al., 2024: DiffDA: A diffusion model for weather-scale Data Assimilation. arXiv, 2401.05932, <https://doi.org/10.48550/arXiv.2401.05932>.
- Huang, S. X., J. J. Teng, J. Xiang, et al., 2003: Generalized variational optimization analysis method of 3-D wind field. Proceedings of the National Symposium on Hydrodynamics and National Conference on Hydrodynamics, China Ocean Press, Beijing, 131–140. (in Chinese)
- Hunt, B. R., E. J. Kostelich, and I. Szunyogh, 2007: Efficient data assimilation for spatiotemporal chaos: A local ensemble transform Kalman filter. *Phys. D Nonlinear Phenom.*, **230**, 112–126, <https://doi.org/10.1016/j.physd.2006.11.008>.
- Irvine, E. A., S. L. Gray, J. Methven, et al., 2011: Forecast impact of targeted observations: Sensitivity to observation error and proximity to steep orography. *Mon. Wea. Rev.*, **139**, 69–78, <https://doi.org/10.1175/2010MWR3459.1>.
- Jansa, A., P. Arbogast, A. Doerenbecher, et al., 2011: A new approach to sensitivity climatologies: The DTS-MEDEX-2009 campaign. *Nat. Hazards Earth Syst. Sci.*, **11**, 2381–2390, <https://doi.org/10.5194/nhess-11-2381-2011>.
- Jerger, D., 2013: Radar forward operator for verification of cloud resolving simulations within the COSMO model. Ph.D. dissertation, Karlsruher Institut für Technologie, Karlsruhe, <https://doi.org/10.5445/KSP/1000038411>.
- Jiang, L., W. S. Duan, and H. L. Liu, 2022: The most sensitive initial error of sea surface height anomaly forecasts and its implication for target observations of mesoscale eddies. *J. Phys. Oceanogr.*, **52**, 723–740, <https://doi.org/10.1175/JPO-D-21-0200.1>.
- Jiang, L., W. S. Duan, and H. Wang, 2024: The sensitive area for targeting observations of paired mesoscale eddies associated with sea surface height anomaly forecasts. *J. Geophys. Res. Oceans*, **129**, e2023JC020572, <https://doi.org/10.1029/2023JC020572>.
- Jiao, M. Y., 2010: *Modern Numerical Weather Prediction Operations*. Meteorological Press, Beijing, 260 pp. (in Chinese)
- Johnson, B. T., C. Dang, P. Stegmann, et al., 2023: The Community Radiative Transfer Model (CRTM): Community-focused collaborative model development accelerating research to operations. *Bull. Amer. Meteor. Soc.*, **104**, E1817–E1830, <https://doi.org/10.1175/BAMS-D-22-0015.1>.
- Jones, T. A., D. J. Stensrud, P. Minnis, et al., 2013: Evaluation of a forward operator to assimilate cloud water path into WRF-DART. *Mon. Wea. Rev.*, **141**, 2272–2289, <https://doi.org/10.1175/MWR-D-12-00238.1>.
- Joo, S., J. Eyre, and R. Marriott, 2013: The impact of MetOp and other satellite data within the Met Office global NWP system using an adjoint-based sensitivity method. *Mon. Wea. Rev.*, **141**, 3331–3342, <https://doi.org/10.1175/MWR-D-12-00232.1>.
- Joo, S.-W., and D.-K. Lee, 2002: The use of ATOVS data in Korea Meteorological Administration (KMA). Proceedings of the 12th International TOVS Study Conference, BMRC, Lorne, Australia, 128–137.
- Jung, Y., G. F. Zhang, and M. Xue, 2008a: Assimilation of simulated polarimetric radar data for a convective storm using the ensemble Kalman filter. Part I: Observation operators for re-

- flectivity and polarimetric variables. *Mon. Wea. Rev.*, **136**, 2228–2245, <https://doi.org/10.1175/2007MWR2083.1>.
- Jung, Y., M. Xue, G. F. Zhang, et al., 2008b: Assimilation of simulated polarimetric radar data for a convective storm using the ensemble Kalman filter. Part II: Impact of polarimetric data on storm analysis. *Mon. Wea. Rev.*, **136**, 2246–2260, <https://doi.org/10.1175/2007MWR2288.1>.
- Kalman, R. E., 1960: A new approach to linear filtering and prediction problems. *J. Basic Eng.*, **82**, 35–45, <https://doi.org/10.1115/1.3662552>.
- Kalman, R. E., and R. S. Bucy, 1961: New results in linear filtering and prediction theory. *J. Basic Eng.*, **83**, 95–108, <https://doi.org/10.1115/1.3658902>.
- Kalnay, E., 2003: *Atmospheric Modeling, Data Assimilation, and Predictability*. Cambridge University Press, Cambridge, 341 pp.
- Kalnay, E., and S.-C. Yang, 2010: Accelerating the spin-up of ensemble Kalman filtering. *Quart. J. Roy. Meteor. Soc.*, **136**, 1644–1651, <https://doi.org/10.1002/qj.652>.
- Kalnay, E., D. L. T. Anderson, A. F. Bennett, et al., 1997: Data assimilation in the ocean and in the atmosphere: What should be next? *J. Meteor. Soc. Japan Ser. II*, **75**, 489–496, [https://doi.org/10.2151/jmsj1965.75.1B\\_489](https://doi.org/10.2151/jmsj1965.75.1B_489).
- Kan, W. L., Y.-N. Shi, J. Yang, et al., 2024: Improvements of the microwave gaseous absorption scheme based on statistical regression and its application to ARMS. *J. Geophys. Res. Atmos.*, **129**, e2024JD040732, <https://doi.org/10.1029/2024JD040732>.
- Kang, J.-S., E. Kalnay, J. J. Liu, et al., 2011: “Variable localization” in an ensemble Kalman filter: Application to the carbon cycle data assimilation. *J. Geophys. Res. Atmos.*, **116**, D09110, <https://doi.org/10.1029/2010JD014673>.
- Karbou, F., É. Gérard, and F. Rabier, 2006: Microwave land emissivity and skin temperature for AMSU-A and -B assimilation over land. *Quart. J. Roy. Meteor. Soc.*, **132**, 2333–2355, <https://doi.org/10.1256/qj.05.216>.
- Karbou, F., E. Gérard, and F. Rabier, 2010: Global 4DVAR assimilation and forecast experiments using AMSU observations over land. Part I: Impacts of various land surface emissivity parameterizations. *Wea. Forecasting*, **25**, 5–19, <https://doi.org/10.1175/2009WAF2222243.1>.
- Kawabata, T., T. Schwitalla, A. Adachi, et al., 2018: Observational operators for dual polarimetric radars in variational data assimilation systems (PolRad VAR v1.0). *Geosci. Model Dev.*, **11**, 2493–2501, <https://doi.org/10.5194/gmd-11-2493-2018>.
- Kelly, G. A. M., G. A. Mills, and W. L. Smith, 1978: Impact of Nimbus-6 temperature soundings on Australian region forecasts. *Bull. Amer. Meteor. Soc.*, **59**, 393–406, <https://doi.org/10.1175/1520-0477-59.4.393>.
- Kleist, D. T., and K. Ide, 2015a: An OSSE-based evaluation of hybrid variational-ensemble data assimilation for the NCEP GFS. Part I: System description and 3D-hybrid results. *Mon. Wea. Rev.*, **143**, 433–451, <https://doi.org/10.1175/MWR-D-13-00351.1>.
- Kleist, D. T., and K. Ide, 2015b: An OSSE-based evaluation of hybrid variational-ensemble data assimilation for the NCEP GFS. Part II: 4DEnVar and hybrid variants. *Mon. Wea. Rev.*, **143**, 452–470, <https://doi.org/10.1175/MWR-D-13-00350.1>.
- Koo, C. C., 1958a: On the equivalency of formulations of weather forecasting as an initial value problem and as an “evolution” problem. *Acta Meteor. Sinica*, **29**, 93–98, <https://doi.org/10.1167/qxxb1958.011>. (in Chinese)
- Koo, C. C., 1958b: On the utilization of past data in numerical weather forecasting. *Acta Meteor. Sinica*, **29**, 176–184, <https://doi.org/10.1167/qxxb1958.019>. (in Chinese)
- Kotsuki, S., K. Shiraishi, and A. Okazaki, 2024: Ensemble data assimilation to diagnose AI-based weather prediction model: A case with ClimaX version 0.3.1. arXiv, 2407.17781, <https://doi.org/10.48550/arXiv.2407.17781>.
- Krishnan, R. G., U. Shalit, and D. Sontag, 2015: Deep Kalman filters. arXiv, 1511.05121, <https://doi.org/10.48550/arXiv.1511.05121>.
- Krishnan, R. G., U. Shalit, and D. Sontag, 2017: Structured inference networks for nonlinear state space models. Proceedings of the 31st AAAI Conference on Artificial Intelligence, AAAI, San Francisco, USA, 2101–2109, <https://doi.org/10.1609/aaai.v31i1.10779>.
- Krzeminski, B., N. Bormann, F. Karbou, et al., 2009: Improved use of surface-sensitive microwave radiances at ECMWF. Proceedings of the EUMETSAT Meteorol. Satell. Conf., Bath, UK, 21–25 September, EUMETSAT, 1–8.
- Lai, A. W., J. Z. Min, J. D. Gao, et al., 2020: Assimilation of radar data, pseudo water vapor, and potential temperature in a 3DVAR framework for improving precipitation forecast of severe weather events. *Atmosphere*, **11**, 182, <https://doi.org/10.3390/atmos11020182>.
- Laloyaux, P., M. Balmaseda, D. Dee, et al., 2016: A coupled data assimilation system for climate reanalysis. *Quart. J. Roy. Meteor. Soc.*, **142**, 65–78, <https://doi.org/10.1002/qj.2629>.
- Lan, W. R., J. Zhu, M. Xue, et al., 2010a: Storm-scale ensemble Kalman filter data assimilation experiments using simulated Doppler radar data. Part I: Perfect model tests. *Chinese J. Atmos. Sci.*, **34**, 640–652, <https://doi.org/10.3878/j.issn.1006-9895.2010.03.15>. (in Chinese)
- Lan, W. R., J. Zhu, M. Xue, et al., 2010b: Storm-scale ensemble Kalman filter data assimilation experiments using simulated Doppler radar data Part II: Imperfect model tests. *Chinese J. Atmos. Sci.*, **34**, 737–753, <https://doi.org/10.3878/j.issn.1006-9895.2010.04.07>. (in Chinese)
- Lei, J., and P. Bickel, 2011: A moment matching ensemble filter for nonlinear non-Gaussian data assimilation. *Mon. Wea. Rev.*, **139**, 3964–3973, <https://doi.org/10.1175/2011MWR3553.1>.
- Lei, L. L., and J. L. Anderson, 2014a: Comparisons of empirical localization techniques for serial ensemble Kalman filters in a simple atmospheric general circulation model. *Mon. Wea. Rev.*, **142**, 739–754, <https://doi.org/10.1175/MWR-D-13-00152.1>.
- Lei, L. L., and J. L. Anderson, 2014b: Impacts of frequent assimilation of surface pressure observations on atmospheric analyses. *Mon. Wea. Rev.*, **142**, 4477–4483, <https://doi.org/10.1175/MWR-D-14-00097.1>.
- Lei, L. L., and J. S. Whitaker, 2016: A four-dimensional incremental analysis update for the ensemble Kalman filter. *Mon. Wea. Rev.*, **144**, 2605–2621, <https://doi.org/10.1175/MWR-D-15-0246.1>.
- Lei, L. L., D. R. Stauffer, S. E. Haupt, et al., 2012: A hybrid nudging-ensemble Kalman filter approach to data assimila-

- tion. Part I: Application in the Lorenz system. *Tellus A Dyn. Meteor. Oceanogr.*, **64**, 18484, <https://doi.org/10.3402/tellusa.v64i0.18484>.
- Lei, L. L., J. L. Anderson, and G. S. Romine, 2015: Empirical localization functions for ensemble Kalman filter data assimilation in regions with and without precipitation. *Mon. Wea. Rev.*, **143**, 3664–3679, <https://doi.org/10.1175/MWR-D-14-00415.1>.
- Lei, L. L., J. S. Whitaker, and C. Bishop, 2018: Improving assimilation of radiance observations by implementing model space localization in an ensemble Kalman filter. *J. Adv. Model. Earth Syst.*, **10**, 3221–3232, <https://doi.org/10.1029/2018MS001468>.
- Lei, L. L., J. S. Whitaker, J. L. Anderson, et al., 2020: Adaptive localization for satellite radiance observations in an ensemble Kalman filter. *J. Adv. Model. Earth Syst.*, **12**, e2019MS001693, <https://doi.org/10.1029/2019MS001693>.
- Lei, L. L., Z. R. Wang, and Z.-M. Tan, 2021: Integrated hybrid data assimilation for an ensemble Kalman filter. *Mon. Wea. Rev.*, **149**, 4091–4105, <https://doi.org/10.1175/MWR-D-21-0002.1>.
- Lei, X. T., X. F. Zhang, W. S. Duan, et al., 2019: Experiment on coordinated observation of offshore typhoon in China. *Adv. Earth Sci.*, **34**, 671–678, <https://doi.org/10.11867/j.issn.1001-8166.2019.07.0671>. (in Chinese)
- Lewis, J. M., and J. C. Derber, 1985: The use of adjoint equations to solve a variational adjustment problem with advective constraints. *Tellus A*, **37A**, 309–322, <https://doi.org/10.1111/j.1600-0870.1985.tb00430.x>.
- Li, G., Z. J. Wu, and H. Zhang, 2016: Bias correction of infrared atmospheric sounding interferometer radiances for data assimilation. *Trans. Atmos. Sci.*, **39**, 72–80, <https://doi.org/10.13878/j.cnki.dqkxxb.20140228001>. (in Chinese)
- Li, J., and G. Q. Liu, 2016: Direct assimilation of Chinese FY-3C Microwave Temperature Sounder-2 radiances in the global GRAPES system. *Atmos. Meas. Tech.*, **9**, 3095–3113, <https://doi.org/10.5194/amt-9-3095-2016>.
- Li, J., C.-Y. Liu, H.-L. Huang, et al., 2005: Optimal cloud-clearing for AIRS radiances using MODIS. *IEEE Trans. Geosci. Remote Sens.*, **43**, 1266–1278, <https://doi.org/10.1109/TGRS.2005.847795>.
- Li, J., Z. K. Qin, and G. Q. Liu, 2016: A new generation of Chinese FY-3C microwave sounding measurements and the initial assessments of its observations. *Int. J. Remote Sens.*, **37**, 4035–4058, <https://doi.org/10.1080/01431161.2016.1207260>.
- Li, J., A. J. Geer, K. Okamoto, et al., 2022a: Satellite all-sky infrared radiance assimilation: Recent progress and future perspectives. *Adv. Atmos. Sci.*, **39**, 9–21, <https://doi.org/10.1007/s00376-021-1088-9>.
- Li, J., Y. R. Zhang, D. Di, et al., 2022b: The influence of sub-footprint cloudiness on three-dimensional horizontal wind from geostationary hyperspectral infrared sounder observations. *Geophys. Res. Lett.*, **49**, e2022GL098460, <https://doi.org/10.1029/2022GL098460>.
- Li, J., Z. K. Qin, G. Q. Liu, et al., 2024: Added benefit of the early-morning-orbit satellite Fengyun-3E on the global microwave sounding of the three-orbit constellation. *Adv. Atmos. Sci.*, **41**, 39–52, <https://doi.org/10.1007/s00376-023-2388-z>.
- Li, J. H., Y. D. Gao, and Q. L. Wan, 2018: Sample optimization of ensemble forecast to simulate a tropical cyclone using the observed track. *Atmos. Ocean*, **56**, 162–177, <https://doi.org/10.1080/07055900.2018.1500881>.
- Li, X., C. Chen, X. Shen, et al., 2020: Review on development of a scalable high-order nonhydrostatic multi-moment constrained finite volume dynamical core. arXiv, 2004.05784, <https://doi.org/10.48550/arXiv.2004.05784>.
- Li, X. L., and Y. Z. Liu, 2019: The improvement of GRAPES global extratropical singular vectors and experimental study. *Acta Meteor. Sinica*, **77**, 552–562, <https://doi.org/10.11676/qxb2019.020>. (in Chinese)
- Li, X. L., J. R. Mecikalski, and D. Posselt, 2017: An ice-phase microphysics forward model and preliminary results of polarimetric radar data assimilation. *Mon. Wea. Rev.*, **145**, 683–708, <https://doi.org/10.1175/MWR-D-16-0035.1>.
- Li, Y. Z., X. G. Wang, and M. Xue, 2012: Assimilation of radar radial velocity data with the WRF hybrid ensemble-3DVAR system for the prediction of Hurricane Ike (2008). *Mon. Wea. Rev.*, **140**, 3507–3524, <https://doi.org/10.1175/MWR-D-12-00043.1>.
- Li, Z. C., 1994: Medium-range numerical weather prediction system at the national meteorological center of China. *Acta Meteor. Sinica*, **52**, 297–307, <https://doi.org/10.11676/qxb1994.038>. (in Chinese)
- Li, Z. C., and G. Q. Qiu, 1992: Operational system for medium-range numerical weather prediction. *Meteor. Mon.*, **18**, 50–52. (in Chinese)
- Li, Z. T., and W. Han, 2024: Impact of HY-2B SMR radiance assimilation on CMA global medium-range weather forecasts. *Quart. J. Roy. Meteor. Soc.*, **150**, 937–957, <https://doi.org/10.1002/qj.4630>.
- Lian, Z. H., and J. S. Xue, 2010: A new surface pressure interpolation scheme for calculation of observations-equivalent quantities lower than model terrain. *J. Trop. Meteor.*, **26**, 489–493, <https://doi.org/10.3969/j.issn.1004-4965.2010.04.014>. (in Chinese)
- Liang, J. Y., K. Terasaki, and T. Miyoshi, 2023: A machine learning approach to the observation operator for satellite radiance data assimilation. *J. Meteor. Soc. Japan Ser. II*, **101**, 79–95, <https://doi.org/10.2151/jmsj.2023-005>.
- Liang, X. D., 2007: An integrating velocity–azimuth process single-Doppler radar wind retrieval method. *J. Atmos. Oceanic Technol.*, **24**, 658–665, <https://doi.org/10.1175/JTECH2047.1>.
- Liu, C. S., Q. N. Xiao, and B. Wang, 2008: An ensemble-based four-dimensional variational data assimilation scheme. Part I: Technical formulation and preliminary test. *Mon. Wea. Rev.*, **136**, 3363–3373, <https://doi.org/10.1175/2008MWR2312.1>.
- Liu, C. S., M. Xue, and R. Kong, 2019: Direct assimilation of radar reflectivity data using 3DVAR: Treatment of hydrometeor background errors and OSSE tests. *Mon. Wea. Rev.*, **147**, 17–29, <https://doi.org/10.1175/MWR-D-18-0033.1>.
- Liu, C. S., M. Xue, and R. Kong, 2020: Direct variational assimilation of radar reflectivity and radial velocity data: Issues with nonlinear reflectivity operator and solutions. *Mon. Wea. Rev.*, **148**, 1483–1502, <https://doi.org/10.1175/MWR-D-19-0149.1>.
- Liu, C. S., H. Q. Li, M. Xue, et al., 2022: Use of a reflectivity operator based on double-moment Thompson microphysics for

- direct assimilation of radar reflectivity in GSI-based hybrid En3DVar. *Mon. Wea. Rev.*, **150**, 907–926, <https://doi.org/10.1175/MWR-D-21-0040.1>.
- Liu, H.-Y., Y. Q. Wang, J. Xu, et al., 2018: A dynamical initialization scheme for tropical cyclones under the influence of terrain. *Wea. Forecasting*, **33**, 641–659, <https://doi.org/10.1175/WAF-D-17-0139.1>.
- Liu, H., J. Xue, J. Gu, et al., 2010: GRAPES 3DVAR radar data assimilation and numerical simulation experiments with a torrential rain case. *Acta Meteoro. Sinica*, **68**, 779–789, <https://doi.org/10.11676/qxxb2010.074>.
- Liu, K., W. H. Guo, L. L. Da, et al., 2021: Improving the thermal structure predictions in the Yellow Sea by conducting targeted observations in the CNOP-identified sensitive areas. *Sci. Rep.*, **11**, 19518, <https://doi.org/10.1038/s41598-021-9894-7>.
- Liu, R. X., Q. F. Lu, C. Q. Wu, et al., 2024: Assimilation of hyperspectral infrared atmospheric sounder data of FengYun-3E satellite and assessment of its impact on analyses and forecasts. *Remote Sens.*, **16**, 908, <https://doi.org/10.3390/rs16050908>.
- Liu, Y., and J. S. Xue, 2014: Assimilation of global navigation satellite radio occultation observations in GRAPES: Operational implementation. *J. Meteor. Res.*, **28**, 1061–1074, <https://doi.org/10.1007/s13351-014-4028-0>.
- Liu, Y. Z., X. S. Shen, and X. L. Li, 2013: Research on the singular vector perturbation of the GRAPES global model based on the total energy norm. *Acta Meteoro. Sinica*, **71**, 517–526, <https://doi.org/10.11676/qxxb2013.043>. (in Chinese)
- Liu, Y. Z., J. D. Gong, L. Zhang, et al., 2019: Influence of linearized physical processes on the GRAPES 4DVAR. *Acta Meteoro. Sinica*, **77**, 196–209, <https://doi.org/10.11676/qxxb2019.013>. (in Chinese)
- Lorenc, A. C., 1981: A global three-dimensional multivariate statistical interpolation scheme. *Mon. Wea. Rev.*, **109**, 701–721, [https://doi.org/10.1175/1520-0493\(1981\)109<0701:AGTDMS>2.0.CO;2](https://doi.org/10.1175/1520-0493(1981)109<0701:AGTDMS>2.0.CO;2).
- Lorenc, A. C., 1986: Analysis methods for numerical weather prediction. *Quart. J. Roy. Meteor. Soc.*, **112**, 1177–1194, <https://doi.org/10.1002/qj.49711247414>.
- Lorenc, A. C., 1997: Development of an operational variational assimilation scheme. *J. Meteor. Soc. Japan Ser. II*, **75**, 339–346, [https://doi.org/10.2151/jmsj1965.75.1B\\_339](https://doi.org/10.2151/jmsj1965.75.1B_339).
- Lorenc, A. C., 2003: The potential of the ensemble Kalman filter for NWP—a comparison with 4D-Var. *Quart. J. Roy. Meteor. Soc.*, **129**, 3183–3203, <https://doi.org/10.1256/qj.02.132>.
- Lorenc, A. C., N. E. Bowler, A. M. Clayton, et al., 2015: Comparison of Hybrid-4DEnVar and Hybrid-4DVar data assimilation methods for Global NWP. *Mon. Wea. Rev.*, **143**, 212–229, <https://doi.org/10.1175/MWR-D-14-00195.1>.
- Lu, N. M., and S. Y. Gu, 2016: The status and prospects of atmospheric microwave sounding by geostationary meteorological satellite. *Adv. Meteor. Sci. Technol.*, **6**, 120–123, <https://doi.org/10.3969/j.issn.2095-1973.2016.01.019>. (in Chinese)
- Lu, Y., F. M. Ren, and W. J. Zhu, 2018: Risk zoning of typhoon disasters in Zhejiang Province, China. *Nat. Hazards Earth Syst. Sci.*, **18**, 2921–2932, <https://doi.org/10.5194/nhess-18-2921-2018>.
- Luo, T. L., S. Ma, W. M. Zhang, et al., 2025: Assimilation of AMSU-A data using the ARMS as an observation operator in the YH4DVAR system. *J. Meteor. Res.*, **39**, 252–271, <https://doi.org/10.1007/s13351-025-4206-2>.
- Luo, Y., X. D. Liang, and M. X. Chen, 2014: Improvement of radial wind data assimilation of single Doppler radar. *J. Meteor. Sci.*, **34**, 620–628, <https://doi.org/10.3969/2013jms.0038>. (in Chinese)
- Lynch, P., and X.-Y. Huang, 1992: Initialization of the HIRLAM model using a digital filter. *Mon. Wea. Rev.*, **120**, 1019–1034, [https://doi.org/10.1175/1520-0493\(1992\)120<1019:ITHMU>2.0.CO;2](https://doi.org/10.1175/1520-0493(1992)120<1019:ITHMU>2.0.CO;2).
- Ma, H., X. D. Liang, Y. Luo, et al., 2016: Application of advanced observation operator of Doppler radar radial velocity assimilation in GRAPES\_3Dvar. *Meteor. Mon.*, **42**, 34–43, <https://doi.org/10.7519/j.issn.1000-0526.2016.01.004>. (in Chinese)
- Ma, Z., J. Li, W. Han, et al., 2021: Four-dimensional wind fields from geostationary hyperspectral infrared sounder radiance measurements with high temporal resolution. *Geophys. Res. Lett.*, **48**, e2021GL093794, <https://doi.org/10.1029/2021GL093794>.
- Malartic, Q., A. Farchi, and M. Bocquet, 2022: State, global, and local parameter estimation using local ensemble Kalman filters: Applications to online machine learning of chaotic dynamics. *Quart. J. Roy. Meteor. Soc.*, **148**, 2167–2193, <https://doi.org/10.1002/qj.4297>.
- Matricardi, M., and A. P. McNally, 2014: The direct assimilation of principal components of IASI spectra in the ECMWF 4D-Var. *Quart. J. Roy. Meteor. Soc.*, **140**, 573–582, <https://doi.org/10.1002/qj.2156>.
- McNally, A. P., and M. Vesperini, 1996: Variational analysis of humidity information from TOVS radiances. *Quart. J. Roy. Meteor. Soc.*, **122**, 1521–1544, <https://doi.org/10.1002/qj.49712253504>.
- McNally, A. P., and P. D. Watts, 2003: A cloud detection algorithm for high-spectral-resolution infrared sounders. *Quart. J. Roy. Meteor. Soc.*, **129**, 3411–3423, <https://doi.org/10.1256/qj.02.208>.
- McPherson, R. D., K. H. Bergman, R. E. Kistler, et al., 1979: The NMC operational global data assimilation system. *Mon. Wea. Rev.*, **107**, 1445–1461, [https://doi.org/10.1175/1520-0493\(1979\)107<1445:TNOGDA>2.0.CO;2](https://doi.org/10.1175/1520-0493(1979)107<1445:TNOGDA>2.0.CO;2).
- Meng, D. M., Y. D. Chen, H. L. Wang, et al., 2019: The evaluation of EnVar method including hydrometeors analysis variables for assimilating cloud liquid/ice water path on prediction of rainfall events. *Atmos. Res.*, **219**, 1–12, <https://doi.org/10.1016/j.atmosres.2018.12.017>.
- Meng, D. M., Z.-M. Tan, J. Li, et al., 2024: Added value of three-dimensional horizontal winds from geostationary interferometric infrared sounder for typhoon forecast in a regional NWP model. *J. Geophys. Res. Atmos.*, **129**, e2024JD040736, <https://doi.org/10.1029/2024JD040736>.
- Meng, Z. Y., and F. Q. Zhang, 2008: Tests of an ensemble Kalman filter for mesoscale and regional-scale data assimilation. Part III: Comparison with 3DVAR in a real-data case study. *Mon. Wea. Rev.*, **136**, 522–540, <https://doi.org/10.1175/2007MWR2106.1>.
- Meng, Z. Y., F. Q. Zhang, D. H. Luo, et al., 2019: Review of Chinese atmospheric science research over the past 70 years:

- Synoptic meteorology. *Sci. China Earth Sci.*, **62**, 1946–1991, <https://doi.org/10.1007/s11430-019-9534-6>.
- Ming, J., and J. A. Zhang, 2018: Direct measurements of momentum flux and dissipative heating in the surface layer of tropical cyclones during landfalls. *J. Geophys. Res. Atmos.*, **123**, 4926–4938, <https://doi.org/10.1029/2017JD028076>.
- Ming, J., J. A. Zhang, R. F. Rogers, et al., 2014: Multiplatform observations of boundary layer structure in the outer rainbands of landfalling typhoons. *J. Geophys. Res. Atmos.*, **119**, 7799–7814, <https://doi.org/10.1002/2014JD021637>.
- Mishchenko, M. I., A. A. Lacis, and L. D. Travis, 1994: Errors induced by the neglect of polarization in radiance calculations for Rayleigh-scattering atmospheres. *J. Quant. Spectrosc. Radiat. Transfer*, **51**, 491–510, [https://doi.org/10.1016/0022-4073\(94\)90149-X](https://doi.org/10.1016/0022-4073(94)90149-X).
- Miyoshi, T., 2011: The Gaussian approach to adaptive covariance inflation and its implementation with the local ensemble transform Kalman filter. *Mon. Wea. Rev.*, **139**, 1519–1535, <https://doi.org/10.1175/2010MWR3570.1>.
- Miyoshi, T., and K. Kondo, 2013: A multiscale localization approach to an ensemble Kalman filter. *SOLA*, **9**, 170–173, <https://doi.org/10.2151/sola.2013-038>.
- Mu, M., W. S. Duan, and B. Wang, 2003: Conditional nonlinear optimal perturbation and its applications. *Nonlinear Processes Geophys.*, **10**, 493–501, <https://doi.org/10.5194/npg-10-493-2003>.
- Mu, M., F. F. Zhou, and H. L. Wang, 2009: A method for identifying the sensitive areas in targeted observations for tropical cyclone prediction: Conditional nonlinear optimal perturbation. *Mon. Wea. Rev.*, **137**, 1623–1639, <https://doi.org/10.1175/2008MWR2640.1>.
- Mu, M., R. Feng, and W. S. Duan, 2017: Relationship between optimal precursors for Indian Ocean Dipole events and optimally growing initial errors in its prediction. *J. Geophys. Res. Oceans*, **122**, 1141–1153, <https://doi.org/10.1002/2016JC012527>.
- Mu, X. Y., Q. Xu, Y. J. Pan, et al., 2019: Contrast experiment of different coordinate remapping schemes in radar velocity data assimilation. *Plateau Meteor.*, **38**, 625–635, <https://doi.org/10.7522/j.issn.1000-0534.2019.00012>. (in Chinese)
- Ohring, G., 1979: Impact of satellite temperature sounding data on weather forecasts. *Bull. Amer. Meteor. Soc.*, **60**, 1142–1147, [https://doi.org/10.1175/1520-0477\(1979\)060<1142:IOS-TSD>2.0.CO;2](https://doi.org/10.1175/1520-0477(1979)060<1142:IOS-TSD>2.0.CO;2).
- Okamoto, K., Y. Takeuchi, Y. Kaido, et al., 2002: Recent developments in assimilation of ATOVS at JMA. Proceedings of the 12th International TOVS Study Conference, BMRC, Lorne, Australia, 226–233.
- Okamoto, K., A. P. McNally, and W. Bell, 2014: Progress towards the assimilation of all-sky infrared radiances: An evaluation of cloud effects. *Quart. J. Roy. Meteor. Soc.*, **140**, 1603–1614, <https://doi.org/10.1002/qj.2242>.
- Oue, M., A. Tatarevic, P. Kollias, et al., 2020: The Cloud-resolving model Radar SIMulator (CR-SIM) Version 3.3: Description and applications of a virtual observatory. *Geosci. Model Dev.*, **13**, 1975–1998, <https://doi.org/10.5194/gmd-13-1975-2020>.
- Palmer, T. N., R. Gelaro, J. Barkmeijer, et al., 1998: Singular vectors, metrics, and adaptive observations. *J. Atmos. Sci.*, **55**, 633–653, [https://doi.org/10.1175/1520-0469\(1998\)055<0633:SVMAAO>2.0.CO;2](https://doi.org/10.1175/1520-0469(1998)055<0633:SVMAAO>2.0.CO;2).
- Panofsky, R. A., 1949: Objective weather-map analysis. *J. Atmos. Sci.*, **6**, 386–392, [https://doi.org/10.1175/1520-0469\(1949\)006<0386:OWMA>2.0.CO;2](https://doi.org/10.1175/1520-0469(1949)006<0386:OWMA>2.0.CO;2).
- Parrish, D. F., and J. C. Derber, 1992: The National Meteorological Center's spectral statistical-interpolation analysis system. *Mon. Wea. Rev.*, **120**, 1747–1763, [https://doi.org/10.1175/1520-0493\(1992\)120<1747:TNCSS>2.0.CO;2](https://doi.org/10.1175/1520-0493(1992)120<1747:TNCSS>2.0.CO;2).
- Peng, Z. Y., L. L. Lei, and Z.-M. Tan, 2024: A hybrid deep learning and data assimilation method for model error estimation. *Sci. China Earth Sci.*, **67**, 3655–3670, <https://doi.org/10.1007/s11430-024-1395-7>.
- Penny, S. G., 2014: The hybrid local ensemble transform Kalman filter. *Mon. Wea. Rev.*, **142**, 2139–2149, <https://doi.org/10.1175/MWR-D-13-00131.1>.
- Penny, S. G., and T. Miyoshi, 2016: A local particle filter for high-dimensional geophysical systems. *Nonlinear Processes Geophys.*, **23**, 391–405, <https://doi.org/10.5194/npg-23-391-2016>.
- Poli, P., P. Moll, D. Puech, et al., 2009: Quality control, error analysis, and impact assessment of FORMOSAT-3/COSMIC in numerical weather prediction. *Terr. Atmos. Oceanic Sci.*, **20**, 101–113, [https://doi.org/10.3319/TAO.2008.01.21.02\(F3C\)](https://doi.org/10.3319/TAO.2008.01.21.02(F3C)).
- Poterjoy, J., 2016: A localized particle filter for high-dimensional nonlinear systems. *Mon. Wea. Rev.*, **144**, 59–76, <https://doi.org/10.1175/MWR-D-15-0163.1>.
- Poterjoy, J., and F. Q. Zhang, 2015: Systematic comparison of four-dimensional data assimilation methods with and without the tangent linear model using hybrid background error covariance: E4DVar versus 4DEnVar. *Mon. Wea. Rev.*, **143**, 1601–1621, <https://doi.org/10.1175/MWR-D-14-00224.1>.
- Poterjoy, J., and F. Q. Zhang, 2016: Comparison of hybrid four-dimensional data assimilation methods with and without the tangent linear and adjoint models for predicting the life cycle of Hurricane Karl (2010). *Mon. Wea. Rev.*, **144**, 1449–1468, <https://doi.org/10.1175/MWR-D-15-0116.1>.
- Prates, C., C. Sahin, and D. S. Richardson, 2009: Report on PREVIEW Data Targeting System. ECMWF Tech. Memo., 581, 31 pp.
- Putnam, B., M. Xue, Y. Jung, et al., 2019: Ensemble Kalman filter assimilation of polarimetric radar observations for the 20 May 2013 Oklahoma tornadic supercell case. *Monthly Weather Review*, **147**, 2511–2533.
- Qin, X. H., and M. Mu, 2012: Influence of conditional nonlinear optimal perturbations sensitivity on typhoon track forecasts. *Quart. J. Roy. Meteor. Soc.*, **138**, 185–197, <https://doi.org/10.1002/qj.902>.
- Qin, X. H., W. S. Duan, P.-W. Chan, et al., 2023: Effects of dropsonde data in field campaigns on forecasts of tropical cyclones over the western North Pacific in 2020 and the role of CNOP sensitivity. *Adv. Atmos. Sci.*, **40**, 791–803, <https://doi.org/10.1007/s00376-022-2136-9>.
- Qu, A. X., S. H. Ma, J. Li, et al., 2009: The initialization of tropical cyclones in the NMC global model Part II: Implementation. *Acta Meteor. Sinica*, **67**, 727–735, <https://doi.org/10.11676/qxb2009.073>. (in Chinese)
- Qu, A. X., S. H. Ma, and J. Zhang, 2016: Updated experiments of tropical cyclone initialization in global model T639. *Meteor. Mon.*, **42**, 664–673, <https://doi.org/10.7519/j.issn.1000-0526>.

- 2016.06.002.** (in Chinese)
- Qu, A. X., S. H. Ma, J. Zhang, et al., 2022: Typhoon initialization in the CMA global forecast system. *Acta Meteor. Sinica*, **80**, 269–279, <https://doi.org/10.11676/qxb2022.014>. (in Chinese)
- Rabier, F., A. McNally, E. Andersson, et al., 1998: The ECMWF implementation of three-dimensional variational assimilation (3D-Var). II: Structure functions. *Quart. J. Roy. Meteor. Soc.*, **124**, 1809–1829, <https://doi.org/10.1002/qj.49712455003>.
- Rabier, F., N. Fourrié, D. Chafai, et al., 2002: Channel selection methods for infrared atmospheric sounding interferometer radiances. *Quart. J. Roy. Meteor. Soc.*, **128**, 1011–1027, <https://doi.org/10.1256/0035900021643638>.
- Rabier, F., P. Gauthier, C. Cardinali, et al., 2008: An update on THORPEX-related research in data assimilation and observing strategies. *Nonlinear Processes Geophys.*, **15**, 81–94, <https://doi.org/10.5194/npg-15-81-2008>.
- Rasp, S., M. S. Pritchard, and P. Gentine, 2018: Deep learning to represent subgrid processes in climate models. *Proc. Natl. Acad. Sci. USA*, **115**, 9684–9689, <https://doi.org/10.1073/pnas.1810286115>.
- Robert, C. P., and G. Cassela, 2004: *Monte Carlo Statistical Methods*. 2nd ed. Springer-Verlag, New York, 645 pp, <https://doi.org/10.1007/978-1-4757-4145-2>.
- Saha, S., S. Moorthi, H.-L. Pan, et al., 2010: The NCEP climate forecast system reanalysis. *Bull. Amer. Meteor. Soc.*, **91**, 1015–1058, <https://doi.org/10.1175/2010BAMS3001.1>.
- Sakov, P., D. S. Oliver, and L. Bertino, 2012: An iterative EnKF for strongly nonlinear systems. *Mon. Wea. Rev.*, **140**, 1988–2004, <https://doi.org/10.1175/MWR-D-11-00176.1>.
- Salonen, K., and N. Bormann, 2015: Atmospheric Motion Vector Observations in the ECMWF System: Fourth Year Report. EUMETSAT/ECMWF Fellowship Programme Research Report No. 36, European Centre for Medium Range Weather Forecasts, Shinfield Park, 1–32.
- Santitissadeekorn, N., and C. Jones, 2015: Two-stage filtering for joint state-parameter estimation. *Mon. Wea. Rev.*, **143**, 2028–2042, <https://doi.org/10.1175/MWR-D-14-00176.1>.
- Sasaki, Y., 1970: Some basic formalisms in numerical variational analysis. *Mon. Wea. Rev.*, **98**, 875–883, [https://doi.org/10.1175/1520-0493\(1970\)098<875:SBFINV>2.3.CO;2](https://doi.org/10.1175/1520-0493(1970)098<875:SBFINV>2.3.CO;2).
- Saunders, R., E. Andersson, G. Kelly, et al., 1997: Developments in assimilating global TOVS data at the UK Met Office. Proceedings of the 9th International TOVS Study Conference, ECMWF, Igls, Austria, 417–428.
- Saunders, R., J. Hocking, E. Turner, et al., 2018: An update on the RTTOV fast radiative transfer model (currently at version 12). *Geosci. Model Dev.*, **11**, 2717–2737, <https://doi.org/10.5194/gmd-11-2717-2018>.
- Schröttle, J., M. Weissmann, L. Scheck, et al., 2020: Assimilating visible and infrared radiances in idealized simulations of deep convection. *Mon. Wea. Rev.*, **148**, 4357–4375, <https://doi.org/10.1175/MWR-D-20-0002.1>.
- Shao, A. M., C. J. Qiu, X. J. Wang, et al., 2016: Using the Newtonian relaxation technique in numerical sensitivity studies. *Sci. China Earth Sci.*, **59**, 2454–2462, <https://doi.org/10.1007/s11430-016-0033-3>.
- Shapiro, M., and A. Thorpe, 2004: THORPEX International Science Plan. WMO/TD-No. 1246, WMO, Geneva, 1–57.
- Shen, X. S., J. J. Wang, Z. C. Li, et al., 2020: China's independent and innovative development of numerical weather prediction. *Acta Meteor. Sinica*, **78**, 451–476, <https://doi.org/10.11676/qxb2020.030>. (in Chinese)
- Sheng, C. Y., D. Q. Xue, T. Lei, et al., 2006: Comparative experiments between effects of doppler radar data assimilation and increasing horizontal resolution on short-range prediction. *Acta Meteor. Sinica*, **64**, 293–307, <https://doi.org/10.3321/j.issn:0577-6619.2006.03.004>. (in Chinese)
- Slivinski, L. C., D. E. Lippi, J. S. Whitaker, et al., 2022: Overlapping windows in a global hourly data assimilation system. *Mon. Wea. Rev.*, **150**, 1317–1334, <https://doi.org/10.1175/MWR-D-21-0214.1>.
- Sluka, T. C., S. G. Penny, E. Kalnay, et al., 2016: Assimilating atmospheric observations into the ocean using strongly coupled ensemble data assimilation. *Geophys. Res. Lett.*, **43**, 752–759, <https://doi.org/10.1002/2015GL067238>.
- Smith, P. J., A. M. Fowler, and A. S. Lawless, 2015: Exploring strategies for coupled 4D-Var data assimilation using an idealised atmosphere-ocean model. *Tellus A Dyn. Meteor. Oceanogr.*, **67**, 27025, <https://doi.org/10.3402/tellusa.v67.27025>.
- Smith, W. L., P. K. Rao, R. Koffler, et al., 1970: The determination of sea-surface temperature from satellite high resolution infrared window radiation measurements. *Mon. Wea. Rev.*, **98**, 604–611, [https://doi.org/10.1175/1520-0493\(1970\)098<604:TDSST>2.3.CO;2](https://doi.org/10.1175/1520-0493(1970)098<604:TDSST>2.3.CO;2).
- Snyder, C., 1996: Summary of an informal workshop on adaptive observations and FASTEX. *Bull. Amer. Meteor. Soc.*, **77**, 953–961, <https://doi.org/10.1175/1520-0477-77.5.953>.
- Snyder, C., T. Bengtsson, P. Bickel, et al., 2008: Obstacles to high-dimensional particle filtering. *Mon. Wea. Rev.*, **136**, 4629–4640, <https://doi.org/10.1175/2008MWR2529.1>.
- Sodhi, J. S., and F. Fabry, 2022: Benefits of smoothing backgrounds and radar reflectivity observations for multiscale data assimilation with an ensemble Kalman filter at convective scales: A proof-of-concept study. *Mon. Wea. Rev.*, **150**, 589–601, <https://doi.org/10.1175/MWR-D-21-0130.1>.
- Spiller, E. T., A. Budhiraja, K. Ide, et al., 2008: Modified particle filter methods for assimilating Lagrangian data into a point-vortex model. *Phys. D Nonlinear Phenom.*, **237**, 1498–1506, <https://doi.org/10.1016/j.physd.2008.03.023>.
- Stoffelen, A., and D. Anderson, 1997: Scatterometer data interpretation: Measurement space and inversion. *J. Atmos. Ocean. Technol.*, **14**, 1298–1313, [https://doi.org/10.1175/1520-0426\(1997\)014<1298:SDIMSA>2.0.CO;2](https://doi.org/10.1175/1520-0426(1997)014<1298:SDIMSA>2.0.CO;2).
- Storto, A., G. De Magistris, S. Falchetti, et al., 2021: A neural network-based observation operator for coupled ocean-acoustic variational data assimilation. *Mon. Wea. Rev.*, **149**, 1967–1985, <https://doi.org/10.1175/MWR-D-20-0320.1>.
- Sugiura, N., T. Awaji, S. Masuda, et al., 2008: Development of a four-dimensional variational coupled data assimilation system for enhanced analysis and prediction of seasonal to interannual climate variations. *J. Geophys. Res. Oceans*, **113**, C10017, <https://doi.org/10.1029/2008JC004741>.
- Sun, J. N., and N. A. Crook, 1997: Dynamical and microphysical retrieval from Doppler radar observations using a cloud model and its adjoint. Part I: Model development and simulated data experiments. *J. Atmos. Sci.*, **54**, 1642–1661, [https://doi.org/10.1175/1520-0469\(1997\)054<1642:DAMRFD>2.0.CO;2](https://doi.org/10.1175/1520-0469(1997)054<1642:DAMRFD>2.0.CO;2).

- Sun, J. N., and N. A. Crook, 1998: Dynamical and microphysical retrieval from Doppler radar observations using a cloud model and its adjoint. Part II: Retrieval experiments of an observed Florida convective storm. *J. Atmos. Sci.*, **55**, 835–852, [https://doi.org/10.1175/1520-0469\(1998\)055<0835:DAMRFD>2.0.CO;2](https://doi.org/10.1175/1520-0469(1998)055<0835:DAMRFD>2.0.CO;2).
- Sun, J. Z., Z. Y. Liu, F. Y. Lu, et al., 2020a: Strongly coupled data assimilation using leading averaged coupled covariance (LACC). Part III: Assimilation of real world reanalysis. *Mon. Wea. Rev.*, **148**, 2351–2364, <https://doi.org/10.1175/MWR-D-19-0304.1>.
- Sun, J. Z., Y. Zhang, J. M. Ban, et al., 2020b: Impact of combined assimilation of radar and rainfall data on short-term heavy rainfall prediction: A case study. *Mon. Wea. Rev.*, **148**, 2211–2232, <https://doi.org/10.1175/MWR-D-19-0337.1>.
- Sun, J., M. Xue, J. W. Wilson, et al., 2014: Use of NWP for nowcasting convective precipitation: Recent progress and challenges. *Bull. Amer. Meteor. Soc.*, **95**, 409–426.
- Talagrand, O., 1997: Assimilation of observations, an introduction. *J. Meteor. Soc. Japan Ser. II*, **75**, 191–209, [https://doi.org/10.2151/jmsj1965.75.1B\\_191](https://doi.org/10.2151/jmsj1965.75.1B_191).
- Tang, J., D. Byrne, J. A. Zhang, et al., 2015: Horizontal transition of turbulent cascade in the near-surface layer of tropical cyclones. *J. Atmos. Sci.*, **72**, 4915–4925, <https://doi.org/10.1175/JAS-D-14-0373.1>.
- Tang, J., J. A. Zhang, P. Chan, et al., 2021: A direct aircraft observation of helical rolls in the tropical cyclone boundary layer. *Sci. Rep.*, **11**, 18771, <https://doi.org/10.1038/s41598-021-9776-7>.
- Temperton, C., and M. Roch, 1991: Implicit normal mode initialization for an operational regional model. *Mon. Wea. Rev.*, **119**, 667–677, [https://doi.org/10.1175/1520-0493\(1991\)119<0667:INMIFA>2.0.CO;2](https://doi.org/10.1175/1520-0493(1991)119<0667:INMIFA>2.0.CO;2).
- Thépaut, J.-N., R. N. Hoffman, and P. Courtier, 1993: Interactions of dynamics and observations in a four-dimensional variational assimilation. *Mon. Wea. Rev.*, **121**, 3393–3414, [https://doi.org/10.1175/1520-0493\(1993\)121<3393:IODAOI>2.0.CO;2](https://doi.org/10.1175/1520-0493(1993)121<3393:IODAOI>2.0.CO;2).
- Thiébaux, H. J., and M. A. Pedder, 1987: *Spatial Objective Analysis*. Academic Press, London, 299 pp.
- Tian, X. J., and X. B. Feng, 2015: A non-linear least squares enhanced POD-4DVar algorithm for data assimilation. *Tellus A Dyn. Meteor. Oceanogr.*, **67**, 25340, <https://doi.org/10.3402/tellusa.v67.25340>.
- Tian, X. J., H. Q. Zhang, X. B. Feng, et al., 2018: Nonlinear least squares En4DVar to 4DENVar methods for data assimilation: Formulation, analysis, and preliminary evaluation. *Mon. Wea. Rev.*, **146**, 77–93, <https://doi.org/10.1175/MWR-D-17-0050.1>.
- Tian, Y. D., C. D. Peters-Lidard, K. W. Harrison, et al., 2015: An examination of methods for estimating land surface microwave emissivity. *J. Geophys. Res. Atmos.*, **120**, 11,114–11,128, <https://doi.org/10.1002/2015JD023582>.
- Tippett, M. K., J. L. Anderson, C. H. Bishop, et al., 2003: Ensemble square root filters. *Mon. Wea. Rev.*, **131**, 1485–1490, [https://doi.org/10.1175/1520-0493\(2003\)131<1485:ESRF>2.0.CO;2](https://doi.org/10.1175/1520-0493(2003)131<1485:ESRF>2.0.CO;2).
- Tong, M. J., and M. Xue, 2005: Ensemble Kalman filter assimilation of Doppler radar data with a compressible nonhydrostatic model: OSS experiments. *Mon. Wea. Rev.*, **133**, 1789–1807, <https://doi.org/10.1175/MWR2898.1>.
- Uppala, S., A. Hollingsworth, S. Tibaldi, et al., 1984: Results from two recent observing system experiments at ECMWF. Proceedings of ECMWF Seminar on Data Assimilation Systems and Observing System Experiments with Particular Emphasis on FGGE, Reading, UK, 3–7 September, ECMWF, 165–202.
- van Leeuwen, P. J., 2003: A variance-minimizing filter for large-scale applications. *Mon. Wea. Rev.*, **131**, 2071–2084, [https://doi.org/10.1175/1520-0493\(2003\)131<2071:AVFFLA>2.0.CO;2](https://doi.org/10.1175/1520-0493(2003)131<2071:AVFFLA>2.0.CO;2).
- Wan, Q. L., J. S. Xue, and S. Y. Zhuang, 2005: Study on the variational assimilation technique for the retrieval of wind fields from Doppler radar data. *Acta Meteor. Sinica*, **63**, 129–145, <https://doi.org/10.11676/qxb2005.014>. (in Chinese)
- Wang, B., J. J. Liu, S. D. Wang, et al., 2010: An economical approach to four-dimensional variational data assimilation. *Adv. Atmos. Sci.*, **27**, 715–727, <https://doi.org/10.1007/s00376-009-9122-3>.
- Wang, D., Z. Ruan, G. L. Wang, et al., 2019: A study on assimilation of wind profiling radar data in GRAPES-Meso model. *Chinese J. Atmos. Sci.*, **43**, 634–654, <https://doi.org/10.3878/j.issn.1006-9895.1810.18125>. (in Chinese)
- Wang, H., and W. Han, 2018: The application of assimilating FY4A AGRI water-vapor channel radiances in GRAPES. Proceedings of the 35th Annual Meeting of Chinese Meteorological Society, S9, Chinese Meteorological Society, Hefei, 1–66. (in Chinese)
- Wang, H. L., J. Z. Sun, S. Y. Fan, et al., 2013a: Indirect assimilation of radar reflectivity with WRF 3D-Var and its impact on prediction of four summertime convective events. *J. Appl. Meteor. Climatol.*, **52**, 889–902, <https://doi.org/10.1175/JAMC-D-12-0120.1>.
- Wang, H. L., J. Z. Sun, X. Zhang, et al., 2013b: Radar data assimilation with WRF 4D-Var. Part I: System development and preliminary testing. *Mon. Wea. Rev.*, **141**, 2224–2244, <https://doi.org/10.1175/MWR-D-12-00168.1>.
- Wang, J. C., Z. R. Zhuang, W. Han, et al., 2014: An improvement of background error covariance in the global GRAPES variational data assimilation and its impact on the analysis and prediction: Statistics of the three-dimensional structure of background error covariance. *Acta Meteor. Sinica*, **72**, 62–78, <https://doi.org/10.11676/qxb2014.008>. (in Chinese)
- Wang, J. C., J. D. Gong, and B. Zhao, 2015: A new method for estimating observation error of the COSMIC refractivity data and its impacts on GRAPES-GFS model weather forecasts. *Acta Meteor. Sinica*, **73**, 142–158, <https://doi.org/10.11676/qxb2015.005>. (in Chinese)
- Wang, J. C., J. D. Gong, and R. C. Wang, 2016: Estimation of background error for brightness temperature in GRAPES 3DVar and its application in radiance data background quality control. *Acta Meteor. Sinica*, **74**, 397–409, <https://doi.org/10.11676/qxb2016.026>. (in Chinese)
- Wang, J.-C., J.-D. Gong, and W. Han, 2020: The impact of assimilating FY-3C GNOS GPS radio occultation observations on GRAPES forecasts. *J. Trop. Meteor.*, **26**, 390–401, <https://doi.org/10.46267/j.1006-8775.2020.034>.
- Wang, J. C., X. W. Jiang, X. S. Shen, et al., 2023: Assimilation of ocean surface wind data by the HY-2B satellite in GRAPES: Impacts on analyses and forecasts. *Adv. Atmos. Sci.*, **40**, 44–61, <https://doi.org/10.1007/s00376-022-1349-2>.

- Wang, M. J., K. Zhao, W.-C. Lee, et al., 2018: Microphysical and kinematic structure of convective-scale elements in the inner rainband of Typhoon Matmo (2014) after landfall. *J. Geophys. Res. Atmos.*, **123**, 6549–6564, <https://doi.org/10.1029/2018JD028578>.
- Wang, P., J. Li, J. L. Li, et al., 2014: Advanced infrared sounder subpixel cloud detection with imagers and its impact on radiance assimilation in NWP. *Geophys. Res. Lett.*, **41**, 1773–1780, <https://doi.org/10.1002/2013GL059067>.
- Wang, P., J. Li, Z. L. Li, et al., 2017: The impact of cross-track infrared sounder (CrIS) cloud-cleared radiances on Hurricane Joaquin (2015) and Matthew (2016) forecasts. *J. Geophys. Res. Atmos.*, **122**, 13,201–13,218, <https://doi.org/10.1002/2017JD027515>.
- Wang, R. C., J. D. Gong, and H. Wang, 2021: Impact studies of introducing a large-scale constraint into the kilometer-scale regional variational data assimilation. *Chinese J. Atmos. Sci.*, **45**, 1007–1022, <https://doi.org/10.3878/j.issn.1006-9895.2009.20176>. (in Chinese)
- Wang, R. C., J. D. Gong, and J. Sun, 2024: A reformulation of the minimization control variables in the CMA-MESO km-scale variational assimilation system. *Acta Meteor. Sinica*, **82**, 208–221, <https://doi.org/10.11676/qxxb2024.20230076>. (in Chinese)
- Wang, S. P., D. X. Liao, L. R. Ji, et al., 1984: Status and prospect for the 2000 year of numerical weather prediction. *Meteor. Sci. Technol.*, **5**, 12–15, <https://doi.org/10.19517/j.1671-6345.1984.05.003>. (in Chinese)
- Wang, S. Z., and Z. Q. Liu, 2019: A radar reflectivity operator with ice-phase hydrometeors for variational data assimilation (version 1.0) and its evaluation with real radar data. *Geosci. Model Dev.*, **12**, 4031–4051, <https://doi.org/10.5194/gmd-12-4031-2019>.
- Wang, X. G., and T. Lei, 2014: GSI-based four-dimensional ensemble-variational (4DEnVar) data assimilation: Formulation and single-resolution experiments with real data for NCEP global forecast system. *Mon. Wea. Rev.*, **142**, 3303–3325, <https://doi.org/10.1175/MWR-D-13-00303.1>.
- Wang, X. G., C. Snyder, and T. M. Hamill, 2007: On the theoretical equivalence of differently proposed ensemble-3DVAR hybrid analysis schemes. *Mon. Wea. Rev.*, **135**, 222–227, <https://doi.org/10.1175/MWR3282.1>.
- Wang, X. G., D. M. Barker, C. Snyder, et al., 2008: A hybrid ETKF-3DVAR data assimilation scheme for the WRF model. Part I: Observing system simulation experiment. *Mon. Wea. Rev.*, **136**, 5116–5131, <https://doi.org/10.1175/2008MWR244.1>.
- Wang, X. G., D. Parrish, D. Kleist, et al., 2013: GSI 3DVar-based ensemble-variational hybrid data assimilation for NCEP global forecast system: Single-resolution experiments. *Mon. Wea. Rev.*, **141**, 4098–4117, <https://doi.org/10.1175/MWR-D-12-00141.1>.
- Wang, X. G., H. G. Chipilski, C. H. Bishop, et al., 2021: A multiscale local gain form ensemble transform Kalman filter (MLGETKF). *Mon. Wea. Rev.*, **149**, 605–622, <https://doi.org/10.1175/MWR-D-20-0290.1>.
- Wang, Y. M., and X. G. Wang, 2021: Development of convective-scale static background error covariance within GSI-based hybrid EnVar system for direct radar reflectivity data assimilation. *Mon. Wea. Rev.*, **149**, 2713–2736, <https://doi.org/10.1175/MWR-D-20-0215.1>.
- Wang, Y. M., and X. G. Wang, 2023: Simultaneous multiscale data assimilation using scale-and variable-dependent localization in EnVar for convection allowing analyses and forecasts: Methodology and experiments for a tornadic supercell. *J. Adv. Model. Earth Syst.*, **15**, e2022MS003430, <https://doi.org/10.1029/2022MS003430>.
- Wang, Y. Y., X. M. Shi, L. L. Lei, et al., 2022: Deep learning augmented data assimilation: Reconstructing missing information with convolutional autoencoders. *Mon. Wea. Rev.*, **150**, 1977–1991, <https://doi.org/10.1175/MWR-D-21-0288.1>.
- Weissmann, M., F. Harnisch, C.-C. Wu, et al., 2011: The influence of assimilating dropsonde data on typhoon track and midlatitude forecasts. *Mon. Wea. Rev.*, **139**, 908–920, <https://doi.org/10.1175/2010MWR3377.1>.
- Wen, J., K. Zhao, H. Huang, et al., 2017: Evolution of microphysical structure of a subtropical squall line observed by a polarimetric radar and a disdrometer during OPACC in eastern China. *J. Geophys. Res. Atmos.*, **122**, 8033–8050, <https://doi.org/10.1002/2016JD026346>.
- Wen, L., K. Zhao, G. Chen, et al., 2018: Drop size distribution characteristics of seven typhoons in China. *J. Geophys. Res. Atmos.*, **123**, 6529–6548, <https://doi.org/10.1029/2017JD027950>.
- Weng, F. Z., B. H. Yan, and N. C. Grody, 2001: A microwave land emissivity model. *J. Geophys. Res. Atmos.*, **106**, 20,115–20,123, <https://doi.org/10.1029/2001JD900019>.
- Weng, F. Z., X. W. Yu, Y. H. Duan, et al., 2020: Advanced Radiative Transfer Modeling System (ARMS): A new-generation satellite observation operator developed for numerical weather prediction and remote sensing applications. *Adv. Atmos. Sci.*, **37**, 131–136, <https://doi.org/10.1007/s00376-019-9170-2>.
- Whitaker, J. S., and T. M. Hamill, 2002: Ensemble data assimilation without perturbed observations. *Mon. Wea. Rev.*, **130**, 1913–1924, [https://doi.org/10.1175/1520-0493\(2002\)130<1913:EDAWPO>2.0.CO;2](https://doi.org/10.1175/1520-0493(2002)130<1913:EDAWPO>2.0.CO;2).
- Whitaker, J. S., and T. M. Hamill, 2012: Evaluating methods to account for system errors in ensemble data assimilation. *Mon. Wea. Rev.*, **140**, 3078–3089, <https://doi.org/10.1175/MWR-D-11-00276.1>.
- Whitaker, J. S., T. M. Hamill, X. Wei, et al., 2008: Ensemble data assimilation with the NCEP global forecast system. *Mon. Wea. Rev.*, **136**, 463–482, <https://doi.org/10.1175/2007MWR2018.1>.
- Wolfensberger, D., and A. Berne, 2018: From model to radar variables: A new forward polarimetric radar operator for COSMO. *Atmos. Meas. Tech.*, **11**, 3883–3916, <https://doi.org/10.5194/amt-11-3883-2018>.
- Wu, C.-C., J.-H. Chen, P.-H. Lin, et al., 2007: Targeted observations of tropical cyclone movement based on the adjoint-derived sensitivity steering vector. *J. Atmos. Sci.*, **64**, 2611–2626, <https://doi.org/10.1175/JAS3974.1>.
- Wu, D., K. Zhao, M. R. Kumjian, et al., 2018: Kinematics and microphysics of convection in the outer rainband of Typhoon Nida (2016) revealed by polarimetric radar. *Mon. Wea. Rev.*, **146**, 2147–2159, <https://doi.org/10.1175/MWR-D-17-0320.1>.
- Wulfmeyer, V., A. Behrendt, H. S. Bauer, et al., 2008: The convective and orographically induced precipitation study: A re-

- search and development project of the world weather research program for improving quantitative precipitation forecasting in low-mountain regions. *Bull. Amer. Meteor. Soc.*, **89**, 1477–1486, <https://doi.org/10.1175/2008BAMS2367.1>.
- Xiao, H. Y., W. Han, H. Wang, et al., 2020: Impact of *FY-3D* MWRI radiance assimilation in GRAPES 4DVar on forecasts of Typhoon Shanshan. *J. Meteor. Res.*, **34**, 836–850, <https://doi.org/10.1007/s13351-020-9122-x>.
- Xiao, H. Y., W. Han, P. Zhang, et al., 2023a: Assimilation of data from the MWHS-II onboard the first early morning satellite *FY-3E* into the CMA global 4D-Var system. *Meteor. Appl.*, **30**, e2133, <https://doi.org/10.1002/met.2133>.
- Xiao, H. Y., J. Li, G. Q. Liu, et al., 2023b: Assimilation of AMSU-a surface-sensitive channels in CMA\_GFS 4D-Var system over land. *Wea. Forecasting*, **38**, 1777–1790, <https://doi.org/10.1175/WAF-D-23-0032.1>.
- Xiao, Q. N., and J. Z. Sun, 2007: Multiple-radar data assimilation and short-range quantitative precipitation forecasting of a squall line observed during IHOP\_2002. *Mon. Wea. Rev.*, **135**, 3381–3404, <https://doi.org/10.1175/MWR3471.1>.
- Xiao, Q. N., Y.-H. Kuo, J. Z. Sun, et al., 2005: Assimilation of Doppler radar observations with a regional 3DVAR system: Impact of Doppler velocities on forecasts of a heavy rainfall case. *J. Appl. Meteor.*, **44**, 768–788, <https://doi.org/10.1175/JAM2248.1>.
- Xiao, Y., L. Bai, W. Xue, et al., 2024a: FengWu-4DVar: Coupling the data-driven weather forecasting model with 4D variational assimilation. arXiv, 2312.12455, <https://doi.org/10.48550/arXiv.2312.12455>.
- Xiao, Y., Q. L. Jia, W. Xue, et al., 2024b: VAE-Var: Variational-autoencoder-enhanced variational assimilation. arXiv, 2405.13711, <https://doi.org/10.48550/arXiv.2405.13711>.
- Xie, H., L. Bi, and W. Han, 2024: ZJU-AERO V0.5: An accurate and efficient radar operator designed for CMA-GFS/MESO with capability of simulating non-spherical hydrometeors. *Geosci. Model Dev.*, **17**, 5657–5688, <https://doi.org/10.5194/gmd-17-5657-2024>.
- Xie, H. J., W. Han, and L. Bi, 2023: Assimilating *FY3D-MWRI* 23.8 GHz observations in the CMA-GFS 4DVAR system based on a pseudo all-sky data assimilation method. *Quart. J. Roy. Meteor. Soc.*, **149**, 3014–3043, <https://doi.org/10.1002/qj.4544>.
- Xie, Y., S. Koch, J. McGinley, et al., 2011: A space-time multiscale analysis system: A sequential variational analysis approach. *Mon. Wea. Rev.*, **139**, 1224–1240, <https://doi.org/10.1175/2010MWR3338.1>.
- Xu, J. M., 2020: Pathways on solving problems at algorithm improvements for *FY-2* meteorological satellite at image navigation and wind vector derivation. *J. Nanjing Univ. Inf. Sci. Technol. (Nat. Sci. Ed.)*, **12**, 1–6. (in Chinese)
- Xu, X. F., 2003: Construction, techniques and application of new generation Doppler weather radar network in China. *Eng. Sci.*, **5**, 7–14, <https://doi.org/10.3969/j.issn.1009-1742.2003.06.002>. (in Chinese)
- Xu, Z. F., J. D. Gong, J. J. Wang, et al., 2006: Preliminary study on surface observational data assimilation. *J. Appl. Meteor. Sci.*, **17**, 1–10, <https://doi.org/10.3969/j.issn.1001-7313.2006.z1.001>. (in Chinese)
- Xu, Z. F., J. D. Gong, J. J. Wang, et al., 2007: A study of assimila-
- tion of surface observational data in complex terrain Part I: Influence of the elevation difference between model surface and observation site. *Chinese J. Atmos. Sci.*, **31**, 222–232, <https://doi.org/10.3878/j.issn.1006-9895.2007.02.04>. (in Chinese)
- Xu, Z. F., J. D. Gong, and Z. C. Li, 2009: A study of assimilation of surface observational data in complex terrain Part III: Comparison analysis of two methods on solving the problem of elevation difference between model surface and observation sites. *Chinese J. Atmos. Sci.*, **33**, 1137–1147, <https://doi.org/10.3878/j.issn.1006-9895.2009.06.02>. (in Chinese)
- Xu, Z. F., M. Hao, L. J. Zhu, et al., 2013: On the research and development of GRAPES\_RAFS. *Meteor. Mon.*, **39**, 466–477, <https://doi.org/10.7519/j.issn.1000-0526.2013.04.009>. (in Chinese)
- Xu, Z. F., Y. Wu, J. D. Gong, et al., 2021: Assimilation of 2-m relative humidity observations in CMA-MESO 3DVar system. *Acta Meteor. Sinica*, **79**, 943–955, <https://doi.org/10.11676/qxb2021.060>. (in Chinese)
- Xu, Z. F., L. Zhang, R. C. Wang, et al., 2023: Effect of 2-m temperature data assimilation in the CMA- MESO 3DVAR system. *J. Meteor. Res.*, **37**, 218–233, <https://doi.org/10.1007/s13351-023-2115-9>.
- Xue, J. S., and D. H. Chen, 2008: *Scientific Design and Application of the Numerical Weather Prediction System GRAPES*. Science Press, Beijing, 383 pp. (in Chinese)
- Xue, J. S., C. J. Li, and Z. M. Wang, 1992: Initialization of limited area model based on the principle of nonlinear normal mode initialization. *Chinese J. Atmos. Sci.*, **16**, 686–697, <https://doi.org/10.3878/j.issn.1006-9895.1992.06.06>. (in Chinese)
- Xue, M., Y. Jung, and G. F. Zhang, 2010: State estimation of convective storms with a two-moment microphysics scheme and an ensemble Kalman filter: Experiments with simulated radar data. *Quart. J. Roy. Meteor. Soc.*, **136**, 685–700, <https://doi.org/10.1002/qj.593>.
- Yang, J., S. G. Ding, P. M. Dong, et al., 2020: Advanced radiative transfer modeling system developed for satellite data assimilation and remote sensing applications. *J. Quant. Spectrosc. Radiat. Transf.*, **251**, 107043, <https://doi.org/10.1016/j.jqsrt.2020.107043>.
- Yang, L. C., W. S. Duan, Z. F. Wang, et al., 2022: Toward targeted observations of the meteorological initial state for improving the PM<sub>2.5</sub> forecast of a heavy haze event that occurred in the Beijing–Tianjin–Hebei region. *Atmos. Chem. Phys.*, **22**, 11,429–11,453, <https://doi.org/10.5194/acp-22-11429-2022>.
- Yang, L. C., W. S. Duan, and Z. F. Wang, 2023: An approach to refining the ground meteorological observation stations for improving PM<sub>2.5</sub> forecasts in the Beijing–Tianjin–Hebei region. *Geosci. Model Dev.*, **16**, 3827–3848, <https://doi.org/10.5194/gmd-16-3827-2023>.
- Yang, S.-C., E. Kalnay, and T. Enomoto, 2015: Ensemble singular vectors and their use as additive inflation in EnKF. *Tellus A Dyn. Meteor. Oceanogr.*, **67**, 26536, <https://doi.org/10.3402/tellusa.v67.26536>.
- Yang, Y., C. J. Qiu, J. D. Gong, et al., 2008: Study on Doppler weather radar data assimilation via 3D-Var. *J. Meteor. Sci.*, **28**, 124–132, <https://doi.org/10.3969/j.issn.1009-0827.2008.02.002>. (in Chinese)

- Yano, J.-I., M. Z. Ziemiański, M. Cullen, et al., 2018: Scientific challenges of convective-scale numerical weather prediction. *Bull. Amer. Meteor. Soc.*, **99**, 699–710, <https://doi.org/10.1175/BAMS-D-17-0125.1>.
- Yin, R. Y., W. Han, Z. Q. Gao, et al., 2020: The evaluation of FY4A's Geostationary Interferometric Infrared Sounder (GIIRS) long-wave temperature sounding channels using the GRAPES global 4D-Var. *Quart. J. Roy. Meteor. Soc.*, **146**, 1459–1476, <https://doi.org/10.1002/qj.3746>.
- Yin, R. Y., W. Han, Z. Q. Gao, et al., 2021: Impact of high temporal resolution FY-4A geostationary interferometric infrared sounder (GIIRS) radiance measurements on typhoon forecasts: Maria (2018) case with GRAPES global 4D-Var assimilation system. *Geophys. Res. Lett.*, **48**, e2021GL093672, <https://doi.org/10.1029/2021GL093672>.
- Ying, Y., and F. Q. Zhang, 2015: An adaptive covariance relaxation method for ensemble data assimilation. *Quart. J. Roy. Meteor. Soc.*, **141**, 2898–2906, <https://doi.org/10.1002/qj.2576>.
- Yussouf, N., and D. J. Stensrud, 2010: Impact of phased-array radar observations over a short assimilation period: Observing system simulation experiments using an ensemble Kalman filter. *Mon. Wea. Rev.*, **138**, 517–538, <https://doi.org/10.1175/2009MWR2925.1>.
- Zeng, Y., 2013: Efficient radar forward operator for operational data assimilation within the COSMO-model. Ph.D. dissertation, Karlsruher Institut für Technologie, Karlsruhe, 232 pp, <https://doi.org/10.5445/KSP/1000036921>.
- Zeng, Y. F., U. Blahak, M. Neuper, et al., 2014: Radar beam tracing methods based on atmospheric refractive index. *J. Atmos. Oceanic Technol.*, **31**, 2650–2670, <https://doi.org/10.1175/JTECH-D-13-00152.1>.
- Zeng, Y. F., T. Janjić, A. de Lozar, et al., 2020: Comparison of methods accounting for subgrid-scale model error in convective-scale data assimilation. *Mon. Wea. Rev.*, **148**, 2457–2477, <https://doi.org/10.1175/MWR-D-19-0064.1>.
- Zhang, C. Z., J. S. Xue, Y. R. Feng, et al., 2019: Retrieval of water vapor from radar reflectivity based on Bayesian scheme and its assimilation test. *J. Trop. Meteor.*, **35**, 145–153, <https://doi.org/10.16032/j.issn.1004-4965.2019.013>. (in Chinese)
- Zhang, F., C. Snyder, and J. Z. Sun, 2004: Impacts of initial estimate and observation availability on convective-scale data assimilation with an ensemble Kalman filter. *Mon. Wea. Rev.*, **132**, 1238–1253, [https://doi.org/10.1175/1520-0493\(2004\)132<1238:IOIEAO>2.0.CO;2](https://doi.org/10.1175/1520-0493(2004)132<1238:IOIEAO>2.0.CO;2).
- Zhang, F. Q., Y. H. Weng, J. A. Sippel, et al., 2009a: Cloud-resolving hurricane initialization and prediction through assimilation of Doppler radar observations with an ensemble Kalman filter. *Mon. Wea. Rev.*, **137**, 2105–2125, <https://doi.org/10.1175/2009MWR2645.1>.
- Zhang, F. Q., M. Zhang, and J. A. Hansen, 2009b: Coupling ensemble Kalman filter with four-dimensional variational data assimilation. *Adv. Atmos. Sci.*, **26**, 1–8, <https://doi.org/10.1007/s00376-009-0001-8>.
- Zhang, J. A., R. F. Rogers, D. S. Nolan, et al., 2011: On the characteristic height scales of the hurricane boundary layer. *Mon. Wea. Rev.*, **139**, 2523–2535, <https://doi.org/10.1175/MWR-D-10-05017.1>.
- Zhang, J. A., D. S. Nolan, R. F. Rogers, et al., 2015: Evaluating the impact of improvements in the boundary layer parameterization on hurricane intensity and structure forecasts in HWRF. *Mon. Wea. Rev.*, **143**, 3136–3155, <https://doi.org/10.1175/MWR-D-14-00339.1>.
- Zhang, L., Y. Z. Liu, Y. Liu, et al., 2019: The operational global four-dimensional variational data assimilation system at the China Meteorological Administration. *Quart. J. Roy. Meteor. Soc.*, **145**, 1882–1896, <https://doi.org/10.1002/qj.3533>.
- Zhang, P., X. Q. Hu, Q. F. Lu, et al., 2022: FY-3E: The first operational meteorological satellite mission in an early morning orbit. *Adv. Atmos. Sci.*, **39**, 1–8, <https://doi.org/10.1007/s00376-021-1304-7>.
- Zhang, P., X. Q. Hu, L. Sun, et al., 2024: The on-orbit performance of FY-3E in an early morning orbit. *Bull. Amer. Meteor. Soc.*, **105**, E144–E175, <https://doi.org/10.1175/BAMS-D-22-0045.1>.
- Zhang, S., M. J. Harrison, A. Rosati, et al., 2007: System design and evaluation of coupled ensemble data assimilation for global oceanic climate studies. *Mon. Wea. Rev.*, **135**, 3541–3564, <https://doi.org/10.1175/MWR3466.1>.
- Zhang, X. H., Q. S. Zhang, and J. M. Xu, 2017a: Use of representative pixels of motion for wind vector height assignment of semi-transparent clouds. *J. Appl. Meteor. Sci.*, **28**, 270–282, <https://doi.org/10.11898/1001-7313.20170302>. (in Chinese)
- Zhang, X. H., Y. H. Duan, Y. Q. Wang, et al., 2017b: A high-resolution simulation of Supertyphoon Rammasun (2014)—Part I: Model verification and surface energetics analysis. *Adv. Atmos. Sci.*, **34**, 757–770, <https://doi.org/10.1007/s00376-017-6255-7>.
- Zhang, Y. J., H. Hu, and F. Z. Weng, 2021: The potential of satellite sounding observations for deriving atmospheric wind in all-weather conditions. *Remote Sens.*, **13**, 2947, <https://doi.org/10.3390/rs13152947>.
- Zhao, K., M. J. Wang, M. Xue, et al., 2017: Doppler radar analysis of a tornadic miniature supercell during the landfall of Typhoon Mujigae (2015) in South China. *Bull. Amer. Meteor. Soc.*, **98**, 1821–1831, <https://doi.org/10.1175/BAMS-D-15-00301.1>.
- Zhao, K., H. Huang, M. J. Wang, et al., 2019: Recent progress in dual-polarization radar research and applications in China. *Adv. Atmos. Sci.*, **36**, 961–974, <https://doi.org/10.1007/s00376-019-9057-2>.
- Zhao, Z.-K., C.-X. Liu, Q. Li, et al., 2015: Typhoon air-sea drag coefficient in coastal regions. *J. Geophys. Res. Oceans*, **120**, 716–727, <https://doi.org/10.1002/2014JC010283>.
- Zhen, Y. C., and F. Q. Zhang, 2014: A probabilistic approach to adaptive covariance localization for serial ensemble square-root filters. *Mon. Wea. Rev.*, **142**, 4499–4518, <https://doi.org/10.1175/MWR-D-13-00390.1>.
- Zheng, H., Y. D. Chen, S. W. Zheng, et al., 2023: Radar reflectivity assimilation based on hydrometeor control variables and its impact on short-term precipitation forecasting. *Remote Sens.*, **15**, 672, <https://doi.org/10.3390/rs15030672>.
- Zhou, L. F., L. L. Lei, J. S. Whitaker, et al., 2024: An adaptive channel selection method for assimilating the hyperspectral infrared radiances. *Mon. Wea. Rev.*, **152**, 793–810, <https://doi.org/10.1175/MWR-D-23-0131.1>.
- Zhu, K., Y. Pan, M. Xue, et al., 2013: A regional GSI-based en-

- semble Kalman filter data assimilation system for the rapid refresh configuration: Testing at reduced resolution. *Mon. Wea. Rev.*, **141**, 4118–4139.
- Zhu, L. J., J. D. Gong, L. P. Huang, et al., 2017: Three-dimensional cloud initial field created and applied to GRAPES numerical weather prediction nowcasting. *J. Appl. Meteor. Sci.*, **28**, 38–51, <https://doi.org/10.11898/1001-7313.20170104>. (in Chinese)
- Zhu, M. B., P. J. van Leeuwen, and J. Amezua, 2016: Implicit equal-weights particle filter. *Quart. J. Roy. Meteor. Soc.*, **142**, 1904–1919, <https://doi.org/10.1002/qj.2784>.
- Zhu, Y. Q., J. Derber, A. Collard, et al., 2014: Enhanced radiance bias correction in the National Centers for Environmental Prediction's Gridpoint Statistical Interpolation data assimilation system. *Quart. J. Roy. Meteor. Soc.*, **140**, 1479–1492, <https://doi.org/10.1002/qj.2233>.
- Zhu, Z. Q., F. Z. Weng, and Y. Han, 2024: Vector radiative transfer in a vertically inhomogeneous scattering and emitting atmosphere. Part I: A new discrete ordinate method. *J. Meteor. Res.*, **38**, 209–224, <https://doi.org/10.1007/s13351-024-3076-3>.
- Zhuang, Z. R., R. C. Wang, and X. L. Li, 2020: Application of global large scale information to GRAEPS RAFS system. *Acta Meteor. Sinica*, **78**, 33–47, [https://doi.org/10.11676/qxx\\_b2020.002](https://doi.org/10.11676/qxx_b2020.002). (in Chinese)
- Zou, X. L., 2025: Overview and new opportunities for multi-source data assimilation. *J. Meteor. Res.*, **39**, 1–25, <https://doi.org/10.1007/s13351-025-4140-3>.
- Zupanski, M., 1993: Regional four-dimensional variational data assimilation in a quasi-operational forecasting environment. *Mon. Wea. Rev.*, **121**, 2396–2408, [https://doi.org/10.1175/1520-0493\(1993\)121<2396:RFDVDA>2.0.CO;2](https://doi.org/10.1175/1520-0493(1993)121<2396:RFDVDA>2.0.CO;2).
- Zupanski, M., 2005: Maximum likelihood ensemble filter: Theoretical aspects. *Mon. Wea. Rev.*, **133**, 1710–1726, <https://doi.org/10.1175/MWR2946.1>.



# 数值天气预报资料同化的发展与展望\*

雷荔傑<sup>1</sup> 翁富忠<sup>2</sup> 段晚锁<sup>3</sup> 陈耀登<sup>4</sup> 张林<sup>2</sup> 王瑞春<sup>2</sup> 杨俊<sup>2</sup>  
 秦晓昊<sup>3</sup> 韩威<sup>2</sup> 李俊<sup>5</sup> 闵锦忠<sup>4</sup> 徐枝芳<sup>2</sup> 陆其峰<sup>2</sup> 龚建东<sup>2</sup>  
 LEI Lili<sup>1</sup> WENG Fuzhong<sup>2</sup> DUAN Wansuo<sup>3</sup> CHEN Yaodeng<sup>4</sup> ZHANG Lin<sup>2</sup> WANG Ruichun<sup>2</sup> YANG Jun<sup>2</sup>  
 QIN Xiaohao<sup>3</sup> HAN Wei<sup>2</sup> LI Jun<sup>5</sup> MIN Jinzhong<sup>4</sup> XU Zhifang<sup>2</sup> LU Qifeng<sup>2</sup> GONG Jiandong<sup>2</sup>

1. 南京大学大气科学学院,南京, 210008

2. 中国气象局地球系统数值预报中心,北京, 100081

3. 中国科学院大气物理研究所,北京, 100029

4. 南京信息工程大学气象灾害教育部重点实验室,南京, 210044

5. 国家卫星气象中心,北京, 100081

1. School of Atmospheric Sciences, Nanjing University, Nanjing 210008, China

2. CMA Earth System Modeling and Prediction Centre, Beijing 100081, China

3. Institute of Atmospheric Physics, Chinese Academy of Sciences, Beijing 100029, China

4. Key Laboratory of Meteorological Disaster of Ministry of Education, Nanjing University of Information Science and Technology, Nanjing 210044, China

5. National Satellite Meteorological Centre, Beijing 100081, China

2024-09-24 收稿, 2024-12-24 改回.

雷荔傑, 翁富忠, 段晚锁, 陈耀登, 张林, 王瑞春, 杨俊, 秦晓昊, 韩威, 李俊, 闵锦忠, 徐枝芳, 陆其峰, 龚建东. 2025. 数值天气预报资料同化的发展与展望. 气象学报, 83(3): 503-535

Lei Lili, Weng Fuzhong, Duan Wansuo, Chen Yaodeng, Zhang Lin, Wang Ruichun, Yang Jun, Qin Xiaohao, Han Wei, Li Jun, Min Jinzhong, Xu Zhifang, Lu Qifeng, Gong Jiandong. 2025. Overview and prospect of data assimilation in numerical weather prediction. *Acta Meteorologica Sinica*, 83(3):503-535

**Abstract** For numerical weather prediction (NWP), data assimilation (DA) combines short-term forecasts and various atmospheric observations to achieve optimal initial conditions, based on which subsequent forecasts are launched. With the rapid advancements in numerical models and observing systems, DA has been significantly evolved. Modern methods now can account for uncertainties of state variables across various spatiotemporal scales, incorporate multiscale observation error statistics, and enforce dynamical constraints and model balances. Meanwhile, observations from various platforms, such as ground-based, aircraft, and satellite, have been assimilated. These include data from polar-orbiting and geostationary satellites, radar-derived radial winds and reflectivity, Global Navigation Satellite System (GNSS) radio occultations, etc. To further utilize the advanced observing systems and DA techniques for high-impact weather predictions, target observation strategies have been developed to identify areas where additional observations can yield the greatest predict improvements. Based on the advancements of DA theories and methods, China's operational systems have made significant progress, establishing advanced operational DA systems. Over the past decade, the

\* 资助课题: 国家自然科学基金项目(42192553)。

作者简介: 雷荔傑, 主要从事资料同化和数值天气预报研究。E-mail: lili@nju.edu.cn

通信作者: 龚建东, 主要从事资料同化和数值天气预报研究。E-mail: gongjd@cma.gov.cn

forecast skill of 5 d global weather prediction has improved by approximately 15%. The article reviews a century of development in DA, and discusses future directions, including the advanced DA methods, operational frameworks, integration of novel observations, and the synergy between DA and artificial intelligence.

**Key words** Data assimilation, Multi-source observations, Atmospheric predictability, Numerical weather prediction

**摘要** 资料同化是结合数值天气预报与多源大气观测资料,以获得最能代表大气状态的数值天气预报所需初值的方法。随着数值模式和观测系统的迅速发展,资料同化已发展为可考虑大气不同时、空尺度不确定性特征、不同种类观测误差特性,具有动力约束、满足模式平衡性的先进理论和方法。也有越来越多的包括地面、飞机和卫星等多手段大气观测资料得以同化使用,包括极轨、静止气象卫星测量的辐射亮温,雷达探测的径向风和反射率因子信息,全球导航卫星系统无线电掩星探测资料等。为进一步改进高影响天气事件的数值预报,目标观测技术持续发展,指导获得最大预报正影响的观测区域。基于资料同化理论和方法的发展,中国的资料同化业务系统也得到了长足进步,建立了先进的资料同化业务系统,5 d全球天气预报水平在过去10年提升了约15%。在回顾过去百年资料同化发展历程的基础上,讨论了未来资料同化方法和业务系统框架的发展、新型观测资料的使用以及同化与人工智能的结合等研究方向。

**关键词** 资料同化, 多源观测, 大气可预报性, 数值天气预报

中图法分类号 P435

## 1 引言

数值天气预报为一初值问题,即给定当前大气状态、侧边界和上、下边界条件,数值模式能预报大气的未来状态。可见,预报的准确性依赖于初值的精确度。而初值的获取是基于所能获取的信息得到大气状态的最优估计(Talagrand, 1997),实际中通常结合观测资料和短期预报而得到大气状态的优化估计,这就是“资料同化”(Daley, 1991; Kalnay, 2003)。

在天气预报资料同化发展初期,经验的资料同化方法得以发展,如插值方案(Panofsky, 1949; Gilchrist, et al, 1954)、逐步订正(Cressman, 1959)、牛顿松弛(Hoke, et al, 1976)等客观分析方法。而同期,中国学者创新地提出了基于近期历史演变资料进行未来状态预报的思想,将天气预报初值问题转换为使用天气历史演变的外推预报(顾震潮, 1958a, 1958b)。进一步将近似描述大气过程的微分方程的求解问题等价地转换为使用多时刻历史观测资料的泛函数极值问题(丑纪范, 1974),这也是后来迅速发展并在数值天气预报中广泛应用的变分方法的主要思想。随着数值模式的发展,中国学者深化资料同化理论,提出数值天气预报是一个初值问题,也是一个反问题(丑纪范, 2007),通过资料同化优化初始条件、边界条件及模式参数估计等。但不稳定性问题带来了挑战,为此,在资料同化中引入数学物理反问题的正则化思想,在目标泛

函数中增加稳定泛函数,可有效解决不稳定性及计算的不稳定性(黄思训等, 2003)。在业务应用领域,中国气象局早期主要依赖于引进的同化技术。从2000年开始,中国气象局团队致力于发展基于变分的资料同化理论和方法,逐步建立了GRAPES-MESO(现为CMA-MESO)区域三维变分同化系统和GRAPES(现为CMA-GFS)全球四维变分同化系统,实现了业务化运行(薛纪善等, 2008; Zhang, et al, 2019; 沈学顺等, 2020),并有效提升了全球业务预报水平(图1)。

数值天气预报资料同化在优化的算法外,还需要高效充分地吸收观测资料信息。在20世纪70年代,卫星反演产品就开始同化到数值模式中,并对预报产生较大贡献(Smith, et al, 1970a, 1970b)。得益于快速辐射传输模式和变分同化技术的发展(Saunders, et al, 2018; Weng, et al, 2020; Johnson, et al, 2023),卫星资料同化在20世纪90年代从早期的同化反演产品演变到了直接同化卫星观测的亮温,进一步加强了卫星资料在数值天气预报中的重要性(Eyre, et al, 2020)。2009年,中国全球/区域一体化数值预报模式(GRAPES)实现准业务运行,显著推进了卫星资料在中国数值预报模式中的应用,特别是中国的风云(FY)气象卫星观测资料。2015年,FY-2D云导风产品实现在GRAPES中的同化应用。2016年,FY-3C微波探测资料和掩星资料进入业务应用(Li, et al, 2016a, 2016b)。此后,FY-4A/B、FY-3D/E各类载荷相继得到同化应用,

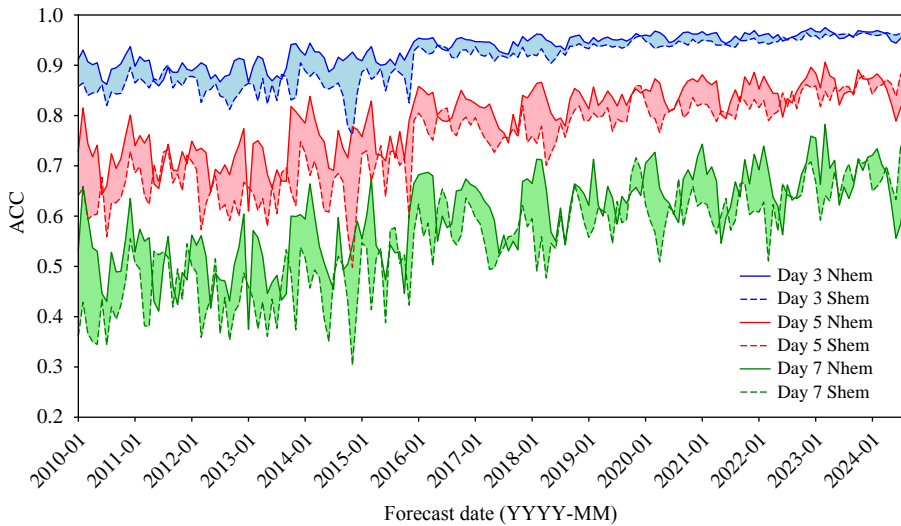


图 1 中国气象局全球数值天气预报水平进展(2010 年 1 月—2024 年 8 月北半球及南半球 500 hPa 高度场第 3、5、7 天距平相关系数(ACC)月平均演变特征, 实线: 北半球; 虚线: 南半球)

Fig. 1 Progress of global NWP by CMA (monthly mean evolution of ACC of 500 hPa geopotential height for 3rd, 5th, and 7th day, respectively, from January 2010 to August 2024; solid lines are for the northern hemisphere, and dashed lines are for the southern hemisphere)

标志着风云卫星资料的定量应用迈上新台阶。此外, 雷达资料也为监测和研究对流尺度天气提供了重要的手段, 中国学者同化雷达资料改善了对流尺度天气的同化和预报效果(陈敏等, 2014; Shao, et al, 2016; 陈耀登等, 2018; Sun, et al, 2020a)。

目标观测策略的提出, 推动了资料同化的精细化, 即在有限的“敏感区域”进行高质量加密观测, 通过同化加密观测, 改进初始场质量, 进而提高高影响天气事件的预报精度。针对敏感区域识别问题, 中国学者考虑大气海洋运动的非线性本质, 提出用条件非线性最优扰动(CNOP)方法识别敏感区的策略, 而且发现在 CNOP 识别的敏感区内获得的加密观测资料, 较在传统的基于线性近似方法确定的敏感区内获得的资料, 能够更加有效地提高高影响天气事件的预报水平。

文中首先对数值天气预报资料同化的理论和方法发展、多源观测资料的同化进展、目标观测策略的提出和发展, 以及中国业务天气预报资料同化系统的进步做了整体回顾; 进一步, 对资料同化在当前数值模式、观测资料、数据科学和人工智能迅速发展环境下的挑战和机遇进行了展望。

## 2 资料同化方法和理论

随着数值模式、观测系统和计算科学的发展,

资料同化方法和理论经历了从早期经验的客观分析, 到以统计估计理论为基础的分析理论, 再到结合大气动力学的同化方法。这里着重对已在数值天气预报中实现业务化并具有统计理论支撑的资料同化方法展开讨论, 对还未实现业务化的非线性、耦合资料同化等方法在未来展望中论述。

### 2.1 变分方法

以统计估计理论为基础的分析方法在 20 世纪 80 年代前后得以发展。Eliassen 等 (1960) 首先推导了基于观测和背景场向量的多元最优插值方程。随后发展的最优插值方案(Optimal Interpolation, OI)在物理空间寻找最优权重矩阵, 比如格点上 (McPherson, et al, 1979) 或者有限体积元上 (Lorenc, 1981), 并基于短期预报与无线电测风探空观测的差值估计背景误差协方差(Hollingsworth, et al, 1986; Thiébaux, et al, 1987)。Gandin (1963) 也独立推导了多元最优插值方程, 并应用于苏联的客观分析。最优插值方案成为 20 世纪 80—90 年代初的业务分析方案。

不同于最优插值方案通过“影响半径”局部求解更新权重, 三维变分(Three-Dimensional Variational, 3DVar; Sasaki, 1970)则通过全局优化算法求得目标函数的极小值, 获得极小化的控制变量。三维变分还有一类观测空间形式, 即物理空间

分析方案(PSAS; Da Silva, et al, 1995), 在观测(物理)空间寻求目标函数的极小化。三维变分、物理空间分析方案、最优插值在解的形式上具有等价性(Lorenc, 1986), 但三维变分和物理空间分析方案相对于最优插值有更具一般性和全局性的背景误差协方差, 例如基于针对同一时刻不同预报差值的方法等(Parrish, et al, 1992; Rabier, et al, 1998)。

四维变分(Four-Dimensional Variational, 4DVar; Lewis, et al, 1985; Courtier, et al, 1990)是三维变分的一个重要推广。相对于三维变分, 四维变分可以考虑观测资料在同化窗内的时间分布(Daley, 1991), 还能隐式地获得背景误差协方差随时间的演变(Thépaut, et al, 1993)。为更好地求得最优解, 四维变分可写作增量的形式(Courtier, et al, 1994; Lorenc, 1997), 寻找相对参考状态的最优扰动而非直接寻找最优状态, 还可以通过“预处理”实现求解的加速(Parrish, et al, 1992; Derber, et al, 1999)。强约束的四维变分假设模式是完美的(Sasaki, 1970), 为突破这一假设, 可以对模式误差进行订正(Derber, 1989; Zupanski, 1993)或使用弱约束来表征模式误差(Bennett, 1992; Egbert, et al, 1994; Bennett, et al, 1996)。当模式完美、初始时刻背景误差协方差正确时, 四维变分分析在同化窗结束时刻的分析值与广义卡尔曼滤波相同(Lorenc, 1986)。自20世纪90年代中期起, 三维变分和四维变分方法成为主流的业务分析方案。

## 2.2 集合卡尔曼滤波

最优插值和三维变分使用静态的背景误差协方差, 但“日变化误差”揭示了流依赖背景误差协方差的重要性(Kalnay, et al, 1997)。卡尔曼滤波(Kalman Filter, KF; Kalman, 1960; Kalman, et al, 1961)使用由模式随时间演变而得到的背景误差协方差, 为四维资料同化建立了数学框架。扩展卡尔曼滤波(Extended Kalman Filter, EKF; Ghil, et al, 1981; Daley, 1995)是卡尔曼滤波在非线性模式中的推广, 可为大气状态及其误差协方差提供最佳的线性无偏估计(BLUE), 是资料同化的“金标准”; 但其计算量非常大, 因为需要基于线性模式矩阵更新误差协方差。

集合卡尔曼滤波(Ensemble Kalman Filter, EnKF; Evensen, 1994; Houtekamer, et al, 1996)是一个简化扩展卡尔曼滤波的途径, 其利用蒙特卡罗

方法估计误差协方差。集合卡尔曼滤波可以近似得到卡尔曼滤波的分析解, 适用于高维动力系统, 并提供集合预报所需的初始条件(Houtekamer, et al, 2005a, 2014)。最初的集合卡尔曼滤波是一种随机滤波, 需要扰动观测获得一致的分析解和分析误差协方差(Burgers, et al, 1998; Houtekamer, et al, 1998)。为避免扰动观测带来的虚假相关, 确定性滤波方法得以提出, 比如集合调整卡尔曼滤波(Ensemble Adjustment Kalman Filter, EAKF; Anderson, 2001)、集合均方根滤波(Ensemble Square Root Filter, EnSRF; Whitaker, et al, 2002)、局地集合转置卡尔曼滤波(Local Ensemble Transform Kalman Filter, LETKF; Bishop, et al, 2001; Hunt, et al, 2007)等。确定性滤波方法利用分析误差背景场求解最优更新权重, 并且在没有协方差局地化时获得一致的解(Tippett, et al, 2003)。在集合卡尔曼滤波分析场的基础上, 利用不同时刻的样本相关可以实现对未来观测的同化, 即集合卡尔曼平滑(Ensmeble Kalman Smoother, EnKS; Evensen, et al, 2000)。

集合卡尔曼滤波应用于实际高维大气时, 有限集合数目、模式误差、线性相关等因素会导致滤波发散, 一个解决的方法是协方差局地化(Covariance Localization; Hamill, 2001; Anderson, 2012), 其通常为观测和模式变量间距离的函数(Gaspari, et al, 1999), 通过调整背景误差协方差矩阵(Houtekamer, et al, 2001; Lei, et al, 2018)或观测误差协方差矩阵(Hunt, et al, 2007)实现。局地化函数可以随观测类型变化(Zhang, et al, 2009a; Lei, et al, 2014a)、随模式变量种类变化(Kang, et al, 2011; Lei, et al, 2015a, 2015b)、随同化时间变化(Anderson, 2007; Chen, et al, 2010), 因此适应性的局地化方法得到发展(Bishop, et al, 2009; Lei, et al, 2014b, 2020; Zhen, et al, 2014; Flowerdew, 2015)。另一个解决滤波发散的办法是协方差膨胀(Covariance Inflation; Anderson, et al, 1999; Houtekamer, et al, 2005b)。协方差膨胀可以经验性或适应性地乘性增加集合扰动(Anderson, 2009; Miyoshi, 2011; El Gharamti, 2018)或将后验集合扰动增加至先验集合扰动或集合离散度(Zhang, et al, 2004; Whitaker, et al, 2012; Ying, et al, 2015)或添加集合扰动(Wang, et al, 2013a, 2013b; Yang, et al, 2015), 并考虑模式的

不确定性(Buizza, et al, 1999; Berner, et al, 2009; Ha, et al, 2015; Zeng, et al, 2020)。自 21 世纪初期, 集合卡尔曼滤波开始在加拿大、美国等业务中心运行(Houtekamer, et al, 2005b; Whitaker, et al, 2008)。

### 2.3 混合集合-变分方法

变分方法使用的静态背景误差协方差矩阵虽为满秩, 但不能捕捉“日变化误差”; 集合卡尔曼滤波利用短期预报建立流依赖背景误差协方差, 但其不满秩且受到样本误差和模式误差的影响。因此, 结合变分和集合卡尔曼滤波的混合同化方法得以发展。混合集合-变分方法可以直接将静态和流依赖的背景误差协方差相结合(Hamill, et al, 2000), 以减少流依赖背景误差协方差不满秩和样本误差的影响(Wang, et al, 2008, 2013a, 2013b; Zhang, et al, 2009b; Kleist, 2015a, 2015b); 静态背景误差协方差也同样可用于集合卡尔曼滤波, 以表征模式误差(Meng, et al, 2008)。集合-四维变分方法(Ensemble 4DVar, E4DVar; Lorenc, 2003; Bonavita, et al, 2012)可以通过 $\alpha$ 控制变量方法实现将流依赖背景误差协方差嵌入变分求解的损失函数, 这与直接混合静态和流依赖背景误差协方差等价(Wang, et al, 2007)。集合-四维变分方法可优于单独的四维变分或集合卡尔曼滤波(Zhang, et al, 2009b; Buehner, et al, 2010a, 2010b)。

相对于集合-四维变分方法, 四维集合-变分方法(4D Ensemble-Var, 4DEnVar; Liu, et al, 2008)利用集合预报获得误差随时间的演变, 而不再需要切线性模式和伴随模式。进一步, 降维投影四维变分方法(Dimension-Reduced Projection 4DVar, DRP-4DVar; Wang, et al, 2010; He, et al, 2017)和非线性最小二乘集合四维变分方法(Nonlinear Least-Squares Ensemble 4DVar, NLS-En4DVar; Tian X J, et al, 2015, 2018)等四维集合-变分方法也相继提出。然而, 四维集合-变分方法无法获得静态背景误差协方差在同化窗内的演变(Wang X G, et al, 2014), 也难以处理局地化矩阵随时间的变化(Bishop, et al, 2009), 因此四维集合-变分不如集合-四维变分方法(Lorenc, et al, 2015; Poterjoy, et al, 2015, 2016a)。

不同于混合背景误差协方差, 混合权重方法(Hybrid Gain; Penny, 2014)将变分所得分析场与

集合卡尔曼滤波分析场进行混合, 该方法也优于单独的集合卡尔曼滤波和使用静态背景误差协方差的四维变分方法(Bonavita, et al, 2015)。自 21 世纪第 2 个 10 年初, 集合-四维变分方法相继在欧洲中期天气预报中心(ECMWF)、英国气象局等业务中心运行(Bonavita, et al, 2012; Clayton, et al, 2013)。随后, 四维集合-变分方法也应用于加拿大和美国等业务预报中心(Buehner, et al, 2015a; Caron, et al, 2015; Kleist, et al, 2015b)。

混合集合-变分方法同时需要变分系统和集合卡尔曼滤波系统, 但两个系统间的不一致性会导致次优的混合集合-变分分析解。局地集成的集合-变分方法(Ensemble Variational Integrated Localized, EVIL; Auligné, et al, 2016)不需要集合框架, 而是利用变分求解所得的分析背景误差协方差构建集合分析场。而集成混合集合-变分方法(Integrated Hybrid Ensemble-Variational, IHEnKF; Lei, et al, 2021)则通过对大样本气候态扰动进行采样以近似静态背景误差协方差, 利用调制的方法在集合卡尔曼滤波框架下实现混合集合-变分方法和混合权重方法; 还能进一步使用混合背景误差协方差更新集合扰动, 从而优于混合集合-变分方法。

### 2.4 多尺度和平衡的资料同化

大气具有多时、空尺度的演变特征, 大气多源观测也能捕捉不同尺度的信息, 因此多尺度资料同化得以提出, 以有效利用多源观测约束大气在不同尺度上的误差。多尺度资料同化可以顺序地分步实现, 先使用更大尺度的局地化半径同化大尺度观测资料(如常规观测), 在更新的分析场上再使用更小尺度的局地化半径同化小尺度观测资料(如雷达观测), 以充分提取不同尺度观测信息(Zhang, et al, 2009a; Xie, et al, 2011; Sodhi, et al, 2022)。也可以使用不同的局地化半径同化相同的观测资料, 再将不同尺度的分析增量结合而得到最终的分析场(Miyoshi, et al, 2013)。不同于分步同化, 多尺度资料同化也可在集合-变分同化框架中或集合同化框架中, 对背景误差协方差应用不同尺度的局地化尺度, 一次性更新能解析的所有尺度信息(Buehner, 2012; Buehner, et al, 2015b; Wang X G, et al, 2021; Wang Y M, et al, 2023)。

数值预报模式使用资料同化所得的分析场作为初值时, 面临初始化冲击, 因此需要平衡的资料

同化, 以减小虚假重力波等噪声对数值预报的影响 (Temperton, et al, 1991)。四维变分方法可以在损失函数中加入平衡约束项。但集合卡尔曼滤波面临其分析场作为初始条件积分时的不平衡, 因此集合卡尔曼滤波可以转换为连续的形式(Bergemann, et al, 2010; Lei, et al, 2012)或是使用更短的同化窗口(He, et al, 2020; Slivinski, et al, 2022), 也可以使用更多当前的观测获得过去更精确的初始条件, 以减小初始化过程(Kalnay, et al, 2010)。对于普适的模式初始化, 可以使用数字滤波将快速振荡略去(Lynch, et al, 1992), 也可以使用分析增量更新方法保持大尺度的分析增量(Bloom, et al, 1996)或是同时保留大尺度和小尺度分析增量在同化窗内演变的四维分析增量更新方法 (Lorenc, et al, 2015; Lei, et al, 2016)。

### 3 多源大气观测资料

#### 3.1 卫星资料

在过去 50 年里, 卫星资料同化在数值天气预报中的作用变得越来越重要。1969 年 4 月, 搭载第一颗温度探测器的“Nimbus 3”卫星发射升空后不久, 其 SIRS 仪器的反演产品就首次被“纳入”美国国家气象中心的客观分析中, 并对太平洋区域的分析场和对全美国的预报产生了较大影响(Smith, et al, 1970a, 1970b)。随后, 国际上也相继开展了一系列卫星产品同化试验(Atkins, et al, 1975; Kelly, 1977; Desmarais, et al, 1978; Druyan, et al, 1978; Kelly, et al, 1978; Gilchrist, 1982; Uppala, et al, 1984), 由于受卫星产品低垂直分辨率以及 2—3 K 温度反演误差的影响, 这一时期的同化试验对预报总体是一个中性的影响, 对南半球的影响更大一些(Ohring, 1979)。Eyre 等(1989)首次提出在数值天气预报中直接同化卫星探测的辐射亮温, 并通过一维变分成功地将 TIROS 垂直探空仪探测的辐射信息同化到数值天气预报系统中(Eyre, et al, 1993)。1995 年 10 月美国国家环境预报中心(NCEP)(Derber, et al, 1998)、1996 年 1 月 ECMWF(Ander-son, et al, 1994; McNally, et al, 1996; Saunders, et al, 1997)率先采用 3DVar 直接同化卫星观测辐射率。ECMWF 于 1997 年 11 月首次在 4DVar 中采用了卫星资料的直接同化技术。随后, 其他一些数值天气预报中心也先后在 3DVar 和 4DVar 系统中

直接同化辐射率(Chouinard, et al, 2002; Joo, et al, 2002; Okamoto, et al, 2002; Li, et al, 2016b)。

#### 3.1.1 快速辐射传输模式

快速辐射传输模式是将大气状态快速映射到观测量, 因此也叫观测算子, 主要由大气气体吸收模块、粒子散射模块、地表发射率模块、辐射传输求解模块以及对应的切线性和伴随模块组成。目前, 主要有 3 个快速辐射传输模式广泛应用于数值天气预报卫星资料同化: 欧洲气象卫星开发组织(EUMETSAT)开发的 Radiative Transfer for the TIROS Operational Vertical Sounder (RTTOV) 模式(Saunders, et al, 2018)、美国国家海洋和大气管理局(NOAA)开发的 Community Radiative Transfer Model (CRTM) 模式(Johnson, et al, 2023)、中国气象局(CMA)开发的 Advanced Radiative Transfer Modeling System (ARMS) 模式(Weng, et al, 2020; Yang, et al, 2020)。ARMS 作为中国自主研发的快速辐射传输模式, 已于 2023 年替代 RTTOV 在 CMA-GFS 中得到业务应用, 其创新性主要体现在:(1)发展了耦合真实光谱响应函数的大气透过率计算方案, 有效改善了微波通道模拟的精度(Kan, et al, 2024); (2)基于 T-Matrix 和离散偶极子近似(DDA)方法构建了非球形云粒子和气溶胶粒子散射数据库, 支撑全天空卫星资料同化(Yang, et al, 2020); (3)发展了基于双尺度海洋粗糙度模型的偏振双向反射分布函数(pBRDF), 完善了微波全极化海-气耦合辐射传输模式的海-气界面双向反射物理机制, 增强了对主被动一体化的卫星辐射传输模拟能力(He, et al, 2023); (4)改进了微波陆表发射率物理模型(LandEM), 发展了 Chen-Weng 粗糙地表反射率模型, 提升了复杂地表发射率估算精度(刘勇洪等, 2025); (5)完善了离散坐标辐射传输理论, 克服了大气散射过程和地表反射过程对方位对称性质的假设和依赖, 发展了通用矢量辐射传输求解方案(VDISORT), 可模拟全谱段卫星斯托克斯矢量辐射(Zhu, et al, 2024)。

#### 3.1.2 红外辐射资料同化

红外辐射资料同化由于光谱特性限制及云区辐射量同化的困难(Li, et al, 2022a), 目前仍然以晴空辐射率直接同化或部分有云的红外辐射资料同化为主。晴空辐射率需要进行精确的云检测, 晴空通道云检测方案通过排序法对参与同化的通道进

行排序, 确定云顶高度, 同化云顶以上的通道, 提高资料利用率(McNally, et al, 2003)。对于部分有云的红外探测同化, Li 等 (2005) 提出了“最优清云”技术, 将部分有云的红外探测量转换为等效晴空辐射量而进行同化, 有效提升了云、雨区红外探测资料的利用率, 并改进了热带气旋预报(Wang P, et al, 2014, 2017)。针对红外辐射率资料云、雨区直接同化的难点, Jones 等 (2013) 和 Chen 等 (2015) 分别采用集合卡尔曼滤波和变分方法成功同化了可见光和近红外探测反演的卫星云水、云冰路径产品; Meng D M 等 (2019) 在扩展控制变量中引入水凝物, 实现了云区红外反演资料的混合同化。

此外, 对数千通道的红外高光谱资料进行辐射传输模拟的计算成本高, 并且难以确定光谱相关的观测误差。因此, 通道相关性处理、主成分分析等技术得以发展, 以实现优选的通道同化(Rabier, et al, 2002; Collard, 2007; Matricardi, et al, 2014; Zhou, et al, 2024)。通常每台仪器同化的通道在 200 个左右, 也避免了光谱区域被未充分表示的可变痕量气体(如臭氧等)影响。中国 CMA-GFS 目前不仅具备同化中国极轨和静止气象卫星红外高光谱 FY-3D/E HIRAS (Liu, et al, 2014)、FY-4A/B GIIRS(Yin, et al, 2021; Han, et al, 2023) 的能力, 也能实时同化 METOP-B/C IASI (李刚等, 2016)、NOAA 20 CRIS 等红外高光谱资料。此外, 红外成像仪资料, 包括 FY-2 VISSR、FY-4A/B AGRI(王皓等, 2018)、H8/H9 AHI 和 GOES-18 ABI 资料等, 都在 CMA-GFS 中实现了业务应用。

### 3.1.3 微波辐射资料同化

在众多卫星仪器中, 微波探测资料具备较强的穿云透雨能力, 可以提供全天空、全地表大气温度和水汽垂直分布信息, 显著改进数值天气预报精度(Bormann, et al, 2019; Li J, et al, 2024)。2009 年, ECMWF 实现了世界上第一个全天空卫星资料业务同化系统(Bauer, et al, 2010)。随后云、雨区卫星资料同化技术相继应用于日本气象厅和 NCEP 业务模式中(Okamoto, 2014; Zhu, et al, 2014)。早期 ECMWF 的云、雨区同化采用 1D-4DVar 的间接同化策略, 对受云、雨影响的卫星观测采用背景场中的温度、湿度作为初猜值, 通过 1DVar 反演出卫星观测对应的整层水汽含量(TWPC), 而后将 TWPC 作为虚拟观测代入 4DVar 同化(Geer, et al,

2008)。由于 1DVar 可以反演出与卫星观测云雨条件匹配的大气状态, 因此可以避免背景场中的晴雨条件与观测资料相悖的问题, 同时还可以通过 1DVar 进行全天空质量控制而不需要采用复杂的云检测方案。但是这种方法反演得到的 TWPC 已经隐含了模式背景场的湿度信息, 后续代入 4DVar 更新背景场时会产生虚假的观测增量(Geer, et al, 2010)。因此, 该方法随后被 ECMWF 全天空直接同化方法取代(Bauer, et al, 2010; Geer, et al, 2010)。CMA-GFS 模式也成功开展了风云卫星微波成像仪的全天空同化, 显著改进了全球水汽的分析和预报精度(Xie, et al, 2023)。在过去 10 余年里, 数值天气预报中卫星资料同化最重要的进展便是云和降水影响下的资料同化技术(Geer, et al, 2018)。

除云、雨影响的同化方法外, 受地表影响的微波资料同化近年来也得到了越来越多的关注, 其难点主要为地表发射率的估计精度。目前同化系统中使用的微波地表发射率估计方法可以分为物理模型方法、统计模型方法和动态反演方法(Tian Y D, et al, 2015)。物理模型方法旨在根据地表发射率与各种地表参数(例如地表类型、植被参数、土壤参数等)之间的物理关系建立数值模型, 但是其计算精度依赖于大量地表参数输入信息的准确估计, 但这些信息却难以获取, 阻碍了此类方法的广泛应用(Weng, et al, 2001)。统计模型方法是指以地表发射率的历史数据集作为实际瞬时发射率的经验或半经验估计值, 例如 TELSEM 数据集(Aires, et al, 2011) 和 CNRM 数据集(Karbou, et al, 2010) 等。这类方法易用性强, 但历史统计数据集难以表征当前瞬时的发射率状态, 对于地表特征的时间变化或亚像元尺度地表特征空间变化的估计能力不足。动态反演方法是指通过计算大气上行、下行辐射以及大气透过率和地表温度, 获取给定观测亮温条件下的地表发射率(Karbou, et al, 2006)。这种方法不仅具有较强的易用性, 同时还可以考虑复杂条件下的发射率动态变化, 因此被大量应用于陆表微波资料同化(Krzeminski, et al, 2009; Baordo, et al, 2016; Xiao, et al, 2023b)。基于动态反演方法, CMA-GFS 模式成功实现了陆面 AMSU 仪器近地表通道的业务同化, 显著改进了全球低层大气的分析和预报精度, 尤其是对陆地占比较大的北半球(Xiao, et al, 2023b)。

### 3.1.4 从双星观测到三星组网

Joo 等 (2013) 发现数值天气预报中 64% 的模式预报误差减小的贡献来自卫星, 而极轨气象卫星数据提供约 90% 的卫星观测带来的误差减小率。2010 年以前, 国际上极轨气象卫星采用上午星和下午星双星组网的探测体系。考虑到双星体系无法在全球数值天气预报模式 6 h 的同化窗内提供完整的全球覆盖, 世界气象组织(WMO)组织专家论证 (WMO, 2009) 提出黎明星、上午星、下午星三轨气象卫星业务组网观测的模式。2014 年, 中国气象局在 FY-3 03 批可研报告中明确要发射黎明星的计划。2021 年 FY-3E 成功发射, 三星组网的观测系统由中国人实现, 有效弥补了极轨卫星在 6 h 同化窗口内的观测差距 (Zhang, et al, 2022)。FY-3E 的观测资料不仅在中国的数值天气预报业务系统应用 (Li J, et al, 2024), 而且还在 ECMWF、英国气象局、日本气象厅、韩国气象厅等多家模式业务应用, 全球观测资料的获取确保了数值天气预报对全球资料的观测需求 (Zhang, et al, 2024)。

## 3.2 雷达资料

雷达资料具有较高的时、空分辨率, 能够捕捉到中、小尺度天气系统信息, 雷达资料的合理利用可有效改善初始场中对流系统的动力和微物理特征, 因此有效地同化雷达观测资料被认为是提高对流性天气数值预报水平的关键之一 (万齐林等, 2005; Sun J, et al, 2014; Sun J Z, et al, 2020b)。

### 3.2.1 雷达资料观测算子

传统多普勒天气雷达探测变量主要是径向风和反射率因子。径向风含有重要的对流系统内部动力特征, 反射率因子包含对流系统内部的微物理信息。雷达径向风在多个资料同化系统中得到了广泛应用, 包括 VDRAS 四维变分同化系统 (Sun, et al, 1997)、ARPS 三维变分同化系统 (Gao, et al, 1999)、WRFDA 系统 (Xiao, et al, 2005)、GRAPES 三维变分同化系统 (刘红亚, 2009) 等。然而, 常规径向风观测算子仅能引入径向风信息, 对于切向风信息的分析存在一定的欠缺。基于在区域方位角内风场均匀的假定, 罗义等 (2014) 将雷达径向风速及其空间变化引入到径向风观测算子当中, 实现了径向风同化时对切向风信息的分析。该径向风观测算子分别被引入到 GSI (Chen, et al, 2017) 和 GRAPES (马昊等, 2016) 同化系统中。

相较于径向风观测算子, 反射率因子观测算子更为复杂。早期研究通过反射率因子与雨水的经验关系, 建立了反射率因子观测算子 (Sun, et al, 1998; Xiao, et al, 2007)。Tong 等 (2005) 和 Gao 等 (2012) 进一步引入了雪和雹等冰相粒子, 建立了基于 Lin 微物理参数化方案的反射率因子观测算子, 分别实现了集合卡尔曼滤波以及变分框架下反射率因子的直接同化。类似地, Hawkness-Smith 等 (2021) 构建了反射率因子观测算子, 实现了英国气象局同化系统对反射率因子的直接同化。Liu 等 (2022) 基于 Thompson 微物理参数化方案引入了雨水数浓度, 建立了基于双参数水凝物粒子的反射率因子观测算子。但反射率因子的观测算子仍较为经验, 观测算子误差也较大。

Jung 等 (2008a) 基于 T 矩阵算法估计了各降水粒子的后向散射截面, 构建了更为准确的反射率因子前向观测算子, 实现了反射率因子的集合卡尔曼滤波同化。Wang 等 (2018) 基于 Jung 等 (2008b) 的反射率因子观测算子, 构建了其切线性和伴随算子, 实现了变分框架下反射率因子的直接同化。Zeng (2013)、Zeng 等 (2014)、Jerger (2014) 在反射率因子观测算子中考虑了不同的物理角度, 构建了三维反射率因子观测算子, 实现了模式中反射率因子的集合卡尔曼滤波同化。Wang 等 (2019) 在 Jung 等 (2008b) 的基础上, 开发了针对冰相粒子的正向反射率因子观测算子, 模拟反射率因子参数化为快速多项式关系的混合比率。这类更复杂、更准确的反射率因子观测算子显著减小了观测算子误差, 为更好地同化雷达反射率因子提供了必要条件。

此外, 已经有许多研究开发和发布了雷达观测算子。Jung 等 (2008b) 实现了一种偏振雷达模拟器, 称为偏振雷达数据模拟器。该模拟器使用球状体来描述水凝物, 并使用在线瑞利近似或离线查找表计算光谱特性 (Mishchenko, et al, 1994), 已应用于低频 S 波段、C 波段和 X 波段雷达。Wolfensberger 等 (2018) 开发了跨平台的偏振雷达观测算子, 该观测算子包含霰粒子的雷达模拟, 其将所有的水凝物粒子描述为均匀的球体。Oue 等 (2020) 开发了云解析模型雷达模拟器, 可模拟偏振雷达和激光雷达观测, 然而其目前仅限于地面平台, 对融化粒子没有明确的处理方法。浙江大学 (ZJU-AERO; Xie, et al, 2023) 设计的精确高效雷达观测算子, 将水凝物

的散射计算和光学特性数据库的构建引入了雷达观测算子, 可以处理大气中的非球形和非均匀水凝物粒子。

### 3.2.2 常规雷达资料同化

径向风观测含有重要的对流系统内部动力特征, 为监测和研究对流尺度天气提供了重要手段(许小峰, 2003; 万齐林等, 2005; Liang, 2007; 杨毅等, 2008; Sun, et al, 2020b)。雷达径向风的同化相对成熟, 能够有效改善对流尺度分析和对流系统的预报效果(Gao, et al, 2004; Xiao, et al, 2005; Li, et al, 2012; 陈敏等, 2014; Zhu, et al, 2014; Shao, et al, 2016; 陈耀登等, 2018; 慕熙昱等, 2019)。

相较于径向风, 反射率因子同化相对更为复杂。目前, 雷达反射率因子同化的方法主要分两类: 直接同化和间接同化。直接同化是将模式变量投影到观测空间, 从而直接比较背景场和观测的雷达反射率因子, 进而通过同化分析过程获得分析场。雷达反射率因子的直接同化取得了较好的应用效果(Sun, et al, 1997; Tong, et al, 2005; Xiao, et al, 2005; 盛春岩等, 2006; Gao, et al, 2012)。

然而, 变分同化直接同化雷达反射率因子也存在挑战: 当背景场中水凝物含量较小时, 代价函数中观测项梯度大, 常使得极小化过程无法有效收敛, 同时非线性反射率因子观测算子难以处理, 常造成水凝物分析不够合理(Sun, et al, 1997; Wang, et al, 2013; Liu, et al, 2019)。增量形式的变分同化通过多次外循环来改善反射率因子观测算子的非线性问题, 但这样会增加计算代价。相较于变分方法, 基于集合卡尔曼滤波的雷达反射率同化可采用非线性观测算子(兰伟仁等, 2010a, 2010b; Yussouf, et al, 2010), 在包含复杂微物理过程的模式中有效吸收雷达反射率因子观测。但非线性观测算子不满足集合卡尔曼滤波的高斯误差分布假设, 而常出现次优解, 特别是密集的强非线性雷达观测, 同时集合卡尔曼滤波还受到采样误差和模式误差的影响(Liu, et al, 2020)。

背景误差协方差在对流尺度资料同化中起重要作用, 合适的背景误差协方差可以得到更协调的分析场(Chen, et al, 2013; 陈娴雅等, 2022; Zheng, et al, 2023)。Wang Y M等(2021)开发了包含水凝物控制变量的静态背景误差协方差, 并将静态背景误差协方差引入混合集合-变分框架, 对超级单体的

预测效果优于集合背景误差协方差。此外, 使用包括垂直和多变量相关的水凝物背景误差协方差同化雷达反射率因子能够明显改善热、动力条件和强降雨预报(Zheng, et al, 2023)。

为避免直接同化时反射率因子非线性观测算子线性化带来的线性近似误差, 目前许多研究和业务中还常采用间接同化方式来同化雷达反射率因子, 即在同化过程中先将雷达反射率因子反演为模式变量, 其通过背景场温度判定反演水凝物的类型及比例, 然后再同化反演所得的模式变量(Wang, et al, 2013a, 2013b)。有研究提出一种新的背景依赖性水凝物反演方法, 即基于模式背景场特征实时更新间接同化中水凝物的类型及比例, 提高了反射率因子同化效果、改进了天气预报效果(Chen, et al, 2020, 2021; 黄静等, 2022)。间接同化方法避免了构建反射率因子观测算子的切线性算子和伴随算子, 改善了代价函数求解的数学条件, 同时计算代价相对直接同化更低, 因此广泛应用于各类研究和业务中(范水勇等, 2013; 张诚忠等, 2019; Lai, et al, 2020)。

### 3.2.3 双偏振雷达资料同化

近年来, 包括中国在内的多个国家都开始进行双偏振雷达的布网升级(Wu, et al, 2018)。双偏振雷达能更准确地识别水凝物相态特征, 双偏振雷达观测资料的有效利用可有效改善数值预报中的水凝物等微物理初始状态(Zhao, et al, 2019)。双偏振雷达观测的同化研究已获得进展, 中国学者构建了基于单、双参微物理方案的双偏振观测算子, 利用集合卡尔曼滤波直接同化双偏振雷达的模拟观测(Jung, et al, 2008a, 2008b; Xue, et al, 2010)。进一步, Putnam等(2019)进行了双偏振雷达真实观测的集合卡尔曼滤波同化, 结果表明偏振观测量的同化改善了偏振量的分析和预报, 获得了正影响, 但其同化的偏振量观测仅限于水平反射率因子及2 km以下的差分反射率因子。

集合卡尔曼滤波方法受有限集合成员数量的限制, 较难合理估计背景场误差协方差, 并面临矩阵不满秩、分析场变量不平衡、模式误差等问题, 因此基于变分方法的双偏振雷达的同化研究也相继开展。Li等(2017)基于变分法, 进行了单站双偏振雷达资料的个例模拟测试, 结果表明额外同化差分反射率因子和比差分相位, 可以进一步改善反射率因子的分析和预报。变分同化方法需要构建双

偏振观测量的切线性算子和伴随算子,为建立更合理的切线性算子和伴随算子,Kawabata等(2018)构建了基于液相粒子的双偏振观测量观测算子的切线性算子和伴随算子,Wang等(2019)建立了包含冰相粒子在内的水平/垂直反射率因子观测算子的切线性算子和伴随算子。

### 3.3 其他观测资料

掩星探测技术被认为是当前大气探测中最具有潜力的手段之一,可以提供全天空全球分布的中性大气和电离层信息,特别是2006年实施的“应用于气象、电离层与气候的星座观测系统”(COSMIC)为掩星资料的同化业务应用创造了条件。对于掩星资料的同化,最适宜的同化量是弯曲角和折射率,观测算子存在一维或二维两种情况。目前全球先进业务数值预报中心的预报业务都同化了掩星资料,并表明掩星资料是数值预报同化系统不可缺少的重要组成部分(Healy, et al, 2005; Poli, et al, 2009; Liu, et al, 2014)。CMA-GFS模式于2009年开始业务同化掩星数据,同化的要素是折射率,同化高度为1—50 km。CMA-GFS较早实现了FY-3D GNOS掩星折射率资料的同化(Wang, et al, 2020)。掩星数据在中国气象局数值预报系统中一直起重要作用,在CMA-GFS中掩星对24 h预报误差的贡献始终保持在前三位。

大气运动矢量(AMV)是资料同化最早关注的卫星资料之一,即使在其他卫星资料大量进入同化系统后,AMV资料在改进数值预报效果中的作用依然是不可忽视的(Forsythe, et al, 2007)。近十几年来,卫星云导风算法在示踪物代表像元选取和高度指定等方面取得了显著进展(许健民, 2020),尤其是风云气象卫星云导风通过运动代表性像元选取和半透明云高估计等改进后(张晓虎等, 2017)。早在2011年,FY-2E的云导风资料已达到国际同类产品水平(Salonen, et al, 2015)。当然,相对其他探测手段,AMV的误差仍比较大,尤其是云的高度指定误差使AMV所代表的大气运动的高度有很大的不确定性。FY-4A高光谱探测仪(GIIRS)垂直方向上数千通道为三维风场的高度指定带来了新的契机,研究表明,三维水平风场可以在晴空和部分有云区域下被有效反演(Ma, et al, 2021; Li, et al, 2022b),并且三维动力信息的合理同化对台风的路径和强度预报具有积极作用(Meng, et al, 2024)。

测风散射仪是一种星载雷达,它从多个方向测量海面的后向散射,由此可以导出海面的风向与风速(Stoffelen, et al, 1997)。卫星对同一片海面测得的一组不同方向的后向散射值,但可以对应多个不同的风向,因而给资料同化带来了新问题。目前同化这类资料一般是先参考背景场从几个可能风向中选取一个与背景场最接近的,也有把多个不同风向的风速同时同化,让同化系统自己根据权重选择。2022年,CMA-GFS 4DVar中实现了对中国海洋二号星(HY-2B)散射计风资料的同化,明显提高了CMA-GFS在洋面上对流层低层的分析场精度(Wang J C, et al, 2023)。2018年,欧洲空间局(ESA)成功发射了全球首颗星载测风激光雷达卫星ADM-Aeolus,它可提供垂直分辨率为0.25—2 km,从地面至30 km高度处的高时空分辨率、近实时全球径向风速。2022年,在CMA-GFS中首次实现Aeolus资料的业务应用,同化Aeolus资料能显著减小热带和南半球风场的分析误差,在热带地区平均分析误差(与ERA5相比)减小幅度能达到10%。在模式预报效果方面,对北半球、南半球和热带前3 d预报的改进比较显著,在东亚地区预报贡献为中性。

此外,中国地面自动气象站网从2008年起不断发展,至2023年形成约7万个站的地自动观测站网。高时、空分辨率地面观测资料成为CMA-MESO系统同化的重要观测资料来源之一,但中国地形复杂,有海拔平均在4000 m以上的“世界屋脊”——青藏高原和海拔平均在1000—2000 m的云贵高原、黄土高原,以及四川盆地等高原与盆地,还有海拔在1000 m以下的丘陵和平原。因此,相对平滑的模式地形与观测站地形存在一定的高度差,徐枝芳等(2006, 2007, 2009)的研究指出,不能有效解决模式与观测站地形高度差异会对地面资料同化带来负面影响。因此,徐枝芳等(2021, 2022)针对复杂地形下的2 m相对湿度和2 m气温资料同化,在CMA-MESO 3DVar系统分别发展了同化方案,提升了同化资料的数量和质量,并改进了地面要素的预报效果。同时,采用静力方程推算的地面气压同化方案替代连治华等(2010)的地面气压外插同化方案,不仅增加了观测资料使用率,同时解决了随地面观测站数增多,降水预报效果变差的问题。

## 4 目标观测策略

对高影响天气事件(如强降水、台风等)的预报,数值预报仍常常出现预报不确定性大的情形。观测数量不足和质量较差,大大限制了高影响天气事件预报水平的提高。研究表明,天气敏感区大气探测数据的充分利用,对于台风等高影响天气的准确预报极为关键(Wang, et al, 2017),如何优化利用资源,仅在有限的敏感区域进行高质量加密观测,成为高影响天气预报新的观测策略,即“目标观测”(Snyder, 1996)。国际全球观测系统研究与可预报性试验(THORPEX)计划聚焦预报对观测的需求,揭示了目标观测在提高台风路径预报能力中的重要作用(Shapiro, et al, 2004)。近年来,中国关于高影响天气事件预报的目标观测研究也取得了重要成果,并在外场试验中得到了成功应用,获得了宝贵的资料(Duan, et al, 2023)。

### 4.1 目标观测理念与可预报性试验

世界气象组织提出的 THORPEX 计划,其主要目的是提高 1—14 d 的高影响天气预报的准确率,延长高影响天气预报的服务时效,并使这些先进的预报产品能够发挥社会经济应用效益,服务于社会。THORPEX 计划提出了“目标观测”理念,作为常规的、固定的观测网的有效补充,使用可移动的观测设备,优先在重要但资料稀缺的区域增加观测,以减小这些区域的初始误差进而抑制预报误差增长。

在 THORPEX 计划的推动下,目标观测外场试验在全球范围迅速开展。大西洋-THORPEX 区域试验(A-TReC)于 2003 年秋季开始实施,收获了大量的常规、遥感观测资料,为提前 1—3 d 对可能影响欧洲的高影响天气预报提供了重要帮助(Rabier, et al, 2008)。2006 年,利用上升和平飘气球携带的探空仪,非洲地区启动了针对西非降水、东风波预报的目标观测外场试验(Agustí-Panareda, et al, 2010)。在高影响天气事件频发的欧洲,为了提高诸如冬季越格陵兰岛的流场畸变、中欧夏季降水、地中海地区秋季暴雨的预报技巧,有规模的外场试验在 2007—2009 年陆续开展(Wulfmeyer, et al, 2008; Prates, et al, 2009; Jansa, et al, 2011)。更大范围的目标观测外场试验于 2008 年在亚太地区(T-PARC)展开,T-PARC 试验在夏季周期中围绕

台风的动力学及可预报性等问题,包括台风的生成、旋转、变性、对下游中纬度地区风暴路径的影响(Elsberry, et al, 2008)等;在冬季周期中则利用飞机及探空观测探索了提高 3 d 后可能影响北美地区的天气系统预报技巧的可行性。此外,目标观测外场试验还覆盖了极地地区(IPY; Irvine, et al, 2011)。

### 4.2 目标观测策略

目标观测要求在关键的敏感区域实施额外观测,进而改善初始场质量,提高高影响天气事件的预报水平。当前目标观测策略主要分为两大类,一类基于分析敏感性,另一类则基于观测敏感性。

分析敏感性方法刻画了预报不确定性(预报误差)对分析场不同位置的扰动(初始误差)的敏感程度。敏感性越强,表明该位置的初始误差将引起更大的预报误差。因此,该位置即为目标观测的敏感区。这类方法主要包括伴随敏感性方法(Bergot, 1999; Wu, et al, 2007)、奇异向量(Singular Vectors, SVs)方法(Palmer, et al, 1998)、集合转换技术(Bishop, et al, 1999)等。在这些方法中,伴随敏感性方法和 SVs 方法被广泛应用于目标观测外场试验(如 T-PARC、IPY 等)。

观测敏感性方法则引入了观测和资料同化技术,通过评估在不同位置引入额外新观测对预报误差的影响来确定目标观测的敏感区。相较于其他位置,能够更多地减小预报误差的位置被识别为敏感区。这类方法的代表有 Hessian SVs 方法(Barkmeijer, 1998)和集合转换卡尔曼滤波(Bishop, et al, 2001),而后者被广泛地应用于目标观测外场试验(如 A-TReC、T-PARC、IPY 等)。针对 T-PARC 夏季周期的外场试验表明,将所获目标观测资料应用于 NCEP 和韩国气象厅的业务预报模式,热带气旋路径的预报误差减小了 20%—40%,应用于 ECMWF 和日本气象厅的业务预报模式时,如果预报时长超过 72 h,则热带气旋路径预报的改善不明显(Weissmann, et al, 2011)。

上述确定敏感区的方法在不同程度上均使用了线性近似,而大气运动具有非线性特征。Mu 等(2009)提出了根据条件非线性最优扰动(Mu, et al, 2003)方法识别目标观测敏感区的思路,构建了依据 CNOP 初始误差特定空间结构和所在地理位置确定目标观测敏感区,进而通过在该区域实施额外

观测,减小观测误差和降低预报误差的新技术。大量观测系统模拟试验表明,在CNOP方法识别的目标观测敏感区内同化资料,对提高热带气旋路径预报技巧具有关键作用,且较在传统方法SVs识别的敏感区内同化资料对预报水平的提高更加明显(Qin, et al, 2012, 2023; Chen, et al, 2013; Feng, et al, 2022; Chan, et al, 2023)。近年来,CNOP方法也被有关院校应用于中国近海海洋环境预报的目标观测理论研究和外场试验,对海洋预报水平的提高取得了明显效果(Liu, et al, 2021)。CNOP正逐渐成为识别大气和海洋及其相关天气气候预报目标观测敏感区行之有效的方法(Mu, et al, 2017; Duan, et al, 2018; Jiang, et al, 2022, 2024; Yang, et al, 2022, 2023),期望未来将其发展为有效提高天气、气候预测水平的业务手段(图2)。

#### 4.3 中国的目标观测实践与经验总结

2009年,中华人民共和国科学技术部、教育部,中国气象局,中国科学院联合正式启动了针对登陆中国台风的10 a重点研究计划(LTCRP)。计划涵盖外场试验、科学实验、技术发展3部分,旨在加强对台风登陆过程的理解,改进台风路径、强度及其引发的强风和降水分布的预报技巧(Duan, et al, 2019)。2008—2018年,LTCRP计划对24个热带气旋开展了外场试验,获得了宝贵数据,深入认识了登陆台风的边界层结构(Zhang J A, et al, 2011, 2015; Ming, et al, 2014, 2018; Bi, et al, 2015; Tang, et al, 2015; Zhao Z K, et al, 2015;

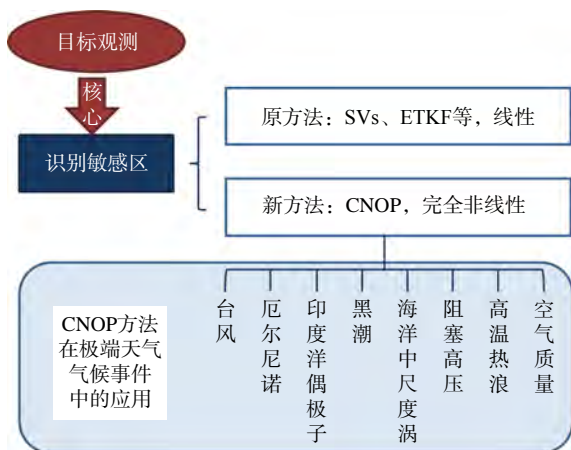


图2 CNOP方法的提出及其在极端天气、气候事件中的应用

Fig. 2 Development of the CNOP and its application in extreme weather and climate events

Wang, et al, 2016, 2018; Zhang X H, et al, 2017; Zhao K, et al, 2017; Wen, et al, 2018; Wu, et al, 2018),同时也促进了新的资料同化技术、短临预报系统、评估体系的发展(Cha, et al, 2013; Wen, et al, 2017; Li, et al, 2018; Liu, et al, 2018; Lu, et al, 2018; Chen H Y, et al, 2019)。

2013年,GRAPES模式中实现了用SVs方法识别目标观测敏感区(刘永柱等,2013;李晓莉等,2019),开展台风预报的目标观测外场试验。GRAPES-SVs预报所关注的区域覆盖中国南方大部分地区及邻近海域( $10^{\circ}$ — $35^{\circ}$ N,  $105^{\circ}$ — $125^{\circ}$ E;刘永柱等,2019;Zhang, et al, 2019)。多家业务和科研单位合作于2020年开始用CNOP方法识别热带气旋目标观测外场试验的敏感区(段晚锁等,2022;Duan, et al, 2023),并对热带气旋海高斯(2020)、美莎克(2020)、灿鸿(2020)、康森(2021)、灿都(2021)、木兰(2022)等实施了外场试验,获得了宝贵资料,显著提高了预报水平(Feng, et al, 2022; Chan, et al, 2023; Qin, et al, 2023)。

LTCRP计划之后,热带气旋目标观测外场试验持续开展。2016年至今,中国香港天文台对中国南海上空的热带气旋开展下投探空观测试验(Chan, et al, 2018)。2020年,中国气象局气象探测中心组织了对热带气旋森拉克(2020)的无人机外场观测试验。这些观测深入理解了热带气旋边界层内滚涡的发生及作用(Chen, et al, 2021; Tang, et al, 2021),同时有效提高了热带气旋路径和强度的预报技巧。以台风艾莎尼(2020)为例,仅同化CNOP识别的敏感区内少量的探空仪观测使得气旋强度预报误差减小程度与同化所有下投探空观测的效果相当。

2016年12月,FY-4A成功发射,为目标观测外场试验提供了新的、强有力的观测手段(Han, et al, 2023)。2018—2021年,FY-4A实施了9次目标观测外场试验,其中8次为热带气旋/台风(雷小途等,2019; Meng Z Y, et al, 2019; Han, et al, 2025)。以热带气旋玛利亚(2018)为例,FY-4A将扫描频率提高至15 min,这部分高频次的卫星观测资料有助于更好地刻画台风周围大气结构(Yin, et al, 2021)。Feng等(2022)的研究表明通过FY-4A获得的CNOP敏感区内的目标观测对热带气旋路径预报的改善,在预报时长大于2.5 d后更为明显,在3—

3.5 d 路径预报误差减小约 50%，尤其在台风灿都（2021）的试验中，对照试验预报该台风将在中国台湾登陆，而同化目标观测后的预报则表明该台风并不会在中国台湾登陆，与实况一致。

2021 年 6 月，FY-4B 成功发射并迅速加入目标观测外场试验观测队伍。2022—2023 年，FY-4B 实施了 3 次目标观测外场试验（包括两个热带气旋/台风）。以台风木兰（2022）为例，FY-4B 观测有效提高了该台风路径、强度及其引发降水的预报水平（Chan, et al, 2023）。在不同化目标观测数据的预报中，台风木兰以西北行登陆中国雷州半岛，而 FY-4B 目标观测数据的同化预报出台风木兰先西行后北折的路径，与实况更为一致。

综上，中国台风目标观测取得了突破性进展，推动了台风预报与观测的互动，实现了敏感区识别的非线性方法研究与实际外场观测实践的结合，为后续台风和其他高影响天气事件预报的目标观测外场试验提供了理论基础和技术支撑。

## 5 中国业务数值预报资料同化系统

### 5.1 业务数值预报同化系统发展历程

建立在理论和方法基础上的资料同化系统是业务数值预报系统的重要组成部分，它通常包括观测实时获取模块、观测预处理子系统和同化子系统，核心是观测资料质量控制和同化方案。从 20 世纪 80 年代至今，随着中国业务数值预报系统的不断发展，资料同化业务系统也经历了由简单到复杂，从引进为主到自主研发的成长过程（图 3）。

中国最早的业务数值预报模式是 1980 年 7 月开始发布传真的原始方程 3 层模式（即 A 模式）和 1982 年 2 月开始业务运行的原始方程北半球 5 层模式（即 B 模式）。当时的同化也叫客观分析，采用较为简单的逐步订正方案，同化的观测以常规资料为主，非常规资料用得很少（王世平等，1984）。

从 20 世纪 80 年代末期开始，国家气象中心逐步建立和发展了 1991 年投入业务使用的 LAFS（Limited Area Forecast System）模式和 1996 年 5 月正式业务运行的 HLAES（High-Resolution LAFS）模式，同时实现了区域资料同化。同化方案采用了改进的 NCEP 的最优插值方案，以高度、风场为三维多变量分析，相对湿度为三维单变量分析，并且使用了非线性正规模初值化方案（薛纪善等，1992），能够同化常规资料和卫星测厚、测湿、云迹风等非常规资料（郭肖容等，1995）。在“九五”期间，国家气象中心开始移植从美国 NCAR 引进的 MM5 中尺度数值预报系统并实时运行，该系统采用逐步订正方案，后来更新为动力张弛方案，同化常规资料（矫梅燕，2010）。

在这个阶段，中国气象局引进 ECMWF 谱模式建立了中国的全球中期天气数值预报业务系统，包括 1991 年 6 月正式投入业务使用的 T42L9 系统，1993 年 10 月开始在中国自行研制的巨型计算机银河-II 上运行的 T63L16 系统，1997 年 7 月在 CRAY C92 上实现业务运行的 T106L19 系统，2002 年 9 月正式业务运行的 T213L31 系统（矫梅燕，2010）。中国气象局在 T 系列全球中期预报业务系统中建立



图 3 中国气象局自主研发的数值天气预报业务同化系统发展历程

Fig. 3 History of the NWP operational data assimilation system independently developed at CMA

了基于最优插值方法的全球资料同化子系统, 并且采用了非线性正规模初值化技术, 使同化结果与预报模式更协调。同化的观测包括国内通信线路和GTS上接收的天气报告(李泽椿等, 1992; 李泽椿, 1994)。在2009年汛期前正式业务运行的T639L60系统中引进了NCEP的GSI变分资料同化系统, 实现了原来由最优插值方案向3DVar同化方案的升级换代, 可以有效同化极轨卫星微波垂直探测仪资料(管成功等, 2008)。

20世纪末至21世纪初, 中国气象局做出了未来数值天气预报业务发展技术路线由引进为主转为自主开发为主的重大决策, 依靠中国科学家自己的力量研发第一代多尺度通用资料同化与数值天气预报系统——GRAPES(薛纪善等, 2008; 沈学顺等, 2020)。2006年7月, 30 km水平分辨率的GRAPES区域模式系统(GRAPES-MESO 2.0版)在国家气象中心业务运行, 它是GRAPES体系中的第一个业务系统, 配备区域等压面3DVar同化子系统, 一天两次冷启动, 同化常规观测资料。2008年汛期前, GRAPES-MESO业务系统升级到2.5版, 水平分辨率提高到15 km, 同时实现了区域模式面3DVar同化。2010年, 基于GRAPES-MESO发展的GRAPES-RAFS(Rapid Analysis and Forecast System; 徐枝芳等, 2013)系统开始准业务运行, 进行3 h间隔的分析预报循环。2014年7月, GRAPES-MESO 4.0版上线, 水平分辨率升级为10 km, 新增了云分析模块, 同时实现了GPS/PW、FY-2E云导风、GNSS/RO等资料的同化应用(黄丽萍等, 2017; 沈学顺等, 2020)。2020年6月, CMA-MESO 5.0版正式业务运行, 同化系统也随之升级为中国区域3 km分辨率的3DVar同化, 3 h分析预报循环(黄丽萍等, 2022)。

GRAPES全球模式系统的第一个正式版本GRAPES-GFS 1.0版在2009年开始准业务运行, 由全球等压面3DVar同化系统提供全球模式的初值。2016年, 25 km水平分辨率的GRAPES-GFS 2.0版正式业务运行, 全球等压面3DVar同化系统更新为全球模式面3DVar同化系统, 避免了同化分析和模式初值之间的空间插值和变量转换引入的额外误差, 改进了背景误差协方差(王金成等, 2014), 同时改进了卫星资料和掩星资料同化(王金成等, 2015, 2016; Han, et al, 2016), GRAPES-

GFS全球模式面3DVar的分析性能达到业务应用要求(王金成等, 2017)。2018年7月, GRAPES-GFS 2.2版实现业务运行, 同化系统由3DVar升级为4DVar(Zhang, et al, 2019)。GRAPES全球四维变分同化系统的业务运行标志着中国业务数值天气预报同化技术迈入国际先进行列, 成为国际上少数具有自主研发和业务应用四维变分同化系统的国家级预报中心之一(沈学顺等, 2020)。2021年, GRAPES-GFS和GRAPES-MESO分别更名为CMA-GFS和CMA-MESO。2023年5月,CMA-GFS 4.0版投入业务应用, 全球4DVar同化系统的水平分辨率从25 km提高到12.5 km, 同时卫星同化使用的快速辐射传输模式从RTTOV更新为国产ARMS, 这是一个重要的节点, 朝向业务同化系统核心技术的自主可控又迈出了关键一步。根据WMO模式检验标准, 选取500 hPa高度场南、北半球距平相关系数(ACC, 图1)历史演变特征为参考, 检验预报效果。可以看到, CMA-GFS全球业务预报系统的预报效果不断提升, 南、北半球预报差异逐渐减小。其中, 第5天北半球500 hPa高度场ACC从2010年9月的0.695, 升到2015年9月的0.768, 至2023年9月已升至0.846(赵滨等, 2024)。

2024年6月, CMA-MESO 6.0版中国1 km分辨率系统通过业务化评审, 开始进行实时业务平行试验, 3DVar同化系统升级为1 km水平分辨率和1 h间隔分析预报循环。与此同时, CMA-GFS 4.2版将全球4DVar升级为全球En4DVar, 已经完成了1 a的回算试验, 分析质量和预报水平系统性优于全球4DVar业务系统的结果, 2024年12月31日业务运行。

## 5.2 全球四维变分同化业务系统

4DVar是3DVar在时间维上的扩展, 所以3DVar同化框架是4DVar同化框架的基础。CMA-GFS全球3/4DVar同化框架采用流函数、非平衡的速度势、非平衡的无量纲气压和比湿作为分析变量, 而速度势和无量纲气压的平衡部分通过动力和统计相结合的方案来计算。因为分析变量之间是相互独立的, 所以对应的背景场误差协方差矩阵是对角矩阵。在此基础上, 单变量的水平相关模型采用二阶自回归相关函数, 然后通过谱滤波来计算, 而水平相关尺度和垂直相关矩阵都是用集合样本统计得到的。

同时, CMA-GFS 全球 3/4DVar 同化框架实施了增量分析方案,使得全球 4DVar 计算观测增量时积分高分辨率预报模式,进行极小化收敛时积分低分辨率切线性模式和伴随模式,不但显著减小了模式积分的计算消耗,而且能够提高目标泛函极小化的收敛效率。

全球切线性模式和伴随模式是全球 4DVar 同化系统的核心部件。CMA-GFS 全球切线性模式和伴随模式是国际上第一个在全球 4DVar 同化业务系统中应用的非静力全球切线性模式和伴随模式,而且两个模式动力框架部分总的计算时间只有全球预报模式动力框架的 3 倍左右,计算性能表现优异。除此之外, CMA-GFS 全球切线性模式和伴随模式接入了较完备的线性化物理过程,包括垂直扩散、次网格地形参数化、大尺度凝结和对流参数化过程(龚建东等, 2019; 刘永柱等, 2019)。

CMA-GFS 全球 4DVar 同化业务系统研发了有预调节功能的 Lanczos-CG 算法和 L-BFGS 算法。缺省配置使用 Lanczos-CG 算法,它的收敛速度更快,收敛过程更平稳。而 L-BFGS 算法的容错能力更好,所以当 Lanczos-CG 算法不收敛时业务系统会自动切换使用 L-BFGS 算法。

GRAPES 全球 4DVar 同化业务系统(4.0 版)的基本设置包括水平分辨率  $0.125^{\circ}/0.75^{\circ}$ (外循环/内循环),垂直层数 87 层,模式积分步长 300 s/900 s(外循环/内循环),同化观测数据的时间窗长度为 6 h, 观测剖分间隔 30 min, 最大极小化迭代次数 50 次。为了兼顾分析预报质量和时效要求,运行一个分析预报循环系统和一个分析预报系统。每天进行 4 次全球 4DVar 同化,同化结束后,生成标准时刻的模式初值,然后再利用这一初值进行 10 d 预报。

CMA-GFS 全球同化系统不但研发了卫星资料的质量控制、云检测、偏差订正等卫星资料同化关键技术,而且建立了国产化的快速辐射传输模式 ARMS, 替代了原先使用的 RTTOV。在卫星资料同化方面, CMA-GFS 4DVar 相继实现了对 FY 极轨系列卫星微波温湿度计(Xiao, et al, 2023a)、微波成像仪(Xiao, et al, 2020)、掩星(Wang, et al, 2020)、FY 静止气象卫星红外高光谱(Yin, et al, 2020, 2021; Han, et al, 2023)、红外成像仪(王皓等, 2018)等,以及 HY-2B 微波成像仪 SMR(Li Z T, et al, 2024)、散射计洋面风(Wang J C, et al, 2023)等

资料的同化。在当前 CMA-GFS 全球 4DVar 系统中,同化的观测包括探空、地面、飞机报、云导风、掩星、散射计风、GPS 可降水量、GNSS 反射计风、NOAA、METOP、FY-3 微波温湿度计、红外高光谱、GCOM 微波成像仪、FY-2 成像仪等资料,其中卫星资料使用量占所有观测数量的 80% 左右,在全球同化中发挥了关键作用。

### 5.3 区域三维变分同化业务系统

中国业务区域数值预报系统 CMA-MESO(原 GRAPES-MESO)主要面向致灾严重的强对流等灾害天气,为短时临近预警和短期天气预报提供数值预报支撑。为应对强对流天气的快速发生、发展,充分利用高时、空分辨率的观测资料和及时校正模式轨迹十分重要,这主要通过 CMA-MESO 千米尺度 3DVar 系统和云分析系统实现。CMA-MESO 系统采用快速同化预报循环更新的方式运行。2020 年 6 月,3 km 分辨率、3 h 更新的 CMA-MESO V5.0 系统实现业务运行(沈学顺等, 2020; 黄丽萍等, 2022); 2024 年 6 月,1 km 分辨率、1 h 更新的 CMA-MESO V6.0 系统通过业务化评审,2024 年 10 月业务运行。

CMA-MESO 千米尺度 3DVar 以 GRAPES 全球区域一体化变分同化框架为基础,面向强对流天气资料同化分析需求开展了针对性开发。在同化分析框架上,从对流尺度系统的动力学特征出发构建新的极小化控制变量,引入简化的连续方程弱约束,实现更加平衡的中小尺度分析(王瑞春等, 2024)。同时,为兼顾大尺度环流的正确描述,还研发了多尺度分析方案,包括:采用多高斯尺度叠加的水平相关模型;全球大尺度信息弱约束;以及中小尺度信息与全球大尺度信息融合的混合(Blending)方案等(庄照荣等, 2020; 王瑞春等, 2021)。千米尺度 3DVar 主要更新风、温、压、湿等变量,云水物质变量则通过云分析系统诊断更新,并通过张弛逼近(Nudging)的方式引入到模式轨迹中(朱立娟等, 2017)。在上述业务系统基础上,研发并初步建成了 CMA-MESO 三维集合变分混合同化(En3DVar)系统,实现流依赖同化分析。进一步,在 En3DVar 框架中新增了云水物质控制变量,为雷达反射率因子直接同化提供基础。

在观测资料应用方面,CMA-MESO 千米尺度 3DVar 充分发挥全球/区域一体化系统共用观测算

子的优势, 实现常规观测、云导风、GNSS(全球导航卫星系统掩星)折射率、洋面风、反射计风等资料的直接同化应用。在此基础上, CMA-MESO 系统积极发展高时、空分辨率资料的同化应用。对于雷达资料, 径向风和风廓线雷达资料在千米尺度 3DVar 中实现直接同化应用, 反射率资料在云分析系统中实现同化应用。针对中国新一代地球静止气象卫星 FY-4A、FY-4B 提供的高时、空分辨率观测资料, 千米尺度 3DVar 也实现直接同化应用, FY-2G 亮温和总云量资料则在云分析系统中应用。面对越来越丰富的地面自动气象站观测, 千米尺度 3DVar 已经实现 10 m 风场、2 m 温度、2 m 湿度、地面气压等全观测要素的有效同化。除了常规地面观测要素, 地基 GNSS 大气可降水量资料也在千米尺度 3DVar 中实现同化应用。多源资料的同化应用丰富了 CMA-MESO 资料同化系统的可应用资料的种类, 可使用的观测资料种类达到 17 种。综合考虑千米尺度 3DVar 和云分析系统, 雷达资料和卫星资料占比最高, 而在千米尺度 3DVar 中, 雷达径向风占比最高。

雷达资料同化对于保证 CMA-MESO 3 km 业务系统的分析和预报性能至关重要, 有无雷达反射率资料的同化对强降水的预报 TS 评分可相差 5—18 个百分点, 径向风的同化也进一步改善了低层风的质量。风廓线雷达的同化应用也显示可改善台风预报的路径和强度(王丹等, 2019)。由于云分析技术依赖于经验关系, 在对流尺度数值模拟中有一定的局限, 因此, 基于 CMA-MESO 1 km 变分同化系统, 开展了雷达反射率变分同化, 双偏振量直接、间接同化技术的研发; 并基于 CMA-MESO En3DVar 系统, 开展了雷达反射率因子水物质同化个例分析。除此之外, 新型地基遥感观测资料应用也受到关注, X 波段天气雷达反射率资料、微波辐射计温湿度廓线产品、云雷达产品等均在 CMA-MESO 系统中实现了同化功能。

#### 5.4 台风观测的资料同化

中国气象局利用全球业务模式系统开展热带气旋预报最早要追溯到 2004 年, 当时基于 T213 全球谱模式发展了由初始涡旋形成、涡旋重定位和涡旋调整 3 部分技术组成的热带气旋初值方案(瞿安祥等, 2009a, 2009b)。2014 年, 该方案中初始涡旋形成技术由人造涡旋嵌入升级为涡旋模型风场和

气压场资料同化吸收技术, 并应用于 T639 全球谱模式(瞿安祥等, 2016)。从 2018 年起, 随着中国自主研发全球模式系统 CMA-GFS 的日益成熟, 发展了一套基于 4DVar 系统、主动吸收高频次热带气旋移动轨迹和中心气压廓线演变趋势信息的热带气旋初值方案(瞿安祥等, 2022)。实际业务应用表明, 该初值方案可以明显改进 CMA-GFS 全球主要海域的热带气旋路径和强度预报效果。未来计划主要有两方面, 一方面大力开展热带气旋初值扰动技术以改进其环流区域流背景误差实时流依赖特征; 另一方面, 基于 En4DVar 技术提高热带气旋观测资料信息的提取幅度和传播效率, 从而提高初值的分析质量。

## 6 资料同化的未来展望

### 6.1 适应高分辨率、长预报时效的资料同化

数值天气预报的一个发展方向是提高数值模式分辨率, 这会带来更多的非线性和非高斯分布的小尺度过程被解析; 同时, 观测系统的发展也会带来更高分辨率、更多非直接的观测信息(图 4)。因此, 目前广泛应用的资料同化方法所假设的高斯分布误差和线性更新就不再适用(Yano, et al, 2018)。迭代的集合卡尔曼滤波(Iterative Ensemble Kalman Filter, IEnKF; Sakov, et al, 2012)利用前一迭代的集合转换矩阵代替线性回归, 更好地捕捉非线性误差增长。进一步, 各类非线性滤波方法得以发展, 包括局地高斯混合滤波(Gaussian Mixture Filter; Bengtsson, et al, 2003)、最大似然集合滤波(Maximum Likelihood Ensemble Filter; Zupanski, 2005)、排序直方图滤波(Rank Histogram Filter; Anderson, 2010)、秩匹配滤波(Lei, et al, 2011)、分位数守恒集合滤波(Quantile-Conserving Ensemble Filter; Anderson, 2022, 2023)等。

还有一类完全贝叶斯、非线性的同化方法是粒子滤波(van Leeuwen, 2009), 所得粒子满足贝叶斯后验分布, 这可以通过重采样(Bootstrap Sampling; Gordon, et al, 1993; Doucet, et al, 2005)、重要性采样(van Leeuwen, 2003; Robert, et al, 2004)或者基于建议分布的重要性采样(Importance Sampling with Proposal; Doucet, et al, 2000; Spiller, et al, 2008)等实现。但粒子滤波在应用于高维动力系统

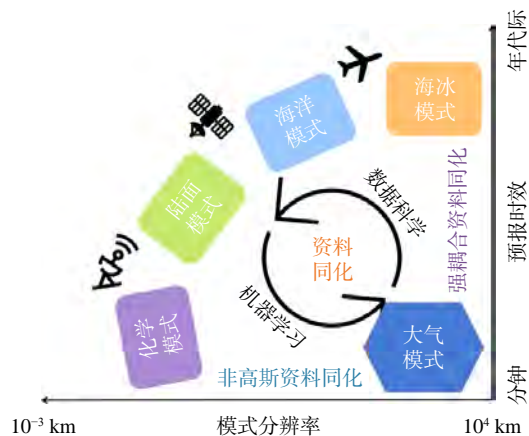


图 4 数值天气预报资料同化的发展展望

Fig. 4 Prospect for the development of data assimilation in NWP

时面临维数诅咒(Curse of Dimensionality; Snyder, et al, 2008)。通常用于减缓维数诅咒的办法包括结合滤波和平滑的隐式粒子滤波(Chorin, et al, 2009)、混合集合卡尔曼滤波的粒子滤波(Santitissadeekorn, et al, 2015)、等权重粒子滤波(Ades, et al, 2015; Zhu, et al, 2016)及局地粒子滤波(Penny, et al, 2016; Poterjoy J, 2016b)等。

数值天气预报的另一个发展方向是延长预报时效,从当前的小于两周的预报时效到季节-年(Seasonal-to-Decadal s2d)的预报时效(图4)。因此,需要耦合大气与地球系统中缓慢变化的组成部分,比如海洋、陆面、冰冻圈等,这些耦合资料同化十分重要。弱耦合同化在各分量模式中同化分量观测,利用耦合模式实现观测信息的跨分量模式传递(Zhang, et al, 2007; Sugiura, et al, 2008; Saha, et al, 2010; Laloyaux, et al, 2016)。进一步,强耦合同化利用观测信息同时更新各分量模式(Sluka, et al, 2016; Sun, et al, 2020b)。相对于弱耦合同化,强耦合同化可以获得更平衡的分析场,进而减小初始化冲击并改进预报(Smith, et al, 2015; Chen X C, et al, 2019; Zhang, et al, 2020)。

## 6.2 混合机器学习的资料同化

机器学习给资料同化、数值模式、预报和预测均带来了新的机遇,尤其是在卫星海量观测数据的高效和有效同化方面。资料同化和机器学习具有相似性,均可看作是贝叶斯理论下的反问题(Geer, 2021)。相对于传统的资料同化,机器学习在捕捉非线性特征、逼近非线性系统、处理海量观测数据

等方面具有优势,因此机器学习和资料同化结合的混合方法得到迅速发展(图4)。直接结合机器学习和资料同化可利用数据驱动、深度学习的预报模型替代数值模式,在循环同化中获得高计算效率的预报。Feng Wu-4DVar 将基于多模态神经网络的风鸟模型与四维变分结合,既利用风鸟模型获得短期预报,又利用深度学习模型的自动微分能力高效获得四维变分的分析解(Xiao, et al, 2024a)。相似地,基于 ViT (Vision Transformer) 神经网络架构的全球天气预报模型 ClimaX 与局地集合转置卡尔曼滤波相结合,可实现循环集合资料同化,同时集合资料同化还可用于诊断基于深度学习的天气模型(Kotsuki, et al, 2024)。

机器学习可以应用于资料同化的各组成部分。观测算子将模式变量转换为对观测的估计,观测算子的线性化计算非常耗时,深度学习可有效建立观测算子及相应的线性算子(Jacobian 矩阵)乃至目前业务同化中普遍被忽略的二阶矩阵(Hessian 矩阵),尤其是建立高度非线性的前向观测算子(Storto, et al, 2021)。此外,基于深度学习的卫星资料观测算子可以替代辐射传输模式,并同时对卫星观测资料进行偏差订正(Liang, et al, 2023)。四维变分所需的伴随模式通常构建难度大、计算需求高,而深度学习模型可直接微分,因此可以利用深度模型对物理参数化方案进行仿真,进而获得相应的切线性模式和伴随模式,并显著提高计算效率(Hatfield, 2021)。局地化是集合卡尔曼滤波成功应用于高维动力系统的关键,但通常使用的局地化函数多为随距离各向对称的,而基于深度学习的局地化则可直接从数据中提取非线性误差特征,获得非对称、非线性的局地化函数(Wang Z R, et al, 2023)。

模式误差是预报误差的重要组成部分,也是资料同化需要重点考虑的误差来源。机器学习可以从不同设置的数值模拟中学习得到由数值模式不能解析而产生的模式误差(Rasp, et al, 2018; Bolton, et al, 2019; Gagne II, et al, 2020; Brajard, et al, 2021)。人工神经网络、深度神经网络和卷积神经网络等不同框架的机器学习,可基于分析场、预报场和观测等信息学到具有不同尺度或非线性特征模式误差,并在资料同化中通过添加等形式表征模式误差(Bonavita, et al, 2020; Farchi, et al, 2021a)。进一步,利用循环资料同化,机器学习可

以基于先验场和后验场在线学习并修正模式误差(Farchi, et al, 2021b; Peng, et al, 2024),或者通过扩充的方法在线同时估计模式变量和模式参数的误差(Bocquet, et al, 2021; Malartic, et al, 2022)。

传统资料同化面临的一个挑战是大气的高维度及其带来的计算复杂性,相应的潜在同化得以提出(Latent Assimilation; Binev, et al, 2017; Arcucci, et al, 2019; Casas, et al, 2020),其在基于机器学习的自编码器的潜在空间进行资料同化,结合机器学习的高计算效率和资料同化的优化分析场等优势。变分方法和集合卡尔曼滤波通常假设误差为高斯分布,而变分自编码器可估计非高斯分布的误差,因此将变分编码器与变分方法相结合,可获得优于传统变分方法的解(Xiao, et al, 2024b)。进一步,机器学习还能与非线性滤波相结合,如深度卡尔曼滤波器(Krishnan, et al, 2015, 2017)和卡尔曼变分自编码器(Fraccaro, et al, 2017)等。DiffDA则基于GraphCast神经网络,利用天气预报模型和去噪扩散模型间的相似,直接产生资料同化分析场(Huang, et al, 2024)。此外,机器学习还能基于不完整或低分辨率的观测网络进行重建和同化(Wang, et al, 2022; Howard, et al, 2024)。

### 6.3 全空卫星、双偏振雷达资料同化

在卫星资料同化方面,中国业务系统中同化的卫星资料仍以晴空下的辐射率资料为主,云雨区资料的同化还未业务应用。新型遥感探测资料,包括降水雷达、风场激光雷达等主动遥感仪器和地基载荷观测资料的同化应用还有待提升。面向地球系统耦合同化应用,快速辐射传输模式需要发展全谱段的含多种大气成分的超高光谱大气层析透过率计算模型,构建基于人工智能的卫星和新型载荷耦合同化观测算子。可见光资料的同化将是未来卫星资料同化应用的一个非常重要的方向,特别是红外和可见光资料的全天空同化将为对流尺度的数值模式提供更精确的分析场(Schrötle, et al, 2020),通过发展更先进的包含云粒子散射特性的辐射传输模型,将能够同化更多受云层影响的红外辐射资料。同时,更精细的陆面过程的描述从而增加地表敏感通道的辐射率同化也将是发展趋势。微波探测资料是对数值天气预报精度贡献最大的观测资料,但是目前微波探测仪仅搭载于低轨气象卫星上,其重访周期长、时间分辨率低,难以提供天气

系统的连续观测信息。中国正在设计建设的静止轨道微波探测系统是对现有微波探测体系的重要补充(卢乃锰等, 2016),不仅可以提供高时变的三维大气热力结构探测信息,同时还可以实现基于水汽追踪方法的全天空不同高度风场产品,为数值预报提供更多的动力场观测信息(Zhang, et al, 2021)。另外,目前卫星数据的同化技术基本上不考虑各仪器观测之间的协同效果。充分考虑各仪器观测之间的协同和互补效应,例如成像和探测资料的联合应用(Di, et al, 2024)提升同化效果,是未来卫星资料同化的重要研究方向。

开发一种合理的基于变分框架的双偏振雷达观测量子十分重要。Li等(2017)基于变分法,进行了单站双偏振雷达资料的个例模拟测试,研究初步表明额外同化差分反射率因子和比差分相移,可以进一步改善反射率因子的分析和预报。变分同化方法需要构建双偏振观测量的切线性算子和伴随算子,为建立更合理的切线性算子和伴随算子,Kawabata等(2018)构建了基于液相粒子的双偏振观测量观测量子的切线性算子和伴随算子,Wang等(2019)研究构建了包含冰相粒子在内的水平/垂直反射率因子观测量子的切线性算子和伴随算子,张海阳等(2024)建立了一套基于水凝物控制变量的双偏振雷达变分直接同化方案,真实个例的循环同化及预报试验表明双偏振雷达资料同化改进了分析场及预报场的热、动力及微物理结构特征。上述关于双偏振雷达观测量子和伴随算子的构建研究,为双偏振雷达偏振量的变分同化工作提供了基础条件。然而,由于双偏振雷达切线性和伴随算子的复杂性和参数化方案的不确定性,更合理的双偏振雷达观测量子仍需要进一步研究,尤其是针对冰相和混合相态的进一步处理。

### 6.4 先进的业务资料同化系统

当前,中国自主研发的全球和区域业务天气预报系统CMA-GFS和CMA-MESO能够有效同化多源观测资料,在日常天气预报预警、气象防灾减灾中发挥了关键支撑作用。但面向无缝隙地球系统数值天气预报,现有模式动力框架难以满足需求。目前国际主要数值预报中心正在发展准均匀网格数值预报系统,中国也基本建成了下一代高精度可扩展大气模式(Li, et al, 2020)。面向下一代模式的高精度可扩展大气同化系统的研制工作正加紧开

展。下一代大气同化系统的发展目标是构建以全球四维变分为核心，全球/区域一体化的集合变分混合同化框架。在此基础上，开展北斗导航探空、云雨区卫星资料、雷达反射率因子、X波段雷达、双偏振雷达、相控阵雷达、地基垂直遥感等多源资料的同化技术研究，推进新型观测资料的业务应用。与此同时，开展人工智能算法在多源资料同化各个领域的应用研究。

面向天气到气候多尺度的无缝隙地球系统数值预报需求，研究地球系统不同圈层的同化技术，以高精度扩展大气同化系统为基础，构建海-陆-气-冰耦合同化系统，实现地球系统不同圈层多源资料的有效同化，为地球系统模式提供协调一致的高质量初值。如图4所示，以期在资料同化方法和理论的发展基础上建立地球系统数值预报和预测的资料同化业务系统。

## 参考文献

- 陈敏, 陈明轩, 范水勇. 2014. 雷达径向风观测在华北区域数值预报系统中的实时三维变分同化应用试验. 气象学报, 72(4): 658-677. Chen M, Chen M X, Fan S Y. 2014. The real-time radar radial velocity 3DVar assimilation experiments for application to an operational forecast model in North China. *Acta Meteor Sinica*, 72(4): 658-677 (in Chinese)
- 陈娴雅, 陈耀登, 孟德明. 2022. 基于云依赖背景场误差协方差的雷达资料同化及对降雨预报影响研究. 气象学报, 80(2): 243-256. Chen X Y, Chen Y D, Meng D M. 2022. Assimilation of radar data based on cloud-dependent background error covariance and its impact on rainfall forecasting. *Acta Meteor Sinica*, 80(2): 243-256 (in Chinese)
- 陈耀登, 陈海琴, 孙娟珍等. 2018. 雷达观测对应模式变量非线性特征及对四维变分同化的影响. 热带气象学报, 34(6): 721-732. Chen Y D, Chen H Q, Sun J Z, et al. 2018. Nonlinear characteristics of model variables corresponding to radar observations and its effects on 4D-Var assimilation. *J Trop Meteor*, 34(6): 721-732 (in Chinese)
- 丑纪范. 1974. 天气数值预报中使用过去资料的问题. 中国科学, 4(6): 635-644. Chou J F. 1974. The usage of past observations in numerical weather prediction. *Scientia Sinica*, 4(6): 635-644 (in Chinese)
- 丑纪范. 2007. 数值天气预报的创新之路: 从初值问题到反问题. 气象学报, 65(5): 673-682. Chou J F. 2007. An innovative road to numerical weather prediction: From initial value problem to inverse problem. *Acta Meteor Sinica*, 65(5): 673-682 (in Chinese)
- 段晚锁, 秦晓昊. 2022. 非线性最优扰动方法在热带气旋目标观测研究和外场试验中的应用. 地球科学进展, 37(2): 165-176. Duan W S, Qin X H. 2022. Application of nonlinear optimal perturbation methods in the targeting observations and field campaigns of tropical cyclones. *Adv Earth Sci*, 37(2): 165-176 (in Chinese)
- 范水勇, 王洪利, 陈敏, 等. 2013. 雷达反射率资料的三维变分同化研究. 气象学报, 71(3): 527-537. Fan S Y, Wang H L, Chen M, et al. 2013. Study of the data assimilation of radar reflectivity with the WRF 3D-Var. *Acta Meteor Sinica*, 71(3): 527-537 (in Chinese)
- 龚建东, 刘永柱, 张林. 2019. 面向四维变分资料同化的 NSAS 积云深对流参数化方案的简化及线性化研究. 气象学报, 77(4): 595-616. Gong J D, Liu Y Z, Zhang L. 2019. A study of simplification and linearization of the NSAS deep convection cumulus parameterization scheme for 4D-Var. *Acta Meteor Sinica*, 77(4): 595-616 (in Chinese)
- 顾震潮. 1958a. 作为初值问题的天气形势数值预报与地面天气历史演变作预报的等值性. 气象学报, 29(2): 93-98. Koo C C. 1958a. On the equivalency of formulations of weather forecasting as an initial value problem and as an "evolution" problem. *Acta Meteor Sinica*, 29(2): 93-98 (in Chinese)
- 顾震潮. 1958b. 天气数值预报中过去资料的使用问题. 气象学报, 29(3): 176-184. Koo C C. 1958b. On the utilization of past data in numerical weather forecasting. *Acta Meteor Sinica*, 29(3): 176-184 (in Chinese)
- 管成功, 陈起英, 佟华等. 2008. T639L60 全球中期预报系统预报试验和性能评估. 气象, 34(6): 11-16. Guan C G, Chen Q Y, Tong H, et al. 2008. Experiments and evaluations of global medium range forecast system of T639L60. *Meteor Mon*, 34(6): 11-16 (in Chinese)
- 郭肖容, 张玉玲, 阎之辉等. 1995. 有限区分析预报系统及其业务应用. 气象学报, 53(3): 306-318. Guo X R, Zhang Y L, Yan Z H, et al. 1995. The limited area analysis and forecast system and its operational application. *Acta Meteor Sinica*, 53(3): 306-318 (in Chinese)
- 黄静, 陈耀登, 陈海琴等. 2022. 实时天气背景依赖的反射率因子间接同化及多暴雨个例试验. 大气科学, 46(3): 691-706. Huang J, Chen Y D, Chen H Q, et al. 2022. Real-time background-dependent indirect assimilation of Radar reflectivity factor and experiments for multi heavy rainfall cases. *Chinese J Atmos Sci*, 46(3): 691-706 (in Chinese)
- 黄丽萍, 陈德辉, 邓莲堂等. 2017. GRAPES\_Meso V4.0 主要技术改进和预报效果检验. 应用气象学报, 28(1): 25-37. Huang L P, Chen D H, Deng L T, et al. 2017. Main technical improvements of GRAPES\_Meso V4.0 and verification. *J Appl Meteor Sci*, 28(1): 25-37 (in Chinese)
- 黄丽萍, 邓莲堂, 王瑞春等. 2022. CMA-MESO 关键技术集成及应用. 应用气象学报, 33(6): 641-654. Huang L P, Deng L T, Wang R C, et al. 2022. Key technologies of CMA-MESO and application to operational forecast. *J Appl Meteor Sci*, 33(6): 641-654 (in Chinese)
- 黄恩训, 滕加俊, 项杰等. 2003. 处理三维流场的广义变分最佳分析方法的理论分析与数值实验[试验]//第十七届全国水动力学研讨会暨第六届全国水动力学学术会议文集. 北京:《水动力学研究与进展》编委会. Huang S X, Teng J J, Xiang J, et al. 2003. Generalized variational optimization analysis method of 3-D wind field//Proceedings of the 17th National Symposium on Hydrodynamics and the 6th National Conference on Hydrodynamics. Beijing: Editorial Board of Journal of Hydrodynamics (in Chinese)
- 矫梅燕. 2010. 现代数值预报业务. 北京: 气象出版社, 206. Jiao M Y. 2010.

- Modern Numerical Weather Prediction Operations. Beijing: China Meteorological Press, 260 (in Chinese)
- 兰伟仁, 朱江, Xue M. 2010a. 风暴尺度天气下利用集合卡尔曼滤波模拟多普勒雷达资料同化试验 I. 不考虑模式误差的情形. 大气科学, 34(3): 640-652. Lan W R, Zhu J, Xue M, et al. 2010a. Storm-scale ensemble Kalman filter data assimilation experiments using simulated doppler Radar data. Part I : Perfect model tests. Chinese J Atmos Sci, 34(3): 640-652 (in Chinese)
- 兰伟仁, 朱江, Xue M, 等. 2010b. 风暴尺度天气下利用集合卡尔曼滤波模拟多普勒雷达资料同化试验 II. 考虑模式误差的情形. 大气科学, 34(4): 737-753. Lan W R, Zhu J, Xue M, et al. 2010b. Storm-scale ensemble Kalman filter data assimilation experiments using simulated doppler Radar data Part II : Imperfect model tests. Chinese J Atmos Sci, 34(4): 737-753 (in Chinese)
- 雷小途, 张雪芬, 段锁锁等. 2019. 近海台风立体协同观测科学试验. 地球科学进展, 34(7): 671-678. Lei X T, Zhang X F, Duan W S, et al. 2019. Experiment on coordinated observation of offshore typhoon in China. Adv Earth Sci, 34(7): 671-678 (in Chinese)
- 李刚, 吴兆军, 张华. 2016. 偏差订正方法在IASI辐射率资料同化中的应用研究. 大气科学学报, 39(1): 72-80. Li G, Wu Z J, Zhang H. 2016. Bias correction of infrared atmospheric sounding interferometer radiances for data assimilation. Trans Atmos Sci, 39(1): 72-80 (in Chinese)
- 李晓莉, 刘永柱. 2019. GRAPES 全球奇异向量方法改进及试验分析. 气象学报, 77(3): 552-562. Li X L, Liu Y Z. 2019. The improvement of GRAPES global extratropical singular vectors and experimental study. Acta Meteor Sinica, 77(3): 552-562 (in Chinese)
- 李泽椿, 裴国庆. 1992. 第一讲 序论: T42 中期数值天气预报业务系统. 气象, 18(6): 50-52. Li Z C, Qiu G Q. 1992. Operational system for medium-range numerical weather prediction. Meteor Mon, 18(6): 50-52 (in Chinese)
- 李泽椿. 1994. 中国国家气象中心中期数值天气预报业务系统. 气象学报, 52(3): 297-307. Li Z C. 1994. Medium-range numerical weather prediction system at the national meteorological center of China. Acta Meteor Sinica, 52(3): 297-307 (in Chinese)
- 连治华, 薛纪善. 2010. 一种新的地面气压插值方案在计算低于模式地形的观测相当量中的研究. 热带气象学报, 26(4): 489-493. Lian Z H, Xue J S. 2010. A new surface pressure interpolation scheme for calculation of observations-equivalent quantities lower than model terrain. J Trop Meteor, 26(4): 489-493 (in Chinese)
- 刘红亚, 薛纪善, 顾建峰等. 2010. 三维变分同化雷达资料暴雨个例试验. 气象学报, (6): 779-789. Liu H Y, Xue J S, Gu J F, et al. 2010. GRAPES-3DVAR radar data assimilation and numerical simulation experiments with a torrential rain case. Acta Meteor Sinica, (6): 779-789 (in Chinese)
- 刘永柱, 沈学顺, 李晓莉. 2013. 基于总能量模的GRAPES全球模式奇异向量扰动研究. 气象学报, 71(3): 517-526. Liu Y Z, Shen X S, Li X L. 2013. Research on the singular vector perturbation of the GRAPES global model based on the total energy norm. Acta Meteor Sinica, 71(3): 517-526 (in Chinese)
- 刘永柱, 龚建东, 张林等. 2019. 线性化物理过程对 GRAPES 4DVAR 同化的影响. 气象学报, 77(2): 196-209. Liu Y Z, Gong J D, Zhang L, et al. 2019. Influence of linearized physical processes on the GRAPES 4DVAR. Acta Meteor Sinica, 77(2): 196-209 (in Chinese)
- 刘勇洪, 翁富忠, 何文英等. 2025. LandEM 模式的改进及在青藏高原地区的初步应用. 气象学报, 83(1): 61-79. Liu, Y H, Weng F Z, He W Y, et al. 2025. Improvement of the LandEM model and its initial application in the Qinghai-Xizang plateau region. Acta Meteor Sinica, 83(1): 61-79 (in Chinese)
- 卢乃锰, 谷松岩. 2016. 静止轨道微波大气探测的技术现状与发展展望. 气象科技进展, 6(1): 120-123. Lu N M, Gu S Y. 2016. The status and prospects of atmospheric microwave sounding by geostationary meteorological satellite. Adv Meteor Sci Technol, 6(1): 120-123 (in Chinese)
- 罗义, 梁旭东, 陈明轩. 2014. 单多普勒雷达径向风同化的改进. 气象科学, 34(6): 9. Luo Y, Liang X D, Chen M X. 2014. Improvement of radial wind data assimilation of single Doppler radar. J Meteor Sci, 34(6): 9 (in Chinese)
- 马昊, 梁旭东, 罗义等. 2016. GRAPES\_3Dvar 中雷达径向风同化改进观测算子的应用. 气象, 42(1): 34-43. Ma H, Liang X D, Luo Y, et al. 2016. Application of advanced observation operator of Doppler radar radial velocity assimilation in GRAPES\_3Dvar. Meteor Mon, 42(1): 34-43 (in Chinese)
- 慕熙昱, 徐琪, 潘玉洁, 等. 2019. 雷达径向速度资料同化中不同坐标转换方案的对比试验. 高原气象, 38(3): 625-635. Mu X Y, Xu Q, Pan Y J, et al. 2019. Contrast experiment of different coordinate remapping schemes in radar velocity data assimilation. Plateau Meteor, 38(3): 625-635 (in Chinese)
- 瞿安祥, 麻素红, Liu Q F 等. 2009a. 全球数值模式中的台风初始化 I : 方案设计. 气象学报, 67(5): 716-726. Qu A X, Ma S H, Liu Q F, et al. 2009a. The initialization of tropical cyclones in the NMC global model part I : Scheme design. Acta Meteor Sinica, 67(5): 716-726 (in Chinese)
- 瞿安祥, 麻素红, 李娟等. 2009b. 全球数值模式中的台风初始化 II : 业务应用. 气象学报, 67(5): 727-735. Qu A X, Ma S H, Li J, et al. 2009b. The initialization of tropical cyclones in the NMC global model part II : Implementation. Acta Meteor Sinica, 67(5): 727-735 (in Chinese)
- 瞿安祥, 麻素红, 张进. 2016. T639 全球模式的台风初始化方案升级试验. 气象, 42(6): 664-673. Qu A X, Ma S H, Zhang J. 2016. Updated experiments of tropical cyclone initialization in global model T639. Meteor Mon, 42(6): 664-673 (in Chinese)
- 瞿安祥, 麻素红, 张进等. 2022. CMA-GFS 全球预报系统中的台风初始化. 气象学报, 80(2): 269-279. Qu A X, Ma S H, Zhang J, et al. 2022. Typhoon initialization in the CMA global forecast system. Acta Meteor Sinica, 80(2): 269-279 (in Chinese)

- 沈学顺,王建捷,李泽椿等.2020.中国数值天气预报的自主创新与发展.气象学报,78(3): 451-476. Shen X S, Wang J J, Li Z C, et al. 2020. China's independent and innovative development of numerical weather prediction. *Acta Meteor Sinica*, 78(3): 451-476 (in Chinese)
- 盛春岩,薛德强,雷霆,等.2006.雷达资料同化与提高模式水平分辨率对短时预报影响的数值对比试验.气象学报,64(3): 293-307. Sheng C Y, Xue D Q, Lei T, et al. 2006. Comparative experiments between effects of doppler radar data assimilation and increasing horizontal resolution on short-range prediction. *Acta Meteor Sinica*, 64(3): 293-307 (in Chinese)
- 万齐林,薛纪善,庄世宇.2005.多普勒雷达风场信息变分同化的试验研究.气象学报,(2): 129-145. Wan Q L, Xue J S, Zhuang S Y. 2005. Study on the variational assimilation technique for the retrieval of wind fields from doppler radar data. *Acta Meteor Sinica*, (2): 129-145 (in Chinese)
- 王丹,阮征,王改利等.2019.风廓线雷达资料在GRAPES-Meso模式中的同化应用研究.大气科学,43(3): 634-654. Wang D, Ruan Z, Wang G L, et al. 2019. A study on assimilation of wind profiling radar data in GRAPES-Meso model. *Chinese J Atmos Sci*, 43(3): 634-654 (in Chinese)
- 王皓,韩威.2018.FY4A AGRI水汽通道辐射率在GRAPES中的同化应用研究//第35届中国气象学会年会S9卫星资料同化.合肥:中国气象学会. Wang H, Han W. 2018. The application of assimilating FY4A AGRI water-vapor channel radiances in GRAPES//35th Annual Meeting of Chinese Meteorological Society, S9, Satellite Data Assimilation. Hefei: Chinese Meteorological Society (in Chinese)
- 王金成,庄照荣,韩威等.2014.GRAPES全球变分同化背景误差协方差的改进及对分析预报的影响:背景误差协方差三维结构的估计.气象学报,72(1): 62-78. Wang J C, Zhuang Z R, Han W, et al. 2014. An improvement of background error covariance in the global GRAPES variational data assimilation and its impact on the analysis and prediction: Statistics of the three-dimensional structure of background error covariance. *Acta Meteor Sinica*, 72(1): 62-78 (in Chinese)
- 王金成,龚建东,赵滨.2015.一种新的COSMIC大气折射率资料观测误差估计方法及在GRAPES全球三维变分同化中的应用.气象学报,73(1): 142-158. Wang J C, Gong J D, Zhao B. 2015. A new method for estimating observation error of the COSMIC refractivity data and its impacts on GRAPES-GFS model weather forecasts. *Acta Meteor Sinica*, 73(1): 142-158 (in Chinese)
- 王金成,龚建东,王瑞春.2016.GRAPES全球三维变分同化中卫星微波温度计亮温的背景误差及在质量控制中的应用.气象学报,74(3): 397-409. Wang J C, Gong J D, Wang R C. 2016. Estimation of background error for brightness temperature in GRAPES 3DVar and its application in radiance data background quality control. *Acta Meteor Sinica*, 74(3): 397-409 (in Chinese)
- 王金成,陆慧娟,韩威等.2017.GRAPES全球三维变分同化业务系统性能.应用气象学报,28(1): 11-24. Wang J C, Lu H J, Han W, et al. 2017. Improvements and performances of the operational GRAPES\_GFS 3Dvar system. *J Appl Meteor Sci*, 28(1): 11-24 (in Chinese)
- 王瑞春,龚建东,王皓.2021.公里尺度区域变分同化中引入大尺度约束的影响研究.大气科学,45(5): 1007-1022. Wang R C, Gong J D, Wang H. 2021. Impact studies of introducing a large-scale constraint into the kilometer-scale regional variational data assimilation. *Chinese J Atmos Sci*, 45(5): 1007-1022 (in Chinese)
- 王瑞春,龚建东,孙健.2024.CMA-MESO千米尺度变分同化系统中极小化控制变量的重构.气象学报,82(2): 208-221. Wang R C, Gong J D, Sun J. 2024. A reformulation of the minimization control variables in the CMA-MESO km-scale variational assimilation system. *Acta Meteor Sinica*, 82(2): 208-221 (in Chinese)
- 王世平,廖洞贤,纪立人等.1984.数值天气预报的现状和2000年展望.气象科技,(5): 12-15. Wang S P, Liao D X, Ji L R. 1984. Status and prospect for the 2000 year of numerical weather prediction. *Meteor Sci Technol*, (5): 12-15 (in Chinese)
- 徐枝芳,龚建东,王建捷等.2006.地面观测资料同化初步研究.应用气象学报,17(S1): 1-10. Xu Z F, Gong J D, Wang J J, et al. 2006. Preliminary study on surface observational data assimilation. *J Appl Meteor Sci*, 17(S1): 1-10 (in Chinese)
- 徐枝芳,龚建东,王建捷等.2007.复杂地形下地面观测资料同化 I.模式地形与观测站地形高度差异对地面资料同化的影响研究.大气科学,31(2): 222-232. Xu Z F, Gong J D, Wang J J, et al. 2007. A study of assimilation of surface observational data in complex terrain part I: Influence of the elevation difference between model surface and observation site. *Chinese J Atmos Sci*, 31(2): 222-232 (in Chinese)
- 徐枝芳,龚建东,李泽椿.2009.复杂地形下地面观测资料同化 III.两种解决模式地形与观测站地形高度差异方法的对比分析.大气科学,33(6): 1137-1147. Xu Z F, Gong J D, Li Z C. 2009. A study of assimilation of surface observational data in complex terrain part III: Comparison analysis of two methods on solving the problem of elevation difference between model surface and observation sites. *Chinese J Atmos Sci*, 33(6): 1137-1147 (in Chinese)
- 徐枝芳,郝民,朱立娟等.2013.GRAPES\_RAFS系统研发.气象,39(4): 466-477. Xu Z F, Hao M, Zhu L J, et al. 2013. On the research and development of GRAPES\_RAFS. *Meteor Mon*, 39(4): 466-477 (in Chinese)
- 徐枝芳,吴洋,龚建东等.2021.CMA-MESO三维变分同化系统2 m相对湿度资料同化研究.气象学报,79(6): 943-955. Xu Z F, Wu Y, Gong J D, et al. 2021. Assimilation of 2 m relative humidity observations in CMA-MESO 3DVar system. *Acta Meteor Sinica*, 79(6): 943-955 (in Chinese)
- 徐枝芳,王瑞春.2022.背景误差尺度分离与多尺度混合滤波技术在CMA-MESO 3 km系统的应用.气象,48(12): 1525-1538. Xu Z F, Wang R C. 2022. Multiscale separation of background error for multiscale filtering in CMA-MESO 3 km resolution system. *Meteor Mon*, 48(12): 1525-1538 (in Chinese)
- 许健民.2020.风云二号气象卫星图像定位和卫星风精度的改善中解决问题的途径.南京信息工程大学学报(自然科学版),12(1): 1-6. Xu J M.

2020. Pathways on solving problems at algorithm improvements for FY-2 meteorological satellite at image navigation and wind vector derivation. *J Nanjing Univ Inf Sci Technol (Nat Sci Ed)*, 12(1): 1-6 (in Chinese)
- 许小峰, 2003. 中国新一代多普勒天气雷达网的建设与技术应用. *中国工程科学*, 5(6): 7-14. Xu X F. 2003. Construction, techniques and application of new generation Doppler weather radar network in China. *Strategic Study of CAE*, 5(6): 7-14 (in Chinese)
- 薛纪善, 李璨玑, 王志明, 1992. 非线性正规模初值化原则在有限区模式的实现. *大气科学*, 16(6): 686-697. Xue J S, Li C J, Wang Z M. 1992. Initialization of limited area model based on the principle of nonlinear normal mode initialization. *Sci Atmos Sinica*, 16(6): 686-697 (in Chinese)
- 薛纪善, 陈德辉. 2008. 数值预报系统 GRAPES 的科学设计与应用. 北京: 科学出版社, 383. Xue J S, Chen D H. 2008. Scientific Design and Application of the Numerical Weather Prediction System GRAPES. Beijing: Science Press, 383 (in Chinese)
- 杨毅, 邱崇践, 龚建东, 等. 利用 3 维变分方法同化多普勒天气雷达资料的试验研究. *气象科学*, 2008, 28(2): 124-132. Yang Y, Qiu C J, Gong J D, et al. Study on Doppler weather radar data assimilation via 3D-Var. *J Meteor Sci*, 2008, 28(2): 124-132 (in Chinese)
- 张诚忠, 薛纪善, 冯业荣, 等. 2019. 基于贝叶斯方案的雷达反射率反演水汽及其同化试验. *热带气象学报*, 35(2): 145-153. Zhang C Z, Xue J S, Feng Y R, et al. 2019. Retrieval of water vapor from radar reflectivity based on bayesian scheme and its assimilation test. *J Tropi Meteor*, 35(2): 145-153 (in Chinese)
- 张海阳, 陈耀登, 孙涛等. 2024. 变分框架下双偏振雷达直接同化算子的构建及其初步应用. *气象学报*, 82(6): 774-787. Zhang H Y, Chen Y D, Sun T, et al. 2024. Construction and preliminary application of a direct assimilation operator for dual polarization radars under the variational assimilation framework. *Acta Meteor Sinica*, 82(6): 774-787 (in Chinese)
- 张晓虎, 张其松, 许健民. 2017. 半透明云风矢量高度算法中代表运动像元的使用. *应用气象学报*, 28(3): 270-282. Zhang X H, Zhang Q S, Xu J M. 2017. Use of representative pixels of motion for wind vector height assignment of semi-transparent clouds. *J Appl Meteor Sci*, 28(3): 270-282 (in Chinese)
- 赵滨, 张莉, 李巧萍等. 2024. CMA 业务预报系统 2023 年度评估报告. 北京: 中国气象局, 51. Zhao B, Zhang L, Li Q P, et al. 2024. Annual evaluation and report of the CMA operational forecast system (2023). Beijing: China Meteorological Administration, 51 (in Chinese)
- 朱立娟, 龚建东, 黄丽萍等. 2017. GRAPES 三维云初始场形成及在短临预报中的应用. *应用气象学报*, 28(1): 38-51. Zhu L J, Gong J D, Huang L P, et al. 2017. Three-dimensional cloud initial field created and applied to GRAPES numerical weather prediction nowcasting. *J Appl Meteor Sci*, 28(1): 38-51 (in Chinese)
- 庄照荣, 王瑞春, 李兴良. 2020. 全球大尺度信息在 3 km GRAPES-RAFS 系统中的应用. *气象学报*, 78(1): 33-46. Zhuang Z R, Wang R C, Li X L. 2020. Application of global large scale information to GRAEPS RAFS system. *Acta Meteor Sinica*, 78(1): 33-46 (in Chinese)
- Ades M, van Leeuwen P J. 2015. The equivalent-weights particle filter in a high-dimensional system. *Quart J Roy Meteor Soc*, 141(687): 484-503
- Agusti-Panareda A, Beljaars A, Cardinali C, et al. 2010. Impacts of assimilating AMMA soundings on ECMWF analyses and forecasts. *Wea Forecasting*, 25(4): 1142-1160
- Aires F, Prigent C, Bernardo F, et al. 2011. A tool to estimate land-surface emissivities at microwave frequencies (TELSEM) for use in numerical weather prediction. *Quart J Roy Meteor Soc*, 137(656): 690-699
- Anderson J L, Anderson S L. 1999. A Monte Carlo implementation of the nonlinear filtering problem to produce ensemble assimilations and forecasts. *Mon Wea Rev*, 127(12): 2741-2758
- Anderson J L. 2001. An ensemble adjustment Kalman filter for data assimilation. *Mon Wea Rev*, 129(12): 2884-2903
- Anderson J L. 2007. Exploring the need for localization in ensemble data assimilation using a hierarchical ensemble filter. *Phys D Nonlinear Phenom*, 230(1-2): 99-111
- Anderson J L. 2009. Spatially and temporally varying adaptive covariance inflation for ensemble filters. *Tellus A*, 61(1): 72-83
- Anderson J L. 2010. A non-Gaussian ensemble filter update for data assimilation. *Mon Wea Rev*, 138(11): 4186-4198
- Anderson J L. 2012. Localization and sampling error correction in ensemble Kalman filter data assimilation. *Mon Wea Rev*, 140(7): 2359-2371
- Anderson J L. 2022. A quantile-conserving ensemble filter framework. Part I: Updating an observed variable. *Mon Wea Rev*, 150(5): 1061-1074
- Anderson J L. 2023. A quantile-conserving ensemble filter framework. Part II: Regression of observation increments in a probit and probability integral transformed space. *Mon Wea Rev*, 151(10): 2759-2777
- Andersson E, Pailleux J, Thépaut J N, et al. 1994. Use of cloud-cleared radiances in three/four-dimensional variational data assimilation. *Quart J Roy Meteor Soc*, 120(517): 627-653
- Arcucci R, Mottet L, Pain C, et al. 2019. Optimal reduced space for variational data assimilation. *J Comput Phys*, 379: 51-69
- Atkins M J, Jones M. 1975. An experiment to determine the value SIRS data in numerical forecasting. *Meteor Mag*, 104: 125-142
- Auligné T, Ménétrier B, Lorenc A C, et al. 2016. Ensemble-variational integrated localized data assimilation. *Mon Wea Rev*, 144(10): 3677-3696
- Baordo F, Geer A J. 2016. Assimilation of SSMIS humidity-sounding channels in all-sky conditions over land using a dynamic emissivity retrieval. *Quart J Roy Meteor Soc*, 142(700): 2854-2866
- Barkmeijer J, Bouttier F, van Gijzen M. 1998. Singular vectors and estimates of the analysis error covariance metric. *Quart J Roy Meteor Soc*, 124(549): 1695-1713
- Bauer P, Geer A J, Lopez P, et al. 2010. Direct 4D-Var assimilation of all-sky radiances. Part I: Implementation. *Quart J Roy Meteor Soc*, 136:

- 1868-1885
- Bengtsson T, Snyder C, Nychka D. 2003. Toward a nonlinear ensemble filter for high-dimensional systems. *J Geophys Res Atmos*, 108(D24): 8775
- Bennett A F. 1992. *Inverse Methods in Physical Oceanography*. Cambridge: Cambridge University Press
- Bennett A F, Chua B S, Leslie L M. 1996. Generalized inversion of a global numerical weather prediction model. *Meteor Atmos Phys*, 60(1): 165-178
- Bergemann K, Reich S. 2010. A mollified ensemble Kalman filter. *Quart J Roy Meteor Soc*, 136(651): 1636-1643
- Bergot T. 1999. Adaptive observations during FASTEX: A systematic survey of upstream flights. *Quart J Roy Meteor Soc*, 125(561): 3271-3298
- Berner J, Shutts G J, Leutbecher M, et al. 2009. A spectral stochastic kinetic energy backscatter scheme and its impact on flow-dependent predictability in the ECMWF ensemble prediction system. *J Atmos Sci*, 66(3): 603-626
- Bi X Y, Gao Z Q, Liu Y G, et al. 2015. Observed drag coefficients in high winds in the near offshore of the South China Sea. *J Geophys Res Atmos*, 120(13): 6444-6459
- Binev P, Cohen A, Dahmen W, et al. 2017. Data assimilation in reduced modeling. *SIAM/ASA J Uncertain Quantif*, 5(1): 1-29
- Bishop C H, Toth Z. 1999. Ensemble transformation and adaptive observations. *J Atmos Sci*, 56(11): 1748-1765
- Bishop C H, Etherton B J, Majumdar S J. 2001. Adaptive sampling with the ensemble transform Kalman filter. Part I : Theoretical aspects. *Mon Wea Rev*, 129(3): 420-436
- Bishop C H, Hodges D. 2009. Ensemble covariances adaptively localized with ECO-RAP. Part 1: Tests on simple error models. *Tellus A*, 61(1): 84-96
- Bloom S C, Takacs L L, da Silva A M, et al. 1996. Data assimilation using incremental analysis updates. *Mon Wea Rev*, 124(6): 1256-1271
- Bocquet M, Farchi A, Malartic Q. 2021. Online learning of both state and dynamics using ensemble Kalman filters. *Found Data Sci*, 3(3): 305-330
- Bolton T, Zanna L. 2019. Applications of deep learning to ocean data inference and subgrid parameterization. *J Adv Model Earth Syst*, 11(1): 376-399
- Bonavita M, Isaksen L, Holm E. 2012. On the use of EDA background error variances in the ECMWF 4D-Var. *Quart J Roy Meteor Soc*, 138(667): 1540-1559
- Bonavita M, Hamrud M, Isaksen L. 2015. EnKF and hybrid gain ensemble data assimilation. Part II : EnKF and hybrid gain results. *Mon Wea Rev*, 143(12): 4865-4882
- Bonavita M, Laloyaux P. 2020. Machine learning for model error inference and correction. *J Adv Model Earth Syst*, 12(12): e2020MS002232
- Bormann N, Lawrence H, Farnan J. 2019. Global observing system experiments in the ECMWF assimilation system. Shinfield Park: ECMWF, 23
- Brajard J, Carrassi A, Bocquet M, et al. 2021. Combining data assimilation and machine learning to infer unresolved scale parametrization. *Philos Trans Roy Soc A Math Phys Eng Sci*, 379(2194): 20200086
- Buehner M, Houtekamer P L, Charette C, et al. 2010a. Intercomparison of variational data assimilation and the ensemble Kalman filter for global deterministic NWP. Part I: Description and single-observation experiments. *Mon Wea Rev*, 138(5): 1550-1566
- Buehner M, Houtekamer P L, Charette C, et al. 2010b. Intercomparison of variational data assimilation and the ensemble Kalman filter for global deterministic NWP. Part II: One-month experiments with real observations. *Mon Wea Rev*, 138(5): 1567-1586
- Buehner M. 2012. Evaluation of a spatial/spectral covariance localization approach for atmospheric data assimilation. *Mon Wea Rev*, 140(2): 617-636
- Buehner M, McTaggart-Cowan R, Beaulne A, et al. 2015a. Implementation of deterministic weather forecasting systems based on ensemble-variational data assimilation at environment Canada. Part I : The global system. *Mon Wea Rev*, 143(7): 2532-2559
- Buehner M, Shlyyeva A. 2015b. Scale-dependent background-error covariance localisation. *Tellus*, 67(1): 28027
- Buizza R, Milleer M, Palmer T N. 1999. Stochastic representation of model uncertainties in the ECMWF ensemble prediction system. *Quart J Roy Meteor Soc*, 125(560): 2887-2908
- Burgers G, van Leeuwen P J, Evensen G. 1998. Analysis scheme in the ensemble Kalman filter. *Mon Wea Rev*, 126(6): 1719-1724
- Caron J F, Milewski T, Buehner M, et al. 2015. Implementation of deterministic weather forecasting systems based on ensemble-variational data assimilation at environment Canada. Part II : The regional system. *Mon Wea Rev*, 143(7): 2560-2580
- Casas C Q, Arcucci R, Wu P, et al. 2020. A reduced order deep data assimilation model. *Phys D Nonlinear Phenom*, 412: 132615
- Cha D H, Wang Y Q. 2013. A dynamical initialization scheme for real-time forecasts of tropical cyclones using the WRF model. *Mon Wea Rev*, 141(3): 964-986
- Chan P W, Wu N G, Zhang C Z, et al. 2018. The first complete dropsonde observation of a tropical cyclone over the South China Sea by the Hong Kong observatory. *Weather*, 73(7): 227-234
- Chan P W, Han W, Mak B, et al. 2023. Ground-space-sky observing system experiment during tropical cyclone Mulan in August 2022. *Adv Atmos Sci*, 40(2): 194-200
- Chen B Y, Mu M, Qin X H. 2013. The impact of assimilating dropwindsonde data deployed at different sites on typhoon track forecasts. *Mon Wea Rev*, 141(8): 2669-2682
- Chen F, Liang X, Ma H. 2017. Application of IVAP-based observation operator in radar radial velocity assimilation: The case of typhoon Fitow. *Mon Wea Rev*, 145: 4187-4203
- Chen H, Chen Y, Gao J, et al. 2020. A radar reflectivity data assimilation method based on background-dependent hydrometeor retrieval: An

- observing system simulation experiment. *Atmospheric Research*, 243: 105022
- Chen H Y, Yu H, Ye G J, et al. 2019. Return period and the trend of extreme disastrous rainstorm events in Zhejiang Province. *J Trop Meteor*, 25(2): 192-200
- Chen N, Tang J, Zhang J A, et al. 2021. On the distribution of helicity in the tropical cyclone boundary layer from dropsonde composites. *Atmos Res*, 249: 105298
- Chen X C, Zhang F Q. 2019. Development of a convection-permitting air-sea-coupled ensemble data assimilation system for tropical cyclone prediction. *J Adv Model Earth Syst*, 11(11): 3474-3496
- Chen Y, Oliver D S. 2010. Cross-covariances and localization for EnKF in multiphase flow data assimilation. *Comput Geosci*, 14(4): 579-601
- Chen Y D, Wang H L, Min J Z, et al. 2015. Variational assimilation of cloud liquid/ice water path and its impact on NWP. *J Appl Meteor Climatol*, 54(8): 1809-1825
- Chorin A J, Tu X M. 2009. Implicit sampling for particle filters. *Proc Natl Acad Sci USA*, 106(41): 17249-17254
- Chouinard C, Hallé J, Charette C, et al. 2002. Recent improvements in the use of TOVS satellite radiances in the unified 3D-Var system of the Canadian meteorological centre// ITSC XII Proceedings. Lorne, 27
- Clayton A M, Lorenc A C, Barker D M. 2013. Operational implementation of a hybrid ensemble/4D-Var global data assimilation system at the Met Office. *Quart J Roy Meteor Soc*, 139(675): 1445-1461
- Collard A D. 2007. Selection of IASI channels for use in numerical weather prediction. *Quart J Roy Meteor Soc*, 133(629): 1977-1991
- Courtier P, Talagrand O. 1990. Variational assimilation of meteorological observations with the direct and adjoint shallow-water equations. *Tellus A*, 42(5): 531-549
- Courtier P, Thépaut J N, Hollingsworth A. 1994. A strategy for operational implementation of 4d-Var, using an incremental approach. *Quart J Roy Meteor Soc*, 120(519): 1367-1387
- Cressman G P. 1959. An operational objective analysis system. *Mon Wea Rev*, 87(10): 367-374
- Da Silva A, Pfaendtner J, Guo J, et al. 1995. Assessing the effects of data selection with DAO's physical-space statistical analysis system// Proceedings of the Second International Symposium on the Assimilation of Observations in Meteorology and Oceanography, Tokyo, Japan. Tokyo, Japan: World Meteorological Organization and Japan Meteorological Agency
- Daley R. 1991. *Atmospheric Data Analysis*. Cambridge: Cambridge University Press
- Daley R. 1995. Estimating the wind field from chemical constituent observations: Experiments with a one-dimensional extended Kalman filter. *Mon Wea Rev*, 123(1): 181-198
- Derber J, Bouttier F. 1999. A reformulation of the background error covariance in the ECMWF global data assimilation system. *Tellus A*, 51(2): 195-221
- Derber J C. 1989. A variational continuous assimilation technique. *Mon Wea Rev*, 117(11): 2437-2446
- Derber J C, Wu W S. 1998. The use of TOVS cloud-cleared radiances in the NCEP SSI analysis system. *Mon Wea Rev*, 126(8): 2287-2299
- Desmarais A J, Tracton S, McPherson P, et al. 1978. The NMC report on the data systems test. NASA Contract S-70252-AG. Camp Springs: National Meteorological Center
- Di D, Li J, Li Z L, et al. 2024. Enhancing clear radiance generation for geostationary hyperspectral infrared sounder using high temporal resolution information. *Geophys Res Lett*, 51(2): e2023GL107194
- Douc R, Cappé O. 2005. Comparison of resampling schemes for particle filtering// ISPA 2005. Proceedings of the 4th International Symposium on Image and Signal Processing and Analysis. Zagreb: IEEE, 64-69
- Doucet A, Godsill S, Andrieu C. 2000. On sequential Monte Carlo sampling methods for Bayesian filtering. *Stat Comput*, 10(3): 197-208
- Druyan L M, Ben-Amram T, Alperson Z, et al. 1978. The impact of VTPR data on numerical forecasts of the Israel meteorological service. *Mon Wea Rev*, 106(6): 859-869
- Duan W S, Li X Q, Tian B. 2018. Towards optimal observational array for dealing with challenges of El Niño-southern oscillation predictions due to diversities of El Niño. *Climate Dyn*, 51(9): 3351-3368
- Duan W S, Yang L C, Mu M, et al. 2023. Recent advances in China on the predictability of weather and climate. *Adv Atmos Sci*, 40(8): 1521-1547
- Duan Y H, Wan Q L, Huang J, et al. 2019. Landfalling tropical cyclone research project (LTCRP) in China. *Bull Amer Meteor Soc*, 100(12): ES447-ES472
- Egbert G D, Bennett A F, Foreman M G G. 1994. TOPEX/POSEIDON tides estimated using a global inverse model. *J Geophys Res Oceans*, 99(12): 24821-24852
- El Gharamti M. 2018. Enhanced adaptive inflation algorithm for ensemble filters. *Mon Wea Rev*, 146(2): 623-640
- Eliassen A, Sawyer J S, Smagorinsky J, et al. 1960. Upper air network requirements for numerical weather prediction. Geneva: World Meteorological Organization
- Elsberry R L, Harr P A. 2008. Tropical cyclone structure (TCS08) field experiment science basis, observational platforms, and strategy. *Asia-Pacific J Atmos Sci*, 44(3): 209-231
- Evensen G. 1994. Sequential data assimilation with a nonlinear quasi-geostrophic model using Monte Carlo methods to forecast error statistics. *J Geophys Res*, 99(C5): 10143-10162
- Evensen G, van Leeuwen P J. 2000. An ensemble Kalman smoother for nonlinear dynamics. *Mon Wea Rev*, 128(6): 1852-1867
- Eyre J R, Lorenc A C. 1989. Direct use of satellite sounding radiances in NWP. *Meteor Mag*, 118: 13-16
- Eyre J R, Kelly G A, McNally A P, et al. 1993. Assimilation of TOVS radiance information through one-dimensional variational analysis. *Quart*

- J Roy Meteor Soc, 119(514): 1427-1463
- Eyre J R, English S J, Forsythe M. 2020. Assimilation of satellite data in numerical weather prediction. Part I : The early years. Quart J Roy Meteor Soc, 146(726): 49-68
- Farchi A, Bocquet M, Laloyaux P, et al. 2021a. A comparison of combined data assimilation and machine learning methods for offline and online model error correction. J Comput Sci, 55: 101468
- Farchi A, Laloyaux P, Bonavita M, et al. 2021b. Using machine learning to correct model error in data assimilation and forecast applications. Quart J Roy Meteor Soc, 147(739): 3067-3084
- Feng J, Qin X H, Wu C Q, et al. 2022. Improving typhoon predictions by assimilating the retrieval of atmospheric temperature profiles from the FengYun-4A's geostationary interferometric infrared sounder (GIIRS). Atmos Res, 280: 106391
- Flowerdew J. 2015. Towards a theory of optimal localisation. Tellus A, 67(1): 25257
- Forsythe M, Berger H, Velden C, et al. 2007. Atmospheric motion vectors: Past, present and future// Proceeding of ECMWF Annual Seminar 2007. Exeter: ECMWF
- Fraccaro M, Kamronn S, Paquet U, et al. 2017. A disentangled recognition and nonlinear dynamics model for unsupervised learning// Proceedings of the 31st International Conference on Neural Information Processing Systems. Long Beach: ACM, 3604-3613
- Gagne II D J, Christensen H M, Subramanian A C, et al. 2020. Machine learning for stochastic parameterization: Generative adversarial networks in the Lorenz' 96 model. J Adv Model Earth Syst, 12(3): e2019MS001896
- Gandin L S. 1963. Objective Analysis of Meteorological Fields. Leningrad: Hydromet Press
- Gao J, Stensrud D J. 2012. Assimilation of reflectivity data in a convective-scale, cycled 3DVAR framework with hydrometeor classification. J Atmos Sci, 69: 1054-1065
- Gao J, Xue M, Shapiro A, et al. 1999. A variational method for the analysis of three-dimensional wind fields from two Doppler radars. Mon Wea Rev, 127: 2128-2142
- Gao J, Xue M, Brewster K, et al. 2004. A three-dimensional variational data analysis method with recursive filter for Doppler radars. J Atmos Ocean Technol, 21(3): 457-469
- Gaspari G, Cohn S E. 1999. Construction of correlation functions in two and three dimensions. Quart J Roy Meteor Soc, 125(554): 723-757
- Geer A J, Bauer P, Lopez P. 2008. Lessons learnt from the operational 1D+4D-Var assimilation of rain-and cloud-affected SSM/I observations at ECMWF. Quart J Roy Meteor Soc, 134(635): 1513-1525
- Geer A J, Bauer P, Lopez P. 2010. Direct 4D-Var assimilation of all-sky radiances. Part II: Assessment. Quart J Roy Meteor Soc, 136(652): 1886-1905
- Geer A J, Lonitz K, Weston P, et al. 2018. All-sky satellite data assimilation at operational weather forecasting centres. Quart J Roy Meteor Soc, 144(713): 1191-1217
- Geer A J. 2021. Learning earth system models from observations: Machine learning or data assimilation?. Philos Trans Roy Soc A Math Phys Eng Sci, 379(2194): 20200089
- Ghil M, Cohn S, Tavantzis J, et al. 1981. Applications of estimation theory to numerical weather prediction// Bengtsson L, Ghil M, Källén E. Dynamic Meteorology: Data Assimilation Methods. New York: Springer, 139-224
- Gilchrist A. 1982. JSC study conference on observing system experiments// Exeter Workshop 1982
- Gilchrist B, Cressman G P. 1954. An experiment in objective analysis. Tellus, 6(4): 309-318
- Gordon N J, Salmond D J, Smith A F M. 1993. Novel approach to non-linear/non-Gaussian Bayesian state estimation. IEE Proc F Radar Signal Process, 140(2): 107-113
- Ha S, Berner J, Snyder C. 2015. A comparison of model error representations in mesoscale ensemble data assimilation. Mon Wea Rev, 143(10): 3893-3911
- Hamill T M, Snyder C. 2000. A hybrid ensemble Kalman filter-3D variational analysis scheme. Mon Wea Rev, 128(8): 2905-2919
- Hamill T M. 2001. Interpretation of rank histograms for verifying ensemble forecasts. Mon Wea Rev, 129(3): 550-560
- Han W, Bormann N. 2016. Constrained adaptive bias correction for satellite radiance assimilation in the ECMWF 4D-Var system. Shinfield Park: ECMWF
- Han W, Yin R Y, Li J, et al. 2023. Assimilation of geostationary hyperspectral infrared sounders (GeoHIS): Progresses and perspectives// Park S K. Numerical Weather Prediction: East Asian Perspectives. Cham: Springer, 205-216
- Han W, Yin R, Li J, Liu Y, Wang J, Li Y, Qin X, Zhang Z, Shen X. 2025. Targeted sounding observations from geostationary satellite and impacts on high impact weather forecasts. Sci China Earth Sci, 68(4): 963-976
- Hawkins-Smith LD, Simonin D. 2021. Radar reflectivity assimilation using hourly cycling 4D-Var in the Met Office Unified Model. Quart J Roy Meteor Soc, 1516-1538
- Hatfield S, Chantry M, Dueben P, et al. 2021. Building tangent-linear and adjoint models for data assimilation with neural networks. J Adv Model Earth Syst, 13(9): e2021MS002521
- He H, Lei L L, Whitaker J S, et al. 2020. Impacts of assimilation frequency on ensemble Kalman filter data assimilation and imbalances. J Adv Model Earth Syst, 12(10): e2020MS002187
- He L L, Weng F Z. 2023. Improved microwave ocean emissivity and reflectivity models derived from two-scale roughness theory. Adv Atmos Sci, 40(10): 1923-1938
- He Y J, Wang B, Liu M M, et al. 2017. Reduction of initial shock in decadal predictions using a new initialization strategy. Geophys Res Lett, 44(16): 8538-8547

- Healy S B, Jupp A M, Marquardt C. 2005. Forecast impact experiment with GPS radio occultation measurements. *Geophys Res Lett*, 32(3): L03804
- Hoke J E, Anthes R A. 1976. The initialization of numerical models by a dynamic-initialization technique. *Mon Wea Rev*, 104(12): 1551-1556
- Hollingsworth A, Shaw D B, Lönnberg P, et al. 1986. Monitoring of observation and analysis quality by a data assimilation system. *Mon Wea Rev*, 114(5): 861-879
- Houtekamer P L, Lefavre L, Derome J, et al. 1996. A system simulation approach to ensemble prediction. *Mon Wea Rev*, 124(6): 1225-1242
- Houtekamer P L, Mitchell H L. 1998. Data assimilation using an ensemble Kalman filter technique. *Mon Wea Rev*, 126(3): 796-811
- Houtekamer P L, Mitchell H L. 2001. A sequential ensemble Kalman filter for atmospheric data assimilation. *Mon Wea Rev*, 129(1): 123-137
- Houtekamer P L, Mitchell H L, Pellerin G, et al. 2005a. Atmospheric data assimilation with an ensemble Kalman filter: Results with real observations. *Mon Wea Rev*, 133(3): 604-620
- Houtekamer P L, Mitchell H L. 2005b. Ensemble Kalman filtering. *Quart J Roy Meteor Soc*, 131(613): 3269-3289
- Houtekamer P L, Deng X X, Mitchell H L, et al. 2014. Higher resolution in an operational ensemble Kalman filter. *Mon Wea Rev*, 142(3): 1143-1162
- Howard L J, Subramanian A, Hoteit I. 2024. A machine learning augmented data assimilation method for high-resolution observations. *J Adv Model Earth Syst*, 16(1): e2023MS003774
- Huang L W, Gianinazzi L, Yu Y J, et al. 2024. DiffDA: A diffusion model for weather-scale data assimilation//41st International Conference on Machine Learning. Vienna: ICML
- Hunt B R, Kostelich E J, Szunyogh I. 2007. Efficient data assimilation for spatiotemporal chaos: A local ensemble transform Kalman filter. *Phys D Nonlinear Phenom*, 230(1-2): 112-126
- Irvine E A, Gray S L, Methven J, et al. 2011. Forecast impact of targeted observations: Sensitivity to observation error and proximity to steep orography. *Mon Wea Rev*, 139(1): 69-78
- Jansa A, Arbogast P, Doerenbecher A, et al. 2011. A new approach to sensitivity climatologies: The DTS-MEDEX-2009 campaign. *Nat Hazards Earth Syst Sci*, 11(9): 2381-2390
- Jerger D. 2014. Radar Forward Operator for Verification of Cloud Resolving Simulations within the COSMO Model. Karlsruhe: Kit Scientific Publishing
- Jiang L, Duan W S, Liu H L. 2022. The most sensitive initial error of sea surface height anomaly forecasts and its implication for target observations of mesoscale eddies. *J Phys Oceanogr*, 52(4): 723-740
- Jiang L, Duan W S, Wang H. 2024. The sensitive area for targeting observations of paired mesoscale eddies associated with sea surface height anomaly forecasts. *J Geophys Res Oceans*, 129(2): e2023JC020572
- Johnson B T, Dang C, Stegmann P, et al. 2023. The community radiative transfer model (CRTM): Community-focused collaborative model development accelerating research to operations. *Bull Amer Meteor Soc*, 104(10): E1817-E1830
- Jones T A, Stensrud D J, Minnis P, et al. 2013. Evaluation of a forward operator to assimilate cloud water path into WRF-DART. *Mon Wea Rev*, 141(7): 2272-2289
- Joo S, Eyre J, Marriott R. 2013. The impact of MetOp and other satellite data within the Met Office global NWP system using an adjoint-based sensitivity method. *Mon Wea Rev*, 141(10): 3331-3342
- Joo S W, Lee D K. 2002. The use of ATOVS data in Korea meteorological administration (KMA)//Proceedings of the 12th International TOVS Study Conference. Lorne: BMRC, 128-137
- Jung Y, Zhang G, Xue M. 2008a. Assimilation of simulated polarimetric radar data for a convective storm using the ensemble Kalman filter. Part I: Observation operators for reflectivity and polarimetric variables. *Mon Wea Rev*, 136: 2228-2245
- Jung Y, Xue M, Zhang G, et al. 2008b. Assimilation of simulated polarimetric radar data for a convective storm using the ensemble Kalman filter. Part II: Impact of polarimetric data on storm analysis. *Mon Wea Rev*, 136(6): 2246-2260
- Kalman R E. 1960. A new approach to linear filtering and prediction problems. *J Basic Eng*, 82(1): 35-45
- Kalman R E, Bucy R S. 1961. New results in linear filtering and prediction theory. *J Basic Eng*, 83(1): 95-108
- Kalnay E, Anderson D L T, Bennett A F, et al. 1997. Data assimilation in the ocean and in the atmosphere: What should be next?. *J Meteor Soc Japan*, 75(1B): 489-496
- Kalnay E. 2003. Atmospheric Modeling, Data Assimilation, and Predictability. New York: Cambridge University Press, 341pp
- Kalnay E, Yang S C. 2010. Accelerating the spin-up of ensemble Kalman filtering. *Quart J Roy Meteor Soc*, 136(651): 1644-1651
- Kan W L, Shi Y N, Yang J, et al. 2024. Improvements of the microwave gaseous absorption scheme based on statistical regression and its application to ARMS. *J Geophys Res Atmos*, 129(13): e2024JD040732
- Kang J S, Kalnay E, Liu J J, et al. 2011. "Variable localization" in an ensemble Kalman filter: Application to the carbon cycle data assimilation. *J Geophys Res Atmos*, 116(D9): D09110
- Karbow F, Gérard É, Rabier F. 2006. Microwave land emissivity and skin temperature for AMSU-A and -B assimilation over land. *Quart J Roy Meteor Soc*, 132(620): 2333-2355
- Karbow F, Gérard E, Rabier F. 2010. Global 4DVAR assimilation and forecast experiments using AMSU observations over land. Part I: Impacts of various land surface emissivity parameterizations. *Wea Forecasting*, 25(1): 5-19
- Kawabata T, Schwitalla T, Adachi A, et al. 2018. Observational operators for dual polarimetric radars in variational data assimilation systems (PolRad VAR v1.0). *Geosci Model Dev*, 11(6): 2493-2501
- Kelly G A M. 1977. A cycling experiment in the Southern Hemisphere using

- VTTPR data. Melbourne: Australian Numerical Meteorology Research Center
- Kelly G A M, Mills G A, Smith W L. 1978. Impact of Nimbus-6 temperature soundings on Australian region forecasts. *Bull Amer Meteor Soc*, 59(4): 393-406
- Kleist D T, Ide K. 2015a. An OSSE-based evaluation of hybrid variational-ensemble data assimilation for the NCEP GFS. Part I: System description and 3D-hybrid results. *Mon Wea Rev*, 143(2): 433-451
- Kleist D T, Ide K. 2015b. An OSSE-based evaluation of hybrid variational-ensemble data assimilation for the NCEP GFS. Part II: 4DEnVar and hybrid variants. *Mon Wea Rev*, 143(2): 452-470
- Kotsuki S, Shiraishi K, Okazaki A. 2024. Ensemble data assimilation to diagnose AI-based weather prediction model: A case with ClimaX. *arXiv*: 2407.17781v2
- Krishnan R G, Shalit U, Sontag D. 2015. Deep Kalman filters. *arXiv*: 1511.05121
- Krishnan R G, Shalit U, Sontag D. 2017. Structured inference networks for nonlinear state space models//31st AAAI Conference on Artificial Intelligence. San Francisco: AAAI, 2101-2109
- Krzeminski B, Bormann N, Karbou F, et al. 2009. Improved use of surface-sensitive microwave radiances at ECMWF//EUMETSAT Meteorol Satell Conf, 21-25
- Lai A, Min J, Gao J, et al. 2020. Assimilation of radar data, pseudo water vapor, and potential temperature in a 3DVAR framework for improving precipitation forecast of severe weather events. *Atmosphere*, 11(2): 182
- Laloyaux P, Balmaseda M, Dee D, et al. 2016. A coupled data assimilation system for climate reanalysis. *Quart J Roy Meteor Soc*, 142(694): 65-78
- Lei J, Bickel P. 2011. A moment matching ensemble filter for nonlinear non-Gaussian data assimilation. *Mon Wea Rev*, 139(12): 3964-3973
- Lei L L, Stauffer D R, Haupt S E, et al. 2012. A hybrid nudging-ensemble Kalman filter approach to data assimilation. Part I: Application in the Lorenz system. *Tellus A*, 64(1): 18484
- Lei L L, Anderson J L. 2014a. Impacts of frequent assimilation of surface pressure observations on atmospheric analyses. *Mon Wea Rev*, 142(12): 4477-4483
- Lei L L, Anderson J L. 2014b. Comparisons of empirical localization techniques for serial ensemble Kalman filters in a simple atmospheric general circulation model. *Mon Wea Rev*, 142(2): 739-754
- Lei L L, Anderson J L, Romine G S. 2015a. Empirical localization functions for ensemble Kalman filter data assimilation in regions with and without precipitation. *Mon Wea Rev*, 143(9): 3664-3679
- Lei L L, Whitaker J S. 2015b. Model space localization is not always better than observation space localization for assimilation of satellite radiances. *Mon Wea Rev*, 143(10): 3948-3955
- Lei L L, Whitaker J S. 2016. A four-dimensional incremental analysis update for the ensemble Kalman filter. *Mon Wea Rev*, 144(7): 2605-2621
- Lei L L, Whitaker J S, Bishop C. 2018. Improving assimilation of radiance observations by implementing model space localization in an ensemble Kalman filter. *J Adv Model Earth Syst*, 10(12): 3221-3232
- Lei L L, Whitaker J S, Anderson J L, et al. 2020. Adaptive localization for satellite radiance observations in an ensemble Kalman filter. *J Adv Model Earth Syst*, 12(8): e2019MS001693
- Lei L L, Wang Z R, Tan Z M. 2021. Integrated hybrid data assimilation for an ensemble Kalman filter. *Mon Wea Rev*, 149(12): 4091-4105
- Lewis J M, Derber J C. 1985. The use of adjoint equations to solve a variational adjustment problem with advective constraints. *Tellus A*, 37(4): 309-322
- Li J, Liu C Y, Huang H L, et al. 2005. Optimal cloud-clearing for AIRS radiances using MODIS. *IEEE Trans Geosci Remote Sens*, 43(6): 1266-1278
- Li J, Liu G Q. 2016a. Direct assimilation of Chinese FY-3C Microwave temperature sounder-2 radiances in the global GRAPES system. *Atmos Meas Tech*, 9(7): 3095-3113
- Li J, Qin Z K, Liu G Q. 2016b. A new generation of Chinese FY-3C microwave sounding measurements and the initial assessments of its observations. *Int J Remote Sens*, 37(17): 4035-4058
- Li J, Geer A J, Okamoto K, et al. 2022a. Satellite all-sky infrared radiance assimilation: Recent progress and future perspectives. *Adv Atmos Sci*, 39(1): 9-21
- Li J, Zhang Y R, Di D, et al. 2022b. The influence of sub-footprint cloudiness on three-dimensional horizontal wind from geostationary hyperspectral infrared sounder observations. *Geophys Res Lett*, 49(11): e2022GL098460
- Li Y, Wang X, Xue M. 2012. Assimilation of radar radial velocity data with the WRF hybrid ensemble-3DVAR system for the prediction of Hurricane Ike (2008). *Mon Wea Rev*, 140(11): 3507-3524
- Li J, Qin Z K, Liu G Q, et al. 2024. Added benefit of the early-morning-orbit satellite Fengyun-3E on the global microwave sounding of the three-orbit constellation. *Adv Atmos Sci*, 41(1): 39-52
- Li J H, Gao Y D, Wan Q L. 2018. Sample optimization of ensemble forecast to simulate a tropical cyclone using the observed track. *Atmos Ocean*, 56(3): 162-177
- Li X, Mecikalski J R, Posselt D. 2017. An ice-phase microphysics forward model and preliminary results of polarimetric radar data assimilation. *Mon Wea Rev*, 145(2): 683-708
- Li Z T, Han W. 2024. Impact of HY-2B SMR radiance assimilation on CMA global medium-range weather forecasts. *Quart J Roy Meteor Soc*, 150(759): 937-957
- Liang J Y, Terasaki K, Miyoshi T. 2023. A machine learning approach to the observation operator for satellite radiance data assimilation. *J Meteor Soc Japan*, 101(1): 79-95
- Liang X. 2007. An integrating velocity-azimuth process single-Doppler radar wind retrieval method. *J Atmos Ocean Technol*, 24: 658-665
- Liu C, Xue M, Kong R. 2019. Direct assimilation of radar reflectivity data

- using 3DVAR: Treatment of hydrometeor background errors and OSSE tests. *Mon Wea Rev*, 147(1): 17-29
- Liu C, Xue M, Kong R. 2020. Direct variational assimilation of radar reflectivity and radial velocity data: Issues with nonlinear reflectivity operator and solutions. *Mon Wea Rev*, 148(4): 1483-1502
- Liu C, Li H, Xue M, et al. 2022. Use of a reflectivity operator based on double-moment thompson microphysics for direct assimilation of radar reflectivity in GSI-based hybrid en3DVar. *Mon Wea Rev*, 150: 907-926
- Liu C S, Xiao Q N, Wang B. 2008. An ensemble-based four-dimensional variational data assimilation scheme. Part I : Technical formulation and preliminary test. *Mon Wea Rev*, 136(9): 3363-3373
- Liu H Y, Wang Y Q, Xu J, et al. 2018. A dynamical initialization scheme for tropical cyclones under the influence of terrain. *Wea Forecasting*, 33(3): 641-659
- Liu K, Guo W H, Da L L, et al. 2021. Improving the thermal structure predictions in the Yellow Sea by conducting targeted observations in the CNOP-identified sensitive areas. *Sci Rep*, 11(1): 19518
- Liu Y, Xue J S. 2014. Assimilation of global navigation satellite radio occultation observations in GRAPES: Operational implementation. *J Meteor Res*, 28(6): 1061-1074
- Lorenc A C. 1981. A global three-dimensional multivariate statistical interpolation scheme. *Mon Wea Rev*, 109(4): 701-721
- Lorenc A C. 1986. Analysis methods for numerical weather prediction. *Quart J Roy Meteor Soc*, 112(474): 1177-1194
- Lorenc A C. 1997. Development of an operational variational assimilation scheme. *J Meteor Soc Japan*, 75(1B): 339-346
- Lorenc A C. 2003. The potential of the ensemble Kalman filter for NWP: A comparison with 4D-Var. *Quart J Roy Meteor Soc*, 129(595): 3183-3203
- Lorenc A C, Bowler N E, Clayton A M, et al. 2015. Comparison of hybrid-4DVar and hybrid-4DVar data assimilation methods for Global NWP. *Mon Wea Rev*, 143(1): 212-229
- Lu Y, Ren F M, Zhu W J. 2018. Risk zoning of typhoon disasters in Zhejiang province, China. *Nat Hazards Earth Syst Sci*, 18(11): 2921-2932
- Lynch P, Huang X Y. 1992. Initialization of the HIRLAM model using a digital filter. *Mon Wea Rev*, 120(6): 1019-1034
- Ma Z, Li J, Han W, et al. 2021. Four-dimensional wind fields from geostationary hyperspectral infrared sounder radiance measurements with high temporal resolution. *Geophys Res Lett*, 48(14): e2021GL093794
- Malartic Q, Farchi A, Bocquet M. 2022. State, global, and local parameter estimation using local ensemble Kalman filters: Applications to online machine learning of chaotic dynamics. *Quart J Roy Meteor Soc*, 148(746): 2167-2193
- Matricardi M, McNally A P. 2014. The direct assimilation of principal components of IASI spectra in the ECMWF 4D-Var. *Quart J Roy Meteor Soc*, 140(679): 573-582
- McNally A P, Vesperini M. 1996. Variational analysis of humidity information from TOVS radiances. *Quart J Roy Meteor Soc*, 122(535): 1521-1544
- McNally A P, Watts P D. 2003. A cloud detection algorithm for high-spectral-resolution infrared sounders. *Quart J Roy Meteor Soc*, 129(595): 3411-3423
- McPherson R D, Bergman K H, Kistler R E, et al. 1979. The NMC operational global data assimilation system. *Mon Wea Rev*, 107(11): 1445-1461
- Meng D M, Chen Y D, Wang H L, et al. 2019. The evaluation of EnVar method including hydrometeors analysis variables for assimilating cloud liquid/ice water path on prediction of rainfall events. *Atmos Res*, 219: 1-12
- Meng D M, Tan Z M, Li J, et al. 2024. Added value of three-dimensional horizontal winds from geostationary interferometric infrared sounder for typhoon forecast in a regional NWP model. *J Geophys Res Atmos*, 129(6): e2024JD040736
- Meng Z Y, Zhang F Q. 2008. Tests of an ensemble Kalman filter for mesoscale and regional-scale data assimilation. Part III: Comparison with 3DVAR in a real-data case study. *Mon Wea Rev*, 136(2): 522-540
- Meng Z Y, Zhang F Q, Luo D H, et al. 2019. Review of Chinese atmospheric science research over the past 70 years: Synoptic meteorology. *Sci China Earth Sci*, 62(12): 1946-1991
- Ming J, Zhang J A, Rogers R F, et al. 2014. Multiplatform observations of boundary layer structure in the outer rainbands of landfalling typhoons. *J Geophys Res Atmos*, 119(13): 7799-7814
- Ming J, Zhang J A. 2018. Direct measurements of momentum flux and dissipative heating in the surface layer of tropical cyclones during landfalls. *J Geophys Res Atmos*, 123(10): 4926-4938
- Mishchenko M I, Lacis A A, Travis L D. 1994. Errors induced by the neglect of polarization in radiance calculations for Rayleigh-scattering atmospheres. *J Quant Spectrosc Radiat Transfer*, 51: 491-510
- Miyoshi T. 2011. The Gaussian approach to adaptive covariance inflation and its implementation with the local ensemble transform Kalman filter. *Mon Wea Rev*, 139(5): 1519-1535
- Miyoshi T, Kondo K. 2013. A multi-scale localization approach to an ensemble Kalman filter. *SOLA*, 9: 170-173
- Mu M, Duan W S, Wang B. 2003. Conditional nonlinear optimal perturbation and its applications. *Nonlinear Process Geophys*, 10(6): 493-501
- Mu M, Zhou F F, Wang H L. 2009. A method for identifying the sensitive areas in targeted observations for tropical cyclone prediction: Conditional nonlinear optimal perturbation. *Mon Wea Rev*, 137(5): 1623-1639
- Mu M, Feng R, Duan W S. 2017. Relationship between optimal precursors for Indian Ocean dipole events and optimally growing initial errors in its prediction. *J Geophys Res Oceans*, 122(2): 1141-1153
- Ohring G. 1979. Impact of satellite temperature sounding data on weather forecasts. *Bull Amer Meteor Soc*, 60(10): 1142-1147
- Okamoto K, Takeuchi Y, Kaido Y, et al. 2002. Recent developments in assimilation of ATOVS at JMA // Proceedings of the 12th International TOVS Study Conference. Lorne: BMRC, 226-233

- Okamoto K, McNally A P, Bell W. 2014. Progress towards the assimilation of all-sky infrared radiances: An evaluation of cloud effects. *Quart J Roy Meteor Soc*, 140(682): 1603-1614
- Oue M, Tatarevic A, Kollias P, et al. 2020. The Cloud-resolving model Radar SIMulator (CR-SIM) Version 3.3: Description and applications of a virtual observatory. *Geosci Model Dev*, 13: 1975-1998
- Palmer T N, Gelaro R, Barkmeijer J, et al. 1998. Singular vectors, metrics, and adaptive observations. *J Atmos Sci*, 55(4): 633-653
- Panofsky R A. 1949. Objective weather-map analysis. *J Atmos Sci*, 6(6): 386-392
- Parrish D F, Derber J C. 1992. The national meteorological center's spectral statistical-interpolation analysis system. *Mon Wea Rev*, 120(8): 1747-1763
- Peng Z Y, Lei L L, Tan Z M. 2024. A hybrid deep learning and data assimilation method for model error estimation. *Sci China Earth Sci*, 67(12): 3655-3670
- Penny S G. 2014. The hybrid local ensemble transform Kalman filter. *Mon Wea Rev*, 142(6): 2139-2149
- Penny S G, Miyoshi T. 2016. A local particle filter for high-dimensional geophysical systems. *Nonlinear Process Geophys*, 23(6): 391-405
- Poli P, Moll P, Puech D, et al. 2009. Quality control, error analysis, and impact assessment of FORMOSAT-3/COSMIC in numerical weather prediction. *Terr Atmos Ocean Sci*, 20(1): 101-113
- Poterjoy J, Zhang F Q. 2015. Systematic comparison of four-dimensional data assimilation methods with and without the tangent linear model using hybrid background error covariance: E4DVar versus 4DEnVar. *Mon Wea Rev*, 143(5): 1601-1621
- Poterjoy J, Zhang F Q. 2016a. Comparison of hybrid four-dimensional data assimilation methods with and without the tangent linear and adjoint models for predicting the life cycle of Hurricane Karl (2010). *Mon Wea Rev*, 144(4): 1449-1468
- Poterjoy J. 2016b. A localized particle filter for high-dimensional nonlinear systems. *Mon Wea Rev*, 144(1): 59-76
- Prates C, Sahin C, Richardson D S. 2009. Report on PREVIEW data targeting system. Reading
- Putnam B, Xue M, Jung Y, et al. 2019. Ensemble Kalman filter assimilation of polarimetric radar observations for the 20 May 2013 Oklahoma tornadic supercell case. *Mon Wea Rev*, 147(7): 2511-2533
- Qin X H, Mu M. 2012. Influence of conditional nonlinear optimal perturbations sensitivity on typhoon track forecasts. *Quart J Roy Meteor Soc*, 138(662): 185-197
- Qin X H, Duan W S, Chan P W, et al. 2023. Effects of dropsonde data in field campaigns on forecasts of tropical cyclones over the western north Pacific in 2020 and the role of CNOP sensitivity. *Adv Atmos Sci*, 40(5): 791-803
- Rabier F, McNally A, Andersson E, et al. 1998. The ECMWF implementation of three-dimensional variational assimilation (3D-Var). II: Structure function. *Quart J Roy Meteor Soc*, 124(550): 1809-1830
- Rabier F, Fourrié N, Chafai D, et al. 2002. Channel selection methods for infrared atmospheric sounding interferometer radiances. *Quart J Roy Meteor Soc*, 128(581): 1011-1027
- Rabier F, Gauthier P, Cardinali C, et al. 2008. An update on THORPEX-related research in data assimilation and observing strategies. *Nonlinear Process Geophys*, 15(1): 81-94
- Rasp S, Pritchard M S, Gentine P. 2018. Deep learning to represent subgrid processes in climate models. *Proc Natl Acad Sci USA*, 115(39): 9684-9689
- Robert C P, Casella G. 2004. *Monte Carlo Statistical Methods*. New York: Springer, 645
- Saha S, Moorthi S, Pan H L, et al. 2010. The NCEP climate forecast system reanalysis. *Bull Amer Meteor Soc*, 91(8): 1015-1058
- Sakov P, Oliver D S, Bertino L. 2012. An iterative EnKF for strongly nonlinear systems. *Mon Wea Rev*, 140(6): 1988-2004
- Salonen K, Bormann N. 2015. Atmospheric motion vector observations in the ECMWF system: Fourth year report. Shinfield Park: ECMWF
- Santitissadeekorn N, Jones C. 2015. Two-stage filtering for joint state-parameter estimation. *Mon Wea Rev*, 143(6): 2028-2042
- Sasaki Y. 1970. Some basic formalisms in numerical variational analysis. *Mon Wea Rev*, 98(12): 875-883
- Saunders R, Andersson E, Kelly G, et al. 1997. Developments in assimilating global TOVS data at the UK Met Office//Proceedings of the 9th International TOVS Study Conference. Igls: ECMWF, 417-428
- Saunders R, Hocking J, Turner E, et al. 2018. An update on the RTTOV fast radiative transfer model (currently at version 12). *Geosci Model Dev*, 11(7): 2712-2737
- Schröttle J, Weissmann M, Scheck L, et al. 2020. Assimilating visible and infrared radiances in idealized simulations of deep convection. *Mon Wea Rev*, 148(11): 4357-4375
- Shao A M, Qiu C J, Wang X J, et al. 2016. Using the Newtonian relaxation technique in numerical sensitivity studies. *Sci China Earth Sci*, 59(12): 2454-2462
- Shapiro M A, Thorpe A J. 2004. THORPEX international science plan: International science plan. Geneva: WMO
- Slivinski L C, Lippi D E, Whitaker J S, et al. 2022. Overlapping windows in a global hourly data assimilation system. *Mon Wea Rev*, 150(6): 1317-1334
- Sluka T C, Penny S G, Kalnay E, et al. 2016. Assimilating atmospheric observations into the ocean using strongly coupled ensemble data assimilation. *Geophys Res Lett*, 43(3): 752-759
- Smith P J, Fowler A M, Lawless A S. 2015. Exploring strategies for coupled 4D-Var data assimilation using an idealised atmosphere-ocean model. *Tellus A*, 67(1): 27025
- Smith W L, Woolf H M, Jacob W J. 1970a. A regression method for obtaining real-time temperature and geopotential height profiles from satellite

- spectrometer measurements and its application to Nimbus 3 "SIRS" observations. *Mon Wea Rev*, 98(8): 582-603
- Smith W L, Rao P K, Koffler R, et al. 1970b. The determination of sea-surface temperature from satellite high resolution infrared window radiation measurements. *Mon Wea Rev*, 98(8): 604-611
- Snyder C. 1996. Summary of an informal workshop on adaptive observations and FASTEX. *Bull Amer Meteor Soc*, 77(5): 953-961
- Snyder C, Bengtsson T, Bickel P, et al. 2008. Obstacles to high-dimensional particle filtering. *Mon Wea Rev*, 136(12): 4629-4640
- Sodhi J S, Fabry F. 2022. Benefits of smoothing backgrounds and radar reflectivity observations for multiscale data assimilation with an ensemble Kalman filter at convective scales: A proof-of-concept study. *Mon Wea Rev*, 150(3): 589-601
- Spiller E T, Budhiraja A, Ide K, et al. 2008. Modified particle filter methods for assimilating Lagrangian data into a point-vortex model. *Phys D Nonlinear Phenom*, 237(10-12): 1498-1506
- Stoffelen A, Anderson D. 1997. Scatterometer data interpretation: Measurement space and inversion. *J Atmos Ocean Technol*, 14(6): 1298-1313
- Storto A, De Magistris G, Falchetti S, et al. 2021. A neural network-based observation operator for coupled ocean-acoustic variational data assimilation. *Mon Wea Rev*, 149(6): 1967-1985
- Sugiura N, Awaji T, Masuda S, et al. 2008. Development of a four-dimensional variational coupled data assimilation system for enhanced analysis and prediction of seasonal to interannual climate variations. *J Geophys Res Oceans*, 113(C10): C10017
- Sun J, Crook N A. 1997. Dynamical and microphysical retrieval from Doppler radar observations using a cloud model and its adjoint. Part I : Model development and simulated data experiments. *J Atmos Sci*, 54: 1642-1661
- Sun J, Crook N A, 1998. Dynamical and microphysical retrieval from Doppler radar observations using a cloud model and its adjoint. Part II : Retrieval experiments of an observed Florida convective storm. *J Atmos Sci*, 55: 835-852
- Sun J, Xue M, Wilson J W, et al. 2014. Use of NWP for nowcasting convective precipitation: Recent progress and challenges. *Bull Amer Meteor Soc*, 95: 409-426
- Sun J Z, Liu Z Y, Lu F Y, et al. 2020a. Strongly coupled data assimilation using leading averaged coupled covariance (LACC). Part III: Assimilation of real world reanalysis. *Mon Wea Rev*, 148(6): 2351-2364
- Sun J Z, Zhang Y, Ban J M, et al. 2020b. Impact of combined assimilation of radar and rainfall data on short-term heavy rainfall prediction: A case study. *Mon Wea Rev*, 148(5): 2211-2232
- Talagrand O. 1997. Assimilation of observations, an introduction. *J Meteor Soc Japan*, 75(1B): 191-209
- Tang J, Byrne D, Zhang J A, et al. 2015. Horizontal transition of turbulent cascade in the near-surface layer of tropical cyclones. *J Atmos Sci*, 72(12): 4915-4925
- Tang J, Zhang J A, Chan P, et al. 2021. A direct aircraft observation of helical rolls in the tropical cyclone boundary layer. *Sci Rep*, 11(1): 18771
- Temperton C, Roch M. 1991. Implicit normal mode initialization for an operational regional model. *Mon Wea Rev*, 119(3): 667-677
- Thépaut J N, Hoffman R N, Courtier P. 1993. Interactions of dynamics and observations in a four-dimensional variational assimilation. *Mon Wea Rev*, 121(12): 3393-3414
- Thiébaux H J, Pedder M A. 1987. Spatial Objective Analysis. London: Academic Press
- Tian X J, Feng X B. 2015. A non-linear least squares enhanced POD-4DVar algorithm for data assimilation. *Tellus A*, 67(1): 25340
- Tian X J, Zhang H Q, Feng X B, et al. 2018. Nonlinear least squares En4DVar to 4DEnVar methods for data assimilation: Formulation, analysis, and preliminary evaluation. *Mon Wea Rev*, 146(1): 77-93
- Tian Y D, Peters-Lidard C D, Harrison K W, et al. 2015. An examination of methods for estimating land surface microwave emissivity. *J Geophys Res Atmos*, 120(21): 11114-11128
- Tippett M K, Anderson J L, Bishop C H, et al. 2003. Ensemble square root filters. *Mon Wea Rev*, 131(7): 1485-1490
- Tong M, Xue M. 2005. Ensemble Kalman filter assimilation of Doppler radar data with a compressible nonhydrostatic model: OSS experiments. *Mon Wea Rev*, 133(7): 1789-1807
- Uppala S, Hollingsworth A, Tibaldi S, et al. 1984. Results from two recent observing system experiments at ECMWF //Proceedings of Seminar on Data Assimilation Systems and Observing System Experiments with Particular Emphasis on FGGE. Shinfield Park: ECMWF, 165-202
- van Leeuwen P J. 2003. A variance-minimizing filter for large-scale applications. *Mon Wea Rev*, 131(9): 2071-2084
- van Leeuwen P J. 2009. Particle filtering in geophysical systems. *Mon Wea Rev*, 137(12): 4089-4114
- Wang B, Liu J J, Wang S D, et al. 2010. An economical approach to four-dimensional variational data assimilation. *Adv Atmos Sci*, 27(4): 715-727
- Wang H, Sun J, Fan S, et al. 2013a. Indirect assimilation of radar reflectivity with WRF 3D-Var and its impact on prediction of four summertime convective events. *J App Meteor Climat*, 52(4): 889-902
- Wang H, Sun J, Zhang X, et al. 2013b. Radar data assimilation with WRF 4D-Var. Part I : System development and preliminary testing. *Mon Wea Rev*, 141(7): 2224-2244
- Wang J C, Gong J D, Han W. 2020. The Impact of assimilating FY-3C GNOS GPS radio occultation observations on GRAPES forecasts. *J Trop Meteor*, 26(4): 390-401
- Wang J C, Jiang X W, Shen X S, et al. 2023. Assimilation of ocean surface wind data by the HY-2B satellite in GRAPES: Impacts on analyses and forecasts. *Adv Atmos Sci*, 40(1): 44-61
- Wang M J, Zhao K, Xue M, et al. 2016. Precipitation microphysics

- characteristics of a Typhoon Matmo (2014) rainband after landfall over Eastern China based on polarimetric radar observations. *J Geophys Res Atmos*, 121(20): 12415-12433
- Wang M J, Zhao K, Lee W C, et al. 2018. Microphysical and kinematic structure of convective-scale elements in the inner rainband of Typhoon Matmo (2014) after landfall. *J Geophys Res Atmos*, 123(12): 6549-6564
- Wang P, Li J, Li J L, et al. 2014. Advanced infrared sounder subpixel cloud detection with imagers and its impact on radiance assimilation in NWP. *Geophys Res Lett*, 41(5): 1773-1780
- Wang P, Li J, Li Z L, et al. 2017. The impact of cross-track infrared sounder (CrIS) cloud-cleared radiances on hurricane Joaquin (2015) and Matthew (2016) forecasts. *J Geophys Res Atmos*, 122(24): 13201-13218
- Wang S, Liu Z. 2019. A radar reflectivity operator with ice-phase hydrometeors for variational data assimilation (version 1.0) and its evaluation with real radar data. *Geosci Model Dev*, 12: 4031-4051
- Wang X G, Snyder C, Hamill T M. 2007. On the theoretical equivalence of differently proposed ensemble-3DVAR hybrid analysis schemes. *Mon Wea Rev*, 135(1): 222-227
- Wang X G, Barker D M, Snyder C, et al. 2008. A hybrid ETKF-3DVAR data assimilation scheme for the WRF model. Part I: Observing system simulation experiment. *Mon Wea Rev*, 136(12): 5116-5131
- Wang X G, Parrish D, Kleist D, et al. 2013. GSI 3DVar-based ensemble-variational hybrid data assimilation for NCEP global forecast system: Single-resolution experiments. *Mon Wea Rev*, 141(11): 4098-4117
- Wang X G, Lei T. 2014. GSI-based four-dimensional ensemble-variational (4DEnVar) data assimilation: Formulation and single-resolution experiments with real data for NCEP global forecast system. *Mon Wea Rev*, 142(9): 3303-3325
- Wang X G, Chipilski H G, Bishop C H, et al. 2021. A multiscale local gain form ensemble transform Kalman filter (MLGETKF). *Mon Wea Rev*, 149(3): 605-622
- Wang Y, Wang X. 2021. Development of convective-scale static background error covariance within GSI-based hybrid EnVar system for direct radar reflectivity data assimilation. *Mon Wea Rev*, 149(8): 2713-2736
- Wang Y M, Wang X G. 2023. Simultaneous multiscale data assimilation using scale-and variable-dependent localization in EnVar for convection allowing analyses and forecasts: Methodology and experiments for a tornadic supercell. *J Adv Model Earth Syst*, 15(5): e2022MS003430
- Wang Y Y, Shi X M, Lei L L, et al. 2022. Deep learning augmented data assimilation: Reconstructing missing information with convolutional autoencoders. *Mon Wea Rev*, 150(8): 1977-1991
- Wang Z R, Lei L L, Anderson J L, et al. 2023. Convolutional neural network-based adaptive localization for an ensemble Kalman filter. *J Adv Model Earth Syst*, 15(10): e2023MS003642
- Weissmann M, Harnisch F, Wu C C, et al. 2011. The influence of assimilating dropsonde data on typhoon track and midlatitude forecasts. *Mon Wea Rev*, 139(3): 908-920
- Wen J, Zhao K, Huang H, et al. 2017. Evolution of microphysical structure of a subtropical squall line observed by a polarimetric radar and a disdrometer during OPACC in Eastern China. *J Geophys Res Atmos*, 122(15): 8033-8050
- Wen L, Zhao K, Chen G, et al. 2018. Drop size distribution characteristics of seven typhoons in China. *J Geophys Res Atmos*, 123(12): 6529-6548
- Weng F Z, Yan B H, Grody N C. 2001. A microwave land emissivity model. *J Geophys Res Atmos*, 106(D17): 20115-20123
- Weng F Z, Yu X W, Duan Y H, et al. 2020. Advanced radiative transfer modeling system (ARMS): A new-generation satellite observation operator developed for numerical weather prediction and remote sensing applications. *Adv Atmos Sci*, 37(2): 131-136
- Whitaker J S, Hamill T M. 2002. Ensemble data assimilation without perturbed observations. *Mon Wea Rev*, 130(7): 1913-1924
- Whitaker J S, Hamill T M, Wei X, et al. 2008. Ensemble data assimilation with the NCEP global forecast system. *Mon Wea Rev*, 136(2): 463-482
- Whitaker J S, Hamill T M. 2012. Evaluating methods to account for system errors in ensemble data assimilation. *Mon Wea Rev*, 140(9): 3078-3089
- Wolfensberger D, Berne A. 2018. From model to radar variables: A new forward polarimetric radar operator for COSMO. *Atmos Meas Tech*, 11: 3883-3916
- World Meteorological Organization (WMO). 2009. The vision for the global observing system in 2025. WMO
- Wu C C, Chen J H, Lin P H, et al. 2007. Targeted observations of tropical cyclone movement based on the adjoint-derived sensitivity steering vector. *J Atmos Sci*, 64(7): 2611-2626
- Wu D, Zhao K, Kumjian M R, et al. 2018. Kinematics and microphysics of convection in the outer rainband of typhoon Nida (2016) revealed by polarimetric radar. *Mon Wea Rev*, 146(7): 2147-2159
- Wulfmeyer V, Behrendt A, Bauer H S, et al. 2008. The convective and orographically induced precipitation study: A research and development project of the world weather research program for improving quantitative precipitation forecasting in low-mountain regions. *Bull Amer Meteor Soc*, 89(10): 1477-1486
- Xiao H Y, Han W, Wang H, et al. 2020. Impact of FY-3D MWRI radiance assimilation in GRAPES 4DVar on forecasts of typhoon shanshan. *J Meteor Res*, 34(4): 836-850
- Xiao H Y, Han W, Zhang P, et al. 2023a. Assimilation of data from the MWHS-II onboard the first early morning satellite FY-3E into the CMA global 4D-Var system. *Meteor Appl*, 30(3): e2133
- Xiao H Y, Li J, Liu G Q, et al. 2023b. Assimilation of AMSU-a surface-sensitive channels in CMA\_GFS 4D-Var system over land. *Wea Forecasting*, 38(9): 1777-1790
- Xiao Q, Kuo Y, Sun J, et al. 2005. Assimilation of Doppler radar observations with a regional 3DVAR system: Impact of Doppler velocities on forecasts of a heavy rainfall case. *J Appl Meteor Climatol*, 44: 768-788

- Xiao Q, Sun J. 2007. Multiple-radar data assimilation and short-range quantitative precipitation forecasting of a squall line observed during IHOP\_2002. *Mon Wea Rev*, 135: 3381-3404
- Xiao Y, Bai L, Xue W, et al. 2024a. FengWu-4DVar: Coupling the data-driven weather forecasting model with 4D variational assimilation. *arXiv*: 2312.12455
- Xiao Y, Jia Q L, Xue W, Bai L. 2024b. VAE-Var: Variational-autoencoder-enhanced variational assimilation. *arXiv*: 2405.13711
- Xie H J, Han W, Bi L. 2023. Assimilating FY3D-MWRI 23.8 GHz observations in the CMA-GFS 4DVAR system based on a pseudo all-sky data assimilation method. *Quart J Roy Meteor Soc*, 149(756): 3014-3043
- Xie Y, Koch S, McGinley J, et al. 2011. A space-time multiscale analysis system: A sequential variational analysis approach. *Mon Wea Rev*, 139(4): 1224-1240
- Xue M, Jung Y, Zhang G. 2010. State estimation of convective storms with a two-moment microphysics scheme and an ensemble Kalman filter: Experiments with simulated radar data. *Quart J Roy Meteor Society*, 136(648): 685-700
- Yang J, Ding S G, Dong P M, et al. 2020. Advanced radiative transfer modeling system developed for satellite data assimilation and remote sensing applications. *J Quant Spectrosc Radiat Transf*, 251: 107043
- Yang L C, Duan W S, Wang Z F, et al. 2022. Toward targeted observations of the meteorological initial state for improving the PM<sub>2.5</sub> forecast of a heavy haze event that occurred in the Beijing-Tianjin-Hebei region. *Atmos Chem Phys*, 22(17): 11429-11453
- Yang L C, Duan W S, Wang Z F. 2023. An approach to refining the ground meteorological observation stations for improving PM<sub>2.5</sub> forecasts in the Beijing-Tianjin-Hebei region. *Geosci Model Dev*, 16(13): 3827-3848
- Yang S C, Kalnay E, Enomoto T. 2015. Ensemble singular vectors and their use as additive inflation in EnKF. *Tellus A*, 67(1): 26536
- Yano J I, Ziemiański M Z, Cullen M, et al. 2018. Scientific challenges of convective-scale numerical weather prediction. *Bull Amer Meteor Soc*, 99(4): 699-710
- Yin R Y, Han W, Gao Z Q, et al. 2020. The evaluation of FY4A's geostationary interferometric infrared sounder (GIIRS) long-wave temperature sounding channels using the GRAPES global 4D-Var. *Quart J Roy Meteor Soc*, 146(728): 1459-1476
- Yin R Y, Han W, Gao Z Q, et al. 2021. Impact of high temporal resolution FY-4A geostationary interferometric infrared sounder (GIIRS) radiance measurements on typhoon forecasts: Maria (2018) case with GRAPES global 4D-Var assimilation system. *Geophys Res Lett*, 48(15): e2021GL093672
- Ying Y, Zhang F Q. 2015. An adaptive covariance relaxation method for ensemble data assimilation. *Quart J Roy Meteor Soc*, 141(692): 2898-2906
- Yussouf N, Stensrud D J. 2010. Impact of phased-array radar observations over a short assimilation period: Observing system simulation experiments using an ensemble Kalman filter. *Mon Wea Rev*, 138(2): 517-538
- Zeng Y. 2013. Efficient Radar Forward Operator for Operational Data Assimilation within the COSMO-model. KIT Scientific Publishing
- Zeng Y, Blahak U, Neuper M, et al. 2014. Radar beam tracing methods based on atmospheric refractive index. *J Atmos Ocean Technol*, 31: 2650-2670
- Zeng Y F, Janjić T, de Lozar A, et al. 2020. Comparison of methods accounting for subgrid-scale model error in convective-scale data assimilation. *Mon Wea Rev*, 148(6): 2457-2477
- Zhang F, Snyder C, Sun J Z. 2004. Impacts of initial estimate and observation availability on convective-scale data assimilation with an ensemble Kalman filter. *Mon Wea Rev*, 132(5): 1238-1253
- Zhang F Q, Weng Y H, Sippel J A, et al. 2009a. Cloud-resolving hurricane initialization and prediction through assimilation of Doppler radar observations with an ensemble Kalman filter. *Mon Wea Rev*, 137(7): 2105-2125
- Zhang F Q, Zhang M, Hansen J A. 2009b. Coupling ensemble Kalman filter with four-dimensional variational data assimilation. *Adv Atmos Sci*, 26(1): 1-8
- Zhang J A, Rogers R F, Nolan D S, et al. 2011. On the characteristic height scales of the hurricane boundary layer. *Mon Wea Rev*, 139(8): 2523-2535
- Zhang J A, Nolan D S, Rogers R F, et al. 2015. Evaluating the impact of improvements in the boundary layer parameterization on hurricane intensity and structure forecasts in HWRF. *Mon Wea Rev*, 143(8): 3136-3155
- Zhang L, Liu Y Z, Liu Y, et al. 2019. The operational global four-dimensional variational data assimilation system at the China meteorological administration. *Quart J Roy Meteor Soc*, 145(722): 1882-1896
- Zhang P, Hu X Q, Lu Q F, et al. 2022. FY-3E: The first operational meteorological satellite mission in an early morning orbit. *Adv Atmos Sci*, 39(1): 1-8
- Zhang P, Hu X Q, Sun L, et al. 2024. The on-orbit performance of FY-3E in an early morning orbit. *Bull Amer Meteor Soc*, 105(1): E144-E175
- Zhang S, Harrison M J, Rosati A, et al. 2007. System design and evaluation of coupled ensemble data assimilation for global oceanic climate studies. *Mon Wea Rev*, 135(10): 3541-3564
- Zhang S Q, Liu Z Y, Zhang X F, et al. 2020. Coupled data assimilation and parameter estimation in coupled ocean-atmosphere models: A review. *Climate Dyn*, 54(11): 5127-5144
- Zhang X H, Duan Y H, Wang Y Q, et al. 2017. A high-resolution simulation of supertyphoon rammasun (2014)—Part I: Model verification and surface energetics analysis. *Adv Atmos Sci*, 34(6): 757-770
- Zhang Y J, Hu H, Weng F Z. 2021. The potential of satellite sounding observations for deriving atmospheric wind in all-weather conditions. *Remote Sens*, 13(15): 2947
- Zhao K, Wang M J, Xue M, et al. 2017. Doppler radar analysis of a tornadic

- miniature supercell during the landfall of typhoon mujigae (2015) in South China. *Bull Amer Meteor Soc*, 98(9): 1821-1831
- Zhao K, Huang H, Wang M, et al. 2019. Recent progress in dual-polarization radar research and applications in China. *Adv Atmos Sci*, 36: 961-974
- Zhao Z K, Liu C X, Li Q, et al. 2015. Typhoon air-sea drag coefficient in coastal regions. *J Geophys Res Oceans*, 120(2): 716-727
- Zhen Y C, Zhang F Q. 2014. A probabilistic approach to adaptive covariance localization for serial ensemble square root filters. *Mon Wea Rev*, 142(12): 4499-4518
- Zheng H, Chen Y, Zheng S, et al. 2023. Radar reflectivity assimilation based on hydrometeor control variables and its impact on short-term precipitation forecasting. *Remote Sensing*, 15(3): 672
- Zhou L F, Lei L L, Whitaker J S, et al. 2024. An adaptive channel selection method for assimilating the hyperspectral infrared radiances. *Mon Wea Rev*, 152(3): 793-810
- Zhu M B, van Leeuwen P J, Amezua J. 2016. Implicit equal-weights particle filter. *Quart J Roy Meteor Soc*, 142(698): 1904-1919
- Zhu Y Q, Derber J, Collard A, et al. 2014. Enhanced radiance bias correction in the national centers for environmental prediction's gridpoint statistical interpolation data assimilation system. *Quart J Roy Meteor Soc*, 140(682): 1479-1492
- Zhu Z Q, Weng F Z, Han Y. 2024. Vector radiative transfer in a vertically inhomogeneous scattering and emitting atmosphere. Part I: A new discrete ordinate method. *J Meteor Res*, 38(2): 209-224
- Zupanski M. 1993. Regional four-dimensional variational data assimilation in a quasi-operational forecasting environment. *Mon Wea Rev*, 121(8): 2396-2408
- Zupanski M. 2005. Maximum likelihood ensemble filter: Theoretical aspects. *Mon Wea Rev*, 133(6): 1710-1726